URS 658-3

COMBINED EFFECTS OF NUCLEAR WEAPONS ON NFSS TYPE STRUCTURES

Final Report
September 1966

Prepared for

OFFICE OF CIVIL DEFENSE
Office of the Secretary of the Army
Washington, D. C. 20310
Contract No. OCD-PS-64-201
OCD Work Unit No. 1126B

Distribution of this document is unlimited.

URS
CORPORATION

DISCLAIMER

URS 658-3

COMBINED EFFECTS OF NUCLEAR WEAPONS ON NFSS TYPE STRUCTURES

Final Report
September 1966

by

Carl K. Wiehle
William L. Durbin
URS CORPORATION
1811 Trousdale Drive
Burlingame, California

Prepared for

OFFICE OF CIVIL DEFENSE
Office of the Secretary of the Army
Washington, D.C. 20310
Contract No. OCD-PS-64-201
OCD Work Unit No. 1126B

ABSTRACT

The primary objective of this program was to examine and evaluate the protection afforded by the types of structures found in the National Fallout Shelter Survey (NFSS) against the combined effects of nuclear weapons. Since a major criterion for the designation of the NFSS structures was the radiation protection factor (PF) of the structure, the approach adopted in this investigation was to examine the sensitivity of the PF for idealized building situations to alteration by air blast and fire damage. To accomplish this, interim techniques were developed for estimation of the air blast loading and damage to selected types of structures. These techniques were developed by utilizing available experimental data together with engineering judgment to modify current generalized blast loading schemes. The procedure adopted to predict damage was to determine the blast loading on each building component and then to compare this loading with the failure loading for the component.

Similarly, by utilizing fire prediction information, a method was developed for determining the fire damage within the building. To predict damage to the various building elements by this procedure, the duration of the peak fire was calculated and then compared with the rated resistance of the components.

ACKNOWLEDGEMENTS

The authors gratefully acknowledge the assistance and guidance of Mr. C. A. Grubb of Stanford Research Institute during the conduct of this program. Similarly, the suggestions and comments of various URS personnel, especially Messrs. A. B. Willoughby, M. B Hawkins, and N. R. Wallace, are gratefully acknowledged.

CONTENTS

ILLUSTRATIONS

ILLUSTRATIONS (Cont.)

TABLES

Section 1
INTRODUCTION

Under Subcontract No. B-81868 (4949A-44)-US, URS Corporation has conducted an investigation of the interaction of nuclear weapon effects and typical shelter structures for the Office of Civil Defense. The purpose of the study was to investigate and evaluate the sensitivity of the protection level afforded by the various types of structures found in the National Fallout Shelter Survey (NFSS) against the combined effects of nuclear weapons. The initial effort was primarily concerned with the establishment of procedures to assess the damage due to air blast and thermal radiation, and to apply these procedures to estimate the damage and the change in radiation fallout protection factor (PF) of idealized structures. An important corollary of the study was to identify and delineate the important problem areas requiring further research.

BACKGROUND

Since the advent of nuclear weapons, considerable effort has been expended to investigate the loading and response of structures and mammals to nuclear blast, the effects of nuclear radiation and methods to protect against it, and the ignition and after-effects of fires generated by thermal radiation. Although structures have been included in nuclear field tests to determine their adequacy in resisting combined nuclear effects, the structural configurations and test parameters investigated have been limited in scope. Also, for the most part, the various effects have been studied and prediction methods developed without consideration for the interrelationships between the phenomena. For instance, the protection afforded by a particular structure in an idealized nuclear radiation environment has been studied extensively, and the radiation protection factors have been determined by methods which are independent of the structural behavior under blast loading. Generally, an engineer concerned with designing for combined nuclear effects has relied on his engineering knowledge of the total environment, rather than on specific guidelines based on research information.

The criterion for the designation of the National Fallout Shelter Survey structures was the radiation protection, or protection factor (PF), afforded by the structure. As long as a shelter is not located in the immediate vicinity of a nuclear explosion, the PF is the most meaningful measure of the shelter protection value.* However, as the distance from ground zero is decreased, the blast overpressure and thermal radiation become increasingly important. It is axiomatic that the areas of blast, nuclear radiation, and thermal radiation effects overlap and that, in such areas, the combined nuclear weapons effects must be considered to adequately describe the protection level of a particular shelter.

Consider the effect of a nuclear explosion on a structure with an interior designated shelter area located in the blast region. Simultaneously with the diffraction around the structure, the pressure wave will enter the structure through doors and through openings created by rapid failure of frangible walls and glass. Even if the shelter area is so located that it is unaffected by the exterior-wall debris, the entering blast wave could produce body translation within the shelter space, as well as internal flying objects. Although considerable research has been conducted to determine the effect of blast waves on mammals (for instance, Ref. 1), it is important to note that the internal pressure-time environment created by a shock wave entering complex geometric configurations is not well defined.**

Depending on the loading function, resistance, geometry, and period of vibration of the exterior walls, interior partitions, floors, roofs, and structural framing, portions or all of the structure could fail or be damaged

---

* It should be noted that the PF relates the dose in the shelter to some standard idealized conditions and not to conditions outside the building housing the shelter.

** In the review of the nuclear weapons blast data conducted by URS for the research reported in Ref. 2 it was found that there was only limited information concerning the internal environment resulting from blast waves entering structures through openings. It is important to emphasize that the paucity of information in this area prevents the formulation of rational prediction schemes for the pressure-time distribution within complex geometries, which is required for a rational evaluation of the possible damage to shelterees.

during or shortly after impingement and passage of the blast wave. Impacting debris could alter significantly the structural integrity of the shelter area and drastically modify its level of protection from other effects.

The thermal radiation from a nuclear detonation can cause simultaneous ignition in fine kindling fuels over large areas. A fraction of these kindling fuels, those suitably located with respect to heavier fuels, can cause small fires, some of which can, in turn, grow and merge into large fires. In addition to direct physical damage to the shelter or shelter facilities, air blast may set the stage for further destruction by making the structure more vulnerable to fire or by producing secondary ignitions. Air flow through the building may be less restricted due to breakage of window glass and blown-out or damaged panels. Combustible materials could be exposed, fire-protective coverings disrupted, and fire control made ineffective by immobilization of fire-fighting equipment and personnel. Also, fire may cause additional structural failure and debris production (Ref. 3). In any event, an important consideration for shelters located throughout the thermally affected area is the sensitivity of the protection level to both direct and secondary ignitions.

Since various levels of blast and fire damage to a structure can drastically affect the radiation-shielding characteristics of designated shelter areas, it is necessary to have available methods for evaluating the combined weapon effects. Such procedures would provide the basis for detailed prediction of damage to NFSS shelters, both for planning purposes and for evaluating the cost of increased fire and blast protection. In this study, URS has attempted to utilize current information to develop methods for predicting the integrated effects of nuclear weapons on the buildings of interest. The approach and limitations of the initial investigation are presented in the following subsection.

APPROACH

Since this study involved the complex interacting effects of radiation, fire, and blast for a very broad range of possible types of buildings, it became necessary to limit the investigation to the most important aspects of

both the weapon effects and the building types. To establish the principal types of construction in use as NFSS shelter structures, an examination was made of the available published information. In general, it was found that the large majority of NFSS buildings belonged to one of the following four categories: wood frame, masonry load bearing wall, multistory reinforced concrete frame, and multistory steel frame. Furthermore, it was also found that over 90 percent of the buildings could be included in the three types of masonry load-bearing wall and steel and reinforced concrete frame. (Refs. 4, 5, 6, 7 and 8). To develop the damage prediction techniques presented in Section 2, it was concluded that the current knowledge of the blast loading and response, and fire rating of large multistory structures precluded differentiating between structures with a steel or reinforced concrete frame. Therefore, for the purpose of this study, only two framing categories were selected for further study: the load-bearing wall and the multistory frame.

In addition, during this phase of the study, information on component building elements required for the damage assesment was catalogued. Since these data are important to PF calculations, fire rating, and blast-resistance estimates, sketches of the more important types of components are included in Appendix A.

Because of the complexity entailed in considering the nuclear weapon effects in detail for the large variety of multistory buildings of interest, it became apparent during the initial period of this investigation that it would be advantageous to make an initial, cursory examination of the possible damage parameters. Essentially, this was a screening process to determine the important parameters requiring further treatment. For example, an examination was made of the effect of ingress of fallout into a building, based on the assumption that the windows had been removed by the air blast or fire. Although current prediction methods are inadequate to determine the actual percentage of ingress or its distribution, its relative importance can be demonstrated by idealized building situations. By assuming various building configurations and percentages of fallout ingress, it was shown that ingress could be an important factor in reducing the PF of some, but not all, shelters. It could be concluded, therefore, that the possibility of window breakage and

the subsequent ingress of fallout into areas of the building adjacent to shelter spaces must be a consideration in any analysis of shelters located in air blast regions.

From the initial examination, it was concluded that current information was inadequate to establish general prediction schemes or even ground rules for the large variety of conceivable situations. However, it was found that meaningful information could be obtained by an examination of limited key situations. This procedure was felt to be adequate at this time since a primary goal of this study was to identify and delineate the important problem areas, even if adequate prediction methods were unavailable or could not be devised within the limits of the program.

Therefore, to demonstrate the protection level sensitivity of typical NFSS building construction, idealized buildings were selected for detailed investigation. In this manner, rational estimates of the interacting weapon effects could be made for comparative purposes and would provide the basis for recommendations of future research. It should be noted that the prediction methods presented in this report should be considered as interim procedures, to be modified and upgraded as the result of additional studies.

REPORT ORGANIZATION

Section 2 contains a discussion and presentation of the methods used in this investigation to determine the protection factor and to predict air blast and fire damage. The use of these techniques is demonstrated in Section 3 by first performing a damage analysis of three idealized structures and then calculating the change in PF for typical shelter areas at various levels of damage to each building. The conclusions and recommendations for further research to upgrade the prediction techniques are presented in Section 4. Sketches of various typical building elements which are useful when making radiation and damage calculations are included in Appendix A. A sample calculation of the pressure buildup as a result of a blast wave entering a room is shown in Appendix B.

Section 2
PREDICTION METHODS

INTRODUCTION

It was not the intention during this investigation to extend the state of knowledge in any of the areas of nuclear weapon effects. Rather, it was the intent to utilize existing information to establish methods for evaluating the protection level sensitivity of the types of construction found in NFSS structures. This required a process of selection or modification of conventional methods for predicting the fallout protection factor, the fire damage, and the air blast damage. The prediction methods used in this investigation are presented in the following sections.

PROTECTION FACTOR PREDICTION

The protection factor (PF) of a shelter is essentially a determinable quantity, i.e., once the geometry and mass thickness of the components are defined, established methods are available for calculating the PF. Consequently, in this study very little effort was devoted to generating new information or modifying existing techniques in the area of nuclear radiation effects.

Defining the geometry and mass thicknesses after the structure has been damaged by blast and/or fire is less determinable than it was prior to damage. For the real case, a structure that was originally of uniform construction would be in a decidely nonuniform condition as a result of partial damage. However, to simplify the calculations, it was assumed for this study that when the failure criterion was satisfied, the components of interest were completely removed.

Another aspect of nuclear radiation effects that could not be handled by conventional techniques was the problem of ingress of fallout particles into the structure. Methods are available for calculating the PF if the amount of ingress is known and the distribution is reasonably uniform. Unfortunately,

no method is currently available for predicting the quantity of ingress, much less the distribution, for even simple geometries.

As a matter of fact, very little definitive work has been done to solve this problem; however, the following preliminary studies are indicative of what might occur if ingress is not prevented. Field measurements were made of ingress of nonradioactive particles of throwout from a volcano in Costa Rica (Refs. 9 and 10). In the first study, the structure considered was a one-story residence with a single 4-sq-ft opening and the following entry conditions: natural ventilation; forced ventilation; and forced ventilation with filtered air. In these tests the mass loading (over a limited area adjacent to the window) inside the house was 2 percent of that outside the house. From these data and the fact that the particles could easily be removed, it was implied that ingress was not much of a problem.

However, in the second study, in which the structure of concern was a schoolroom with a much larger ratio of window area to wall area, the interior mass loadings were significantly larger. In four tests the average mass loading over the entire room ranged from 5 to 15 percent of the exterior loading, (Ref. 10). (To obtain the average mass loading, the total mass of the ingress, in grams, was divided by the total area, in square feet. The percentage of ingress was determined by dividing the density of ingress (gm/sq ft) by the density of the exterior deposit.) Although not too much confidence can be placed on these limited results, there are a few points worth mentioning in connection with this latter study. Intuitively, it seems as though the amount of ingress would be a function of many parameters, including such things as particle size, window area, wind speed, ratio of window area to wall area, and ratio of window area to floor area. It is worthwhile to look at the Costa Rica tests to determine how these parameters compared with typical conditions found in American construction. First, the wind was variable, ranging from 0.7 to >12.0 fps; secondly, the particle size ranged from 44 to 350 μ; thirdly, the ratio of window area to wall area was 0.20; and fourthly, the ratio of window area to floor area was 0.063. Thus, the winds were moderate, the particle size was within the range of interest, and the ratio of window area to wall area was consistent

with construction practices in this country, as was the ratio of window area to floor area.

The third source of information on experimental measurement of ingress came from a model study conducted in a low-speed wind tunnel at Texas Engineering Experimental Station (Ref. 11). In this reference, an example is presented in which the amount of ingress was calculated (based on the experimentally obtained coefficients) for ideal conditions. For the particular circumstances indicated in the example, the interior and exterior mass loadings were equal.

Needless to say, there is still little information on which to base predictions of the ingress of fallout into typical NFSS buildings. For this reason it was decided to investigate the effects on the PF of a range of values for the amount of ingress while assuming uniform distribution of the material entering the building. The results of these calculations are shown in Fig. 1. The uppermost curve represents a basement shelter with the floor above consisting of 6 in. of reinforced concrete (X_o = 75 psf). The total overhead mass, including floors and roof is equal to 250 psf. The exterior walls have a mass thickness of 130 psf with 50 percent openings. The floor area of the building equals 15,000 sq ft. As little as 5 percent ingress spread uniformly over the floor above causes a reduction in PF of about 80 percent. In the second case, the shelter was in the core of the 10th floor of a 12-story building, with ingress spread around the perimeter, i.e., the entire area between the interior partitions and the exterior walls. (This structure is analyzed in detail in Section 3 and a description of the building can be found there.) In this case 5-percent ingress causes a 50-percent reduction in PF. The lowermost curve pertains to a 6-story structure with a core shelter on the 4th floor. In this case, ingress has much less of an effect. These results are consistent with those in Ref. 9, in which it was shown that the percent reduction in PF (for a given amount of ingress) increased sharply as the initial PF increased.* Although it can be argued that in the shelter with a high

* These results seem to be in contrast to the results of a study reported in Ref. 12; however, the apparent anomalies are due to differences in the assumed mass loadings and the distributional patterns.

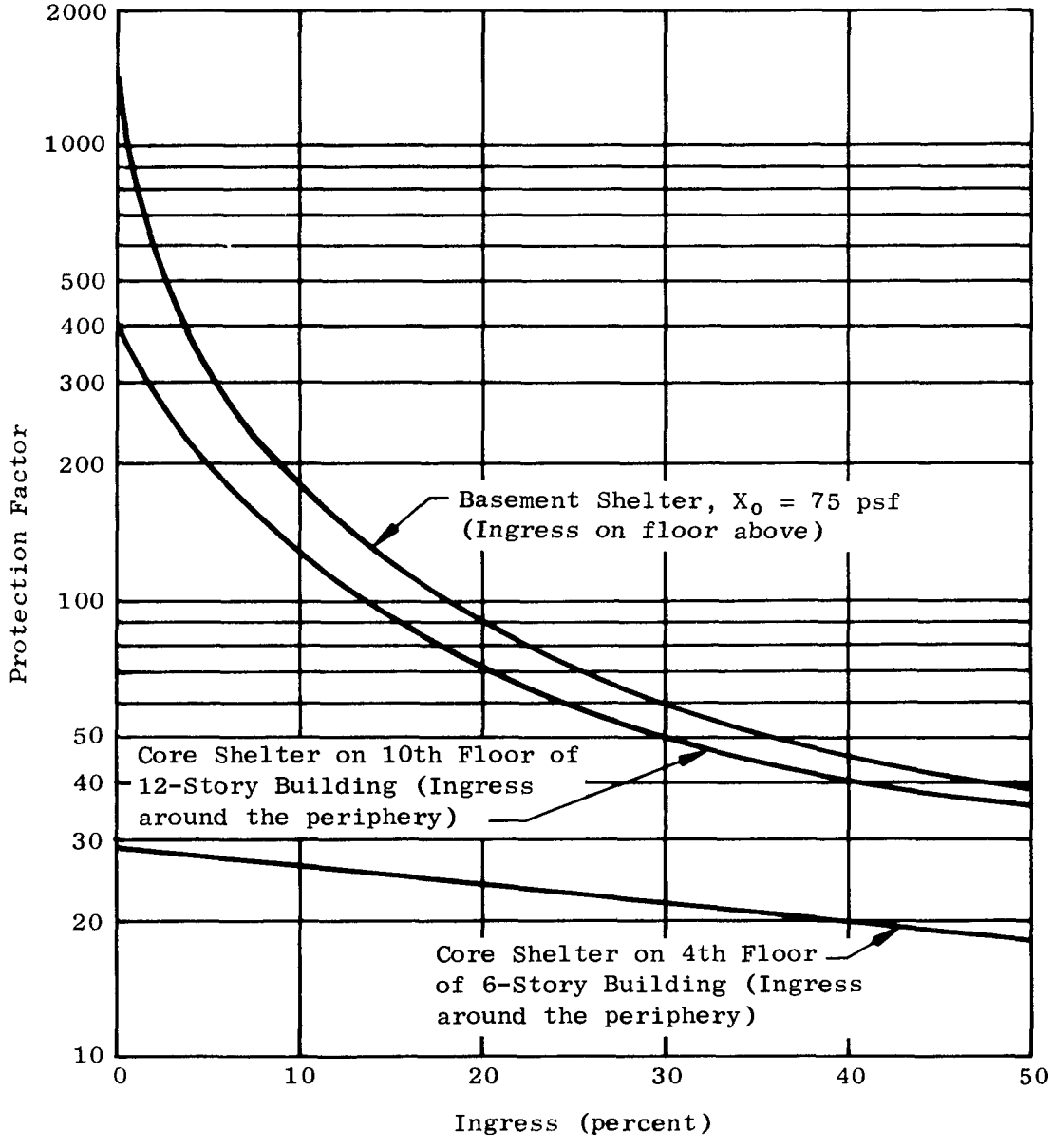

Fig. 1. Protection Factor Versus Ingress for Typical Shelters Within Simplified Structures

initial PF (Fig. 1), the final PF was still relatively large, account should be taken of the reduction in PF in planning exit times, countermeasures, etc.

In the experimental studies mentioned above, it was determined that the distribution of fallout was definitely nonuniform; but because of the paucity of information regarding distributional patterns, it was assumed in the present study that the particles were distributed uniformly over the floor. Generally, the error due to this assumption should be less than the error inherent in the assumption of the magnitude of the average interior mass loading. Because of the lack of sufficient information regarding the magnitude of the average density of ingress to be expected for the conditions examined in the subsequent examples, it was assumed that the ingress was 10 percent of the exterior deposit.

The protection factors for the examples in Section 3 were calculated by the Engineering Method in accordance with the procedures presented in Ref. 13.

FIRE DAMAGE PREDICTIONS

Introduction

Roughly one-third of the energy liberated in an ordinary air burst of a nuclear weapon is in the form of thermal radiation, which can lead to fires over large areas. The actual extent of the affected area is, of course, a function of many parameters. In addition to the source parameters of importance, the extent of damage will also be strongly influenced by the characteristics of the receiver. No attempt will be made to present a sensitivity analysis of these parameters or even to list all of them; rather, the reader is referred to Ref. 14, in which an excellent summary of the state of the art is presented.

In keeping with the approach outlined in Section 1, no effort has been made in this study to extend understanding of the basic phenomena; rather, the objective has been to utilize, wherever possible, existing information on the thermal effects of nuclear weapons. Since this study was concerned

with the damage to selected structures inflicted by the combined effects of nuclear weapons (as opposed to the total effects of fires alone), it was restricted to an examination of fire histories within structures. By restricting the area of concern to fire histories, it was anticipated that the prediction of ignitions (whether primary, secondary, or by fire spread) would be provided by other investigators.

Fire Damage Prediction Model

The specific objective of the fire damage prediction model is to estimate the post-fire condition of the shelter, insofar as the shelter remains adequate for attenuating the nuclear radiation associated with fallout. Since a great deal of work has been done to classify buildings and components with regard to their fire resistance, a method was sought by which the fire ratings could be compared with the duration of the anticipated fires in order to predict the reusability of the structure for shelter purposes.

Reference 15 presents a method for designing fire-resistant components that has been considered in Refs. 14 and 16 as the basis for evaluating fire damage to urban areas. This scheme establishes an indirect relationship between the fire rating and the duration and severity of the anticipated fire. This is done by comparing the area under the standard time–temperature (t–T) curve* used in rating building material with the area under the t–T curve anticipated for the design conditions (See Fig. 2).

The anticipated t–T curve for a particular occupancy can be obtained from Table 1 and from the nonlinear curves in Fig. 3, which were taken from Ref. 15. Knowing the unit fire load (psf) and the occupancy, the duration can be obtained from the linear curves in that figure. With this information the designer can then select the appropriate component such that its equivalent fire rating is greater than the time indicated on the standard curve in Fig. 2.** The basic assumption in this method is that the resistance is

---

* "The standard time–temperature curve...is somewhere near the maximum representative of the severity of a fire likely to occur in the complete burn-out of a brick, wood-joisted building and its contents." (Ref. 15).

** See the example presented in Fig. 3.

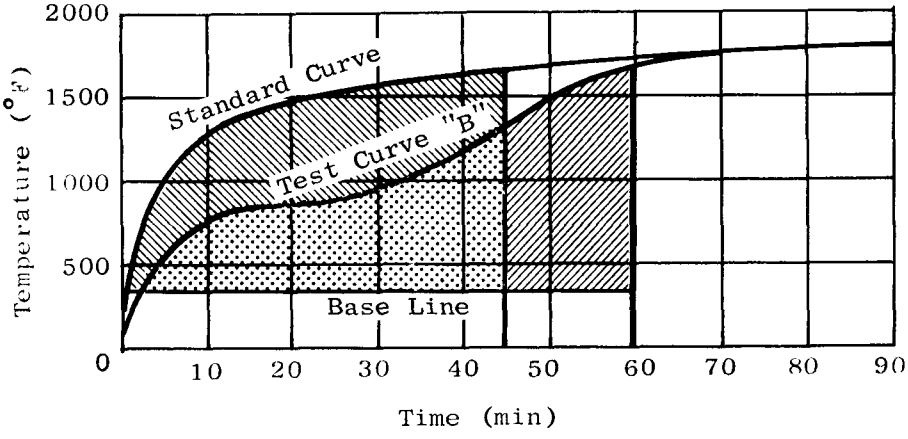

Note: The area, expressed in degree-hours, under the test curve and above a base line for 60 min is the same as the area under the standard time – temperature curve for a 45-min period. Therefore, the severity of the fire under both curves is approximately the same.

Fig. 2. Method for Obtaining the Equivalent Fire Severity Curve (From Ref. 15)

Table 1

FIRE SEVERITY EXPECTED BY OCCUPANCY

(See Fig. 3)

Temperature Curve A (Slight)

Well-arranged office, metal furniture, noncombustible building.
Welding areas containing slight combustibles.
Noncombustible power house.
Noncombustible buildings, slight amount of combustible occupancy.

Temperature Curve B (Moderate)

Cotton and wastepaper storage (baled) and well-arranged, noncombustible building.
Paper-making processes, noncombustible building.
Noncombustible institutional buildings with combustible occupancy.

Temperature Curve C (Moderately Severe)

Well-arranged combustible storage, e.g., wooden patterns, noncombustible buildings.
Machine shop having noncombustible floors.

Temperature Curve D (Severe)

Manufacturing areas, combustible products, noncombustible building.
Congested combustible storage areas, noncombustible building.

Temperature Curve E (Standard Fire Exposure — Severe)

Flammable liquids.
Woodworking areas.
Office, combustible furniture and buildings.
Paper-working, printing, etc.
Furniture manufacturing and finishing.
Machine shop having combustible floors.

(From Ref. 15)

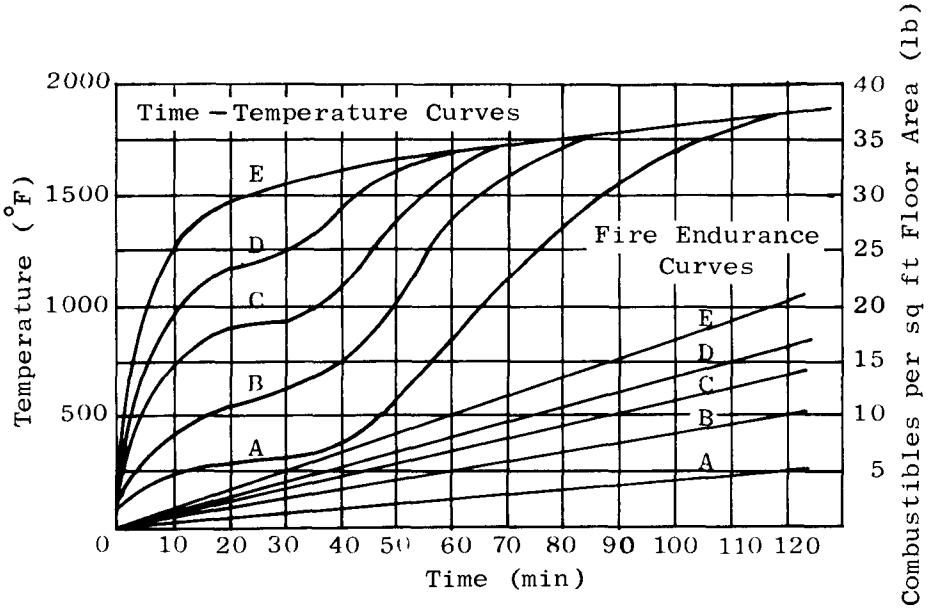

Note: The straight lines indicate the length of fire endurance based upon amounts of combustibles involved. The curved lines indicate the severity expected for the various occupancies (see Table 1). There is no direct relationship between the straight and curved lines, but, for example, 5 lb of combustibles per sq ft will produce a 60-min fire in a "B" occupancy, and a fire severity following the time – temperature curve "B" might be expected. Then, if we assume that the test curve in Fig. 2 is the "B" curve, a fire protection in excess of 45 min would be required for the above conditions.

Fig. 3. Possible Classification of Building Contents for Fire Severity and Duration (From Ref. 15)

a function of both severity and duration. However, because of a lack of information to support this assumption and because of the arbitrary nature of the t − T curves in Fig. 3, it was decided to base the present model upon the methods developed by Illinois Institute of Technology Research Institute (IITRI) and presented in Refs. 17 − 19.

This investigation included studies of initial ignitions, fire histories, and fire spread, a large portion of which involved experimental studies of fire histories within buildings. Consequently, the possibility existed for adapting the information contained in Refs. 17 − 19 to predict the reusability of buildings and their components for attenuating nuclear radiation. Many parameters were measured in these experimental studies, including such things as time to flashover, temperatures, burning rates, and time for penetration of the walls, doors, and ceilings. The quantities of most interest to the prediction method presented herein are burning rates and times for penetration.

Once the anticipated burning rate is determined, the duration of the peak fire, D, can be calculated from the following equation:

$$D = \frac{0.5\ W}{R} \tag{1}$$

where W is the total weight of fuel (lb) and R is the mean burning rate (lb/min). The constant 0.5 was introduced to account for the fact that approximately 50 percent of the fuel is consumed during the time to peak fire.

The mean burning rate can be either fuel-surface controlled or ventilation controlled. If it is fuel-surface controlled:

$$R_s = 0.09\ A_s \tag{2}$$

where A_s is the surface area of the combustible material (sq ft) and R_s is the mean burning rate for fuel-controlled fires (lb/min). If the surface area is relatively large and the ventilation provided is relatively small, then the fire will be ventilation controlled. In this case the burning rate is:

$$R_v = 1.5\ A\ \sqrt{H}\ ^{*} \qquad (3)$$

where A is the window area, H is the window height (ft) and R_v is the mean burning rate for ventilation-controlled fires.

In either case, the magnitude of the fire load must be known in order to calculate the duration. The fire load (lb) is best determined by actual measurements whenever possible, since it is known to vary over wide limits, even for a particular occupancy type. For instance, the unit fire load (psf) for dwellings has been found to vary between 5 and 10 psf. In lieu of actual measurements, unit fire loads of building contents can be obtained from Table 2, which was taken from Ref. 20. In addition, if the structure is of combustible construction, the fire load contributed by it would have to be determined from building drawings.

The model presented herein compares the duration of the peak fire calculated by means of Eq. (1) with the time for penetration of the walls, ceilings, floors, and doors. As mentioned previously, the actual resistance, i.e., the time for penetration (t_p) was measured in the experimental studies at IITRI and presented in Ref. 18. The relationship between t_p and the rated resistance (t_R) of the components is presented in Fig. 4. From these results it appears that there was good correlation between t_p and t_R.** It should be observed that the data were limited to rated resistances

---

* This is for the case of a fire in a room with a single window. For other cases see Ref. 17.

** Actually it was concluded from Ref. 18 that $t_p - t_R = -4$ min; however, the 4 min was dropped for this analysis because it becomes insignificant for the higher fire ratings.

Table 2

UNIT FIRE LOADS OF BUILDING CONTENTS*

Occupancy	PSF Combustible
Apts. and Residential	3.5
Auditoriums and Churches	1
Garage	
Storage	1
Repair	1
Gymnasium	0.3
Hospitals	1.2
Hotels	4
Libraries	24
Manufacturing	
Comb. Mdse., Fabrics and Furniture	13.5
Incombustible	1
Offices	7
Printing Plant	
Newspaper	10
Books	50
Schools	9.5
Storage	
Gen. Mdse.	14
Special	
Stores	
Retail Dept.	7.5
Wholesale	10
Restaurant	2

* From Ref. 20.

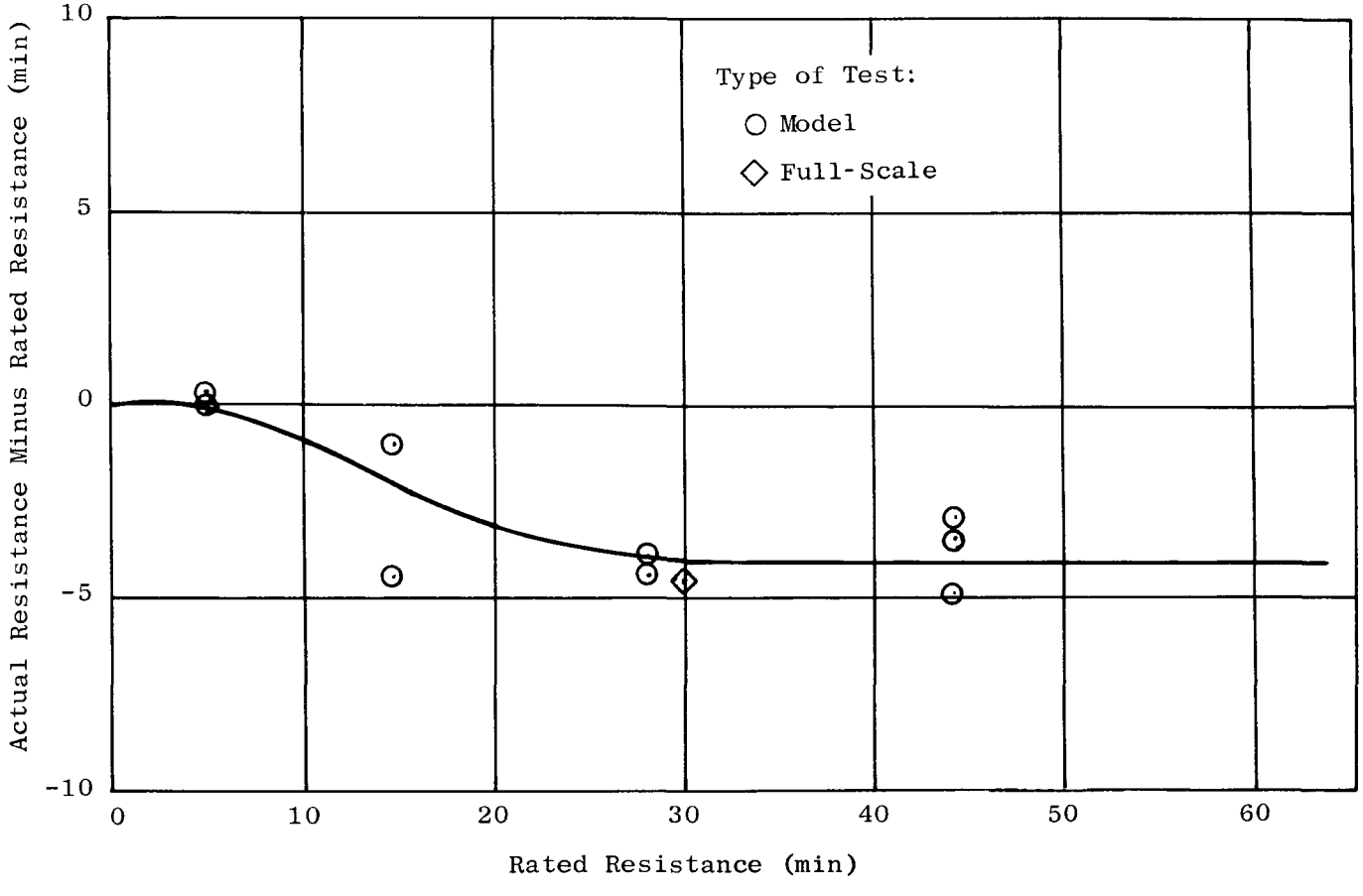

Fig. 4. A Comparison of Actual Fire Behavior of Various Barriers to Their Fire Resistance Rating (From Ref. 16)

of 45 min, whereas many of the NFSS structures have fire resistance ratings in excess of 45 min. However, for the present effort these data were extrapolated to the higher fire ratings.

The implicit assumption in the fire damage prediction model used here is that the resistance is primarily a function of duration, but relatively insensitive to severity. This is implied by the fact that a good correlation was obtained between actual resistance and rated resistance (in Ref. 18) even though the fire ratings were based upon the standard curve and the actual resistances were based upon the fires that actually existed in the field tests. This can be a reasonable assumption and still not contradict the basic assumption of the method presented in Ref. 15 if the effect of severity is small or the variation in severity in the IITRI tests was small. This assumption becomes less uncertain for the times corresponding to the higher fire ratings.

In an actual situation, ignition points within the building would be obtained from an initial ignition model, and the fire history within the entire building could then be determined. If the barriers forming the initial fire areas are of sufficient resistance to contain the fire, then the fire history will be limited. However, if penetration of these barriers does occur, then the next area involved would have to be analyzed to determine if it could contain the fire. Since in the examples presented here, the locations of ignitions were unknown, fires were arbitrarily assumed in the rooms with windows, and the resistance of these areas was determined and assumed to apply throughout the building. This should be adequate to demonstrate the protection level sensitivity for uniform construction and fire loading. For the case of ordinary type construction, e.g., brick bearing wall with wood joists, the prediction of fire damage is obvious, since if an ignition occurs in a building of this type, the building will generally be destroyed by the fire.*

*It was anticipated in this study that there will be no active fire-fighting facilities available.

If the structure of interest is in the range of significant blast damage, then certain parameters in the fire damage prediction model must be altered. For instance, it is clear that the fire resistance of various components can be reduced, or the fire load increased, by the removal of fireproof protective materials by direct air blast or by blast-generated missiles. In addition, of course, the fire hazard in structures can be reduced if fires are smothered by building debris or if active fire suppression is undertaken. However, because of the lack of information in these areas, the latter two conditions could not be included in the damage predictions for this study.

AIR BLAST DAMAGE PREDICTION SCHEMES

Introduction

An important factor in air blast damage predictions is the determination of the free-field pressure—time relationship just prior to the interaction of the wave with the structure. For this study, it was assumed that the blast wave characteristics could be calculated by standard procedures for ideal waves propagating radially outward over an ideal rigid reflecting surface. It should be kept in mind, however, that this is an oversimplification of the actual situation, where many factors influence the determination of a realistic pressure— time relationship. These include terrain, surface type, nonideal waveforms, blast shielding in city complexes, and airborne dust and debris.* Furthermore, it was assumed that the structure was located

* The reader is referred to Ref. 21 for a spectacular demonstration of the structure loading and response, due to a low-pressure, dust-laden precursor blast wave.

in the Mach region, that the duration of the positive phase of the overpressure and dynamic pressure were the same, and that the negative phase could be neglected. Although the negative phase loadings could possibly alter the deposition of debris, or fail damaged structural elements, it is not considered a major damage parameter.

To determine the protection level sensitivity of NFSS structures to the effects of nuclear weapons, it is necessary to predict the incident overpressure level at which damage to various structural components occurs. This requires the determination of the time-dependent load function at any point on or within the building and the establishment of adequate failure criteria for the buildings and members of interest. It was found during this program that the conventional air blast load prediction methods were often inadequate for the determination of damage to multistory buildings in city complexes. This inadequacy results primarily from the fact that the blast load prediction schemes were developed for the design of structures to be located in a nuclear blast environment. For such purposes, certain simplifying assumptions for estimating the unknown factors were justified, since they generally result in adequate structures. Unfortunately, for damage prediction purposes, the application of the design methods without due consideration for the original assumptions can result in large errors.

For example, consider the design assumption for the clearing time of the reflected pulse on the windward face of a partially open rectangular structure. To calculate the design load, it is arbitrarily assumed that if the window openings are less than 30 percent of the exterior wall area, then the overall building dimensions determine the time required for the reflected pulse to reach the stagnation pressure (sum of overpressure and dynamic pressure); on the other hand, if the wall openings are greater than 30 percent, it is assumed that the distance between windows determines this time (Ref. 22). Application of this criterion to large multistory buildings typical of American cities would indicate that the average loading on the front face of a building with slightly less than 30 percent window openings would decay from the reflected peak pressure to a stagnation pressure in hundreds of

milliseconds. However, for an identical building, except with slightly greater than 30 percent window area, the method would show a time of decay in tens of milliseconds.* Such a difference in clearing time can be an important factor in determining the peak incident overpressure at which failure would occur for many actual structural situations. This one example indicates that the application of a design criterion in a general manner, and without consideration for the local conditions, can be misleading for detailed damage prediction. Therefore, it is not sufficient merely to assume that a known free-field pressure—time history can be applied directly to a structural member located at the point of interest in a multistory building. It is also necessary to consider the modification of the free-field pressure as a result of its interaction with the structure.** For the purpose of estimating blast damage for this study, an attempt was made to utilize, wherever possible, the conventional or generalized loading schemes used in design, and to modify these procedures to reflect the available experimental information.

In addition to the determination of the air blast loading, another important aspect of damage prediction is a knowledge of the failure loading*** for each structure and element of interest. Although there is a wealth of failure information reported in the engineering literature, it was beyond the scope of this study to survey the entire field, to extract applicable information, and to correlate the data for application to multistory buildings located in blast environments. The procedure adopted was to utilize the readily available failure information from nuclear field tests and laboratory experiments to obtain solutions to the selected idealized building situations. Unfortunately, however, no test information is available on the loading and

---

* Consider a building with a distance S = 100 ft and the distance between window openings = 10 ft. For less than 30 percent window area, the clearing time, $t_1 \simeq 250$ msec, while for the same building with window area slightly greater than 30 percent, $t_1 \simeq 12$ msec.

** In addition, of course, the interacting free-field shock wave is influenced by many factors, such as the surrounding structures, and the geometry, size, orientation, and response of the building.

*** The establishment of a failure criterion for civil engineering structures is a very complex subject and involves many variable factors (see, for example, Ref. 22). For the purposes of this study, failure is defined as structural collapse or gross structural distortion.

response of typical American multistory buildings subjected to nuclear air blast loading. Therefore, in order to examine realistic situations for the current study, it was necessary to establish both a failure loading and a load prediction method for a particular wall panel located in the idealized structure. This required, first, a review of the weapon test data to determine the failure load for the individual wall panel under actual nuclear air blast loading conditions.* And, second, it was necessary to modify current generalized blast load prediction schemes to relate the test load conditions and the loading anticipated when the panel was located in a realistic multistory building.

During the conduct of this program, it was necessary to review a number of reports in the area of air blast loading and structural response, including the damage information obtained from the atomic attacks on Hiroshima and Nagasaki. After a careful examination, it was concluded that the information from the Japanese cities has limited application for detailed damage predictions for typical multistory buildings in American cities (Refs. 7, 23, and 24). This is primarily due to two factors. First, the heights-of-burst at both Japanese cities were well above the optimum for producing maximum building damage. Thus, most structures were located in the regular reflection region, where the vertical component of load was more predominant than the horizontal component. This produced relatively more damage to the roof and floor systems than would be expected for the Mach region, where horizontal flow predominates. Also, the correlation of structural damage with blast wave characteristics in the regular reflection region is complicated by the double shock effect and the complex flow regime behind the shocks.

Second, as a result of the adoption of an earthquake code in 1924, the multistory structures in Japan were inherently more resistant to blast loadings than comparable structures in most parts of the United States.

---

* It should be noted that although an attempt was made to utilize actual test failure data, an unknown factor is the effect on the response of an element that occurs as a result of the difference in support conditions between the test situation and an actual multistory structure.

This was due primarily to the code requirements for the design for lateral loads, limitation in the height of buildings, and continuity of construction. In general, this resulted in structures that were as monolithic as possible through the use of heavier members, rigid connections, and continuous reinforcement. Diagonal bracing and reinforced concrete shear walls made most of the major structures very well suited to resist large blast forces without undue loss of structural integrity between the frame, walls, and floors. Therefore, since the data from the Japanese cities constitute, essentially, a biased sample, any direct comparison with the damage predicted for American multistory buildings at similar overpressure levels must be made with care.

The development of the loading schemes used in this program is presented in the following subsections, and the failure criteria are discussed, along with the appropriate applications, in Section 3. It was assumed in this study that the structures were located in the Mach region, and were subjected to a clean, sharp-fronted wave. Also, it should be emphasized that only the factors affecting the modifications to the generalized blast loading techniques used for predicting damage are discussed herein; the reader is referred to the standard sources for detailed treatment of the general subject of air blast phenomena (e.g., Refs. 2, 6, 25, and 26).

Loading Schemes

To predict the loading on multistory buildings and their components at successively increasing overpressure levels, it is convenient to consider two general building categories: those structures whose interior partitions fail at a lower incident overpressure level than the exterior walls and those structures whose exterior walls fail at a lower overpressure than the interior partitions. In addition, in order to predict the incident overpressure at which failure of any element occurs, it is necessary to consider the loading for an undamaged or a partially damaged building condition. Although it was not possible within the scope of this effort to treat all such situations, the techniques can be illustrated for the selected idealized buildings by considering the following three cases.

Case No. 1

For this case, the incident overpressure level is less than that required to cause failure of either the exterior walls or the interior partitions. If a plane wave strikes normal to a typical multistory building, the blast wave front reflects from the front exterior wall, enters the windows, and diffracts around the rear of the exterior walls and around the sides and roof of the building.*

The diffracted shock within the structure exerts an average pressure on the back of the front wall which is initially less than the incident overpressure, p_{so}, because of the expansion into the room. During this time an unloading wave is sweeping the front face of the exterior wall laterally outward from all edges of the windows and building. The total effect on the front exterior wall is to reduce the differential pressure acting on it. Quantitative values of pressure on the building cannot be calculated during the diffraction time, although it is usually assumed arbitrarily (e.g., Ref. 22) that if window openings are less than 30 percent of the wall area, the outside dimensions of the building determine this time. For openings greater than 30 percent the dimensions between openings determine the diffraction time.

In any event, however, for the building response (as opposed to response of an element), the reflection of the blast wave from the interior partitions would also apply a load to the structure which is delayed a time equal to ℓ/U (room length divided by shock velocity), the travel time across the room. In another time increment of ℓ/U, the wave reflected from the rear interior partition reaches the window opening. At the present time, analytical techniques are inadequate for determining the strength of the shock front after it enters the window opening and expands into a three-dimensional room. Also, the value of the wave reflected from the interior partition is unknown. Limited field test data indicate that the pressure on some interior walls had a finite rise-time to a pressure approximately equal to the free-field overpressure (Ref. 27). In addition to the reflection of the entering wave front from the rear interior wall, there is a very complex pattern of

* It should be noted that the failure process for window glass is so rapid that no significant reflection of the shock front occurs.

indeterminate multiple reflections and interactions of waves within the room, as well as vortices at window edges. However, in a time approximately equal to 2 ℓ/U, the wave reflected from the rear interior partition reaches the window; this is the first notification to the incoming particles that the partition exists. Room filling ceases as the room and exterior pressures approach equilization.

Building Load. Subsequent to the initial reflection from the front face of the building, there would be a short-duration dip in the average front-face loading because of the window opening. Since the pressure is below that required to fail the interior partitions, the effective average pressure on the front of the building would then increase to the pressure condition on the outside of the front wall, as shown in Fig. 5. However, because of the unknowns involved in describing the pressure—time history, and since the overall building dimensions are large compared to the room size, it was assumed in this study that the variation in average load due to window openings was of minor consideration. Therefore, the average loading on a multistory building with nonfailing exterior and interior walls was calculated in the usual manner for rectangular solid blocks as shown in Fig. 5 (Refs. 2, 6, 25 and 26).

Front Exterior Wall Load. After initial reflection of the wave on the front exterior wall, both the unloading waves on the front surface and the diffraction of the blast wave around the rear surface tend to reduce the net pressure on the wall. In addition, since a condition of nonfailing interior partitions without openings was assumed, the problem is analogous to a shock wave filling a chamber of finite size. Although the actual time-history of the net front load cannot be calculated with available techniques, it would be a function of exterior building pressure and the interior room pressure buildup. Therefore, for this study, the net exterior front wall loading, as shown on the bottom of Fig. 6, was calculated by assuming that the pressure at any time was equal to the front face pressure, as determined in the previous subsection, minus the average interior room pressure, as determined in the following subsection. Since the peak pressure exerted on the exterior walls of the sides and back of the building will be lower

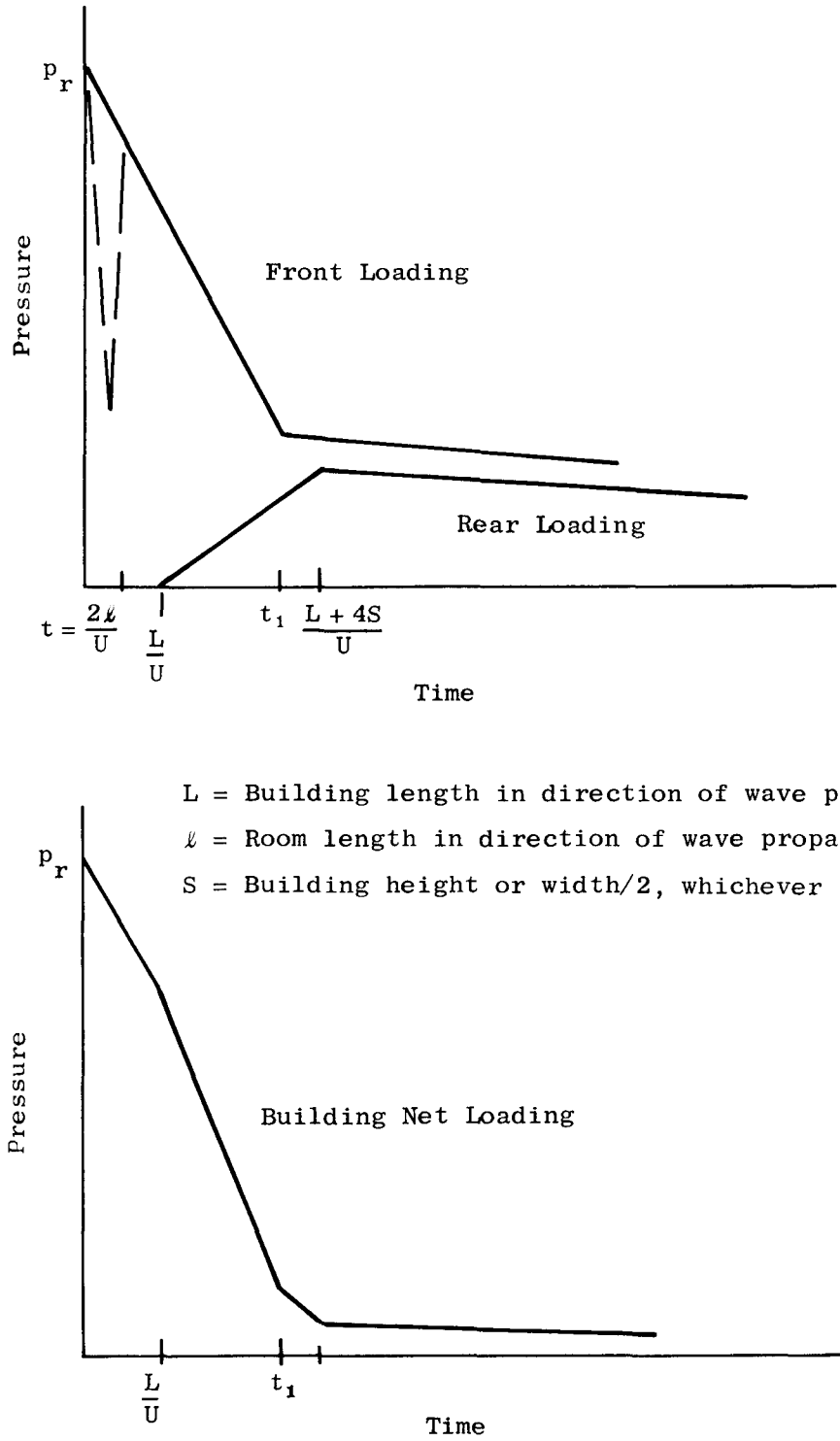

Fig. 5. Average Loading for a Multistory Structure – Exterior and Interior Walls Not Failed

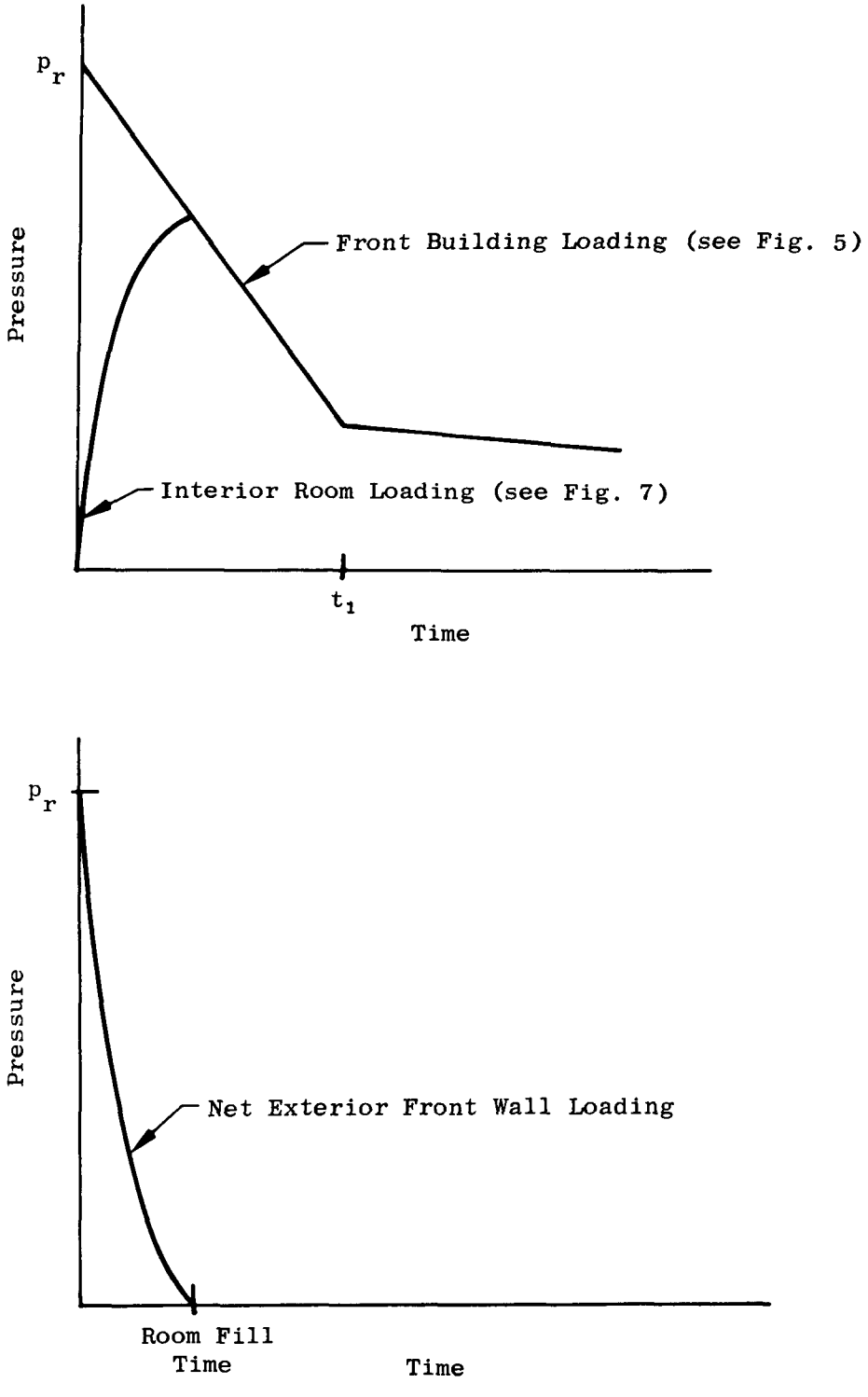

Fig. 6. Average Net Loading on Front Exterior Wall – Exterior and Interior Walls Not Failed

than that on the front wall, the loading on these walls is not critical from the standpoint of damage for the assumed conditions. If required, however, the net loading on these elements could be determined in the same manner by using the appropriate exterior pressure loading.

Interior Partition. The calculation of the loading on the rear interior partition of an outer room of the building is an exceedingly complex problem. At a time $t \simeq \ell/U$ after the wave strikes the building, the rear interior partition is subjected to the initial reflection of the wave front that entered the room. This is a weakened wave front whose reflected peak would be less than the exterior building reflected pressure. Subsequent to the initial reflected pressure jump, complex multiple reflections would occur during room filling. A number of possible methods were investigated in an attempt to determine a rational method for estimating the interior partition loading and the room filling time. For the purpose of this study, the method and experimental coefficients outlined in Ref. 28 for determining the average pressure resulting from a shock wave entering a finite chamber were utilized. The procedure is essentially an iterative process, whereby the magnitude of the interior and exterior pressures are calculated at selected time intervals. A correction, based on an experimentally established relationship, is then applied to the differential pressure existing at each time interval. The process is continued until an approximate equilibrium pressure condition exists, as shown in Fig. 7.

Case No. 2

For this case, the interior partitions fail at a lower incident overpressure level than the exterior walls. If the incident overpressure is of sufficient strength to fail the rear interior partition, both the net building and the front exterior wall loading are affected. Although many factors would influence the loading (e.g., wall failure-time) these cannot be considered in detail with current information. For instance, for a particular set of conditions, there would be an incident overpressure level where failure of the interior partition would occur in the room on the side of the building facing ground zero. Since degradation of the pressure would occur

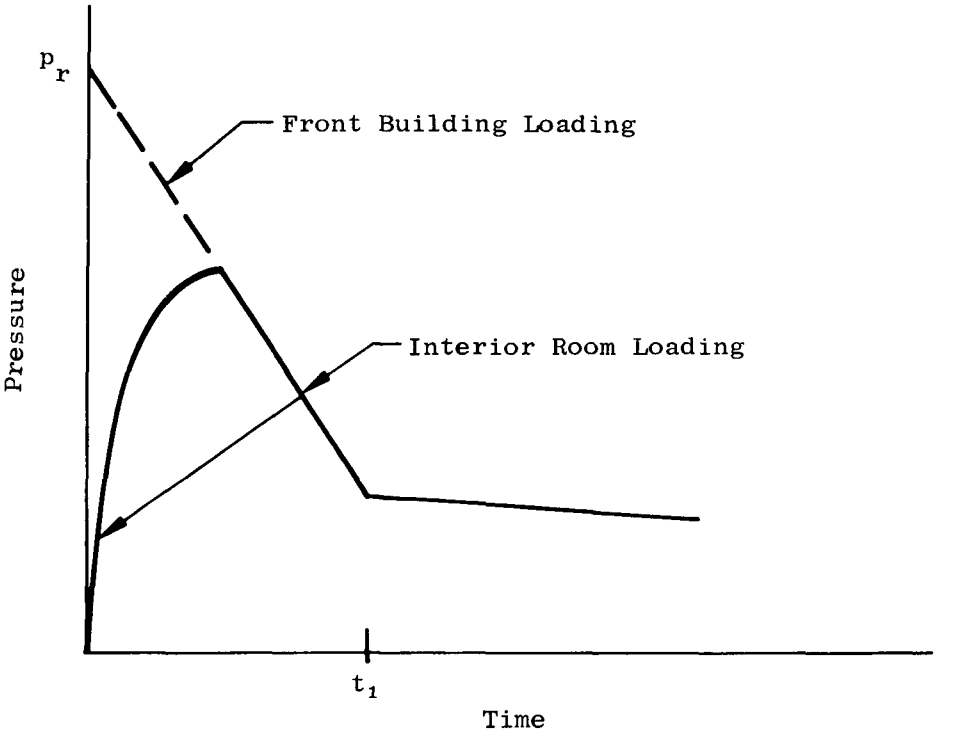

Fig. 7. Average Loading on Back Interior Partition of Outer Room – Exterior and Interior Walls Not Failed

during the failure time of the first partition, failure may not occur at successive partitions throughout the building. Although analysis of data from nuclear field tests and the atomic attacks on Japanese cities (Ref. 7) have shown this to be the case for actual structures, no rational methods exist that could be readily applied for this study. Therefore, for calculation of the loading on the building and exterior walls, it was assumed that when the pressure was of sufficient magnitude to fail the interior partition in the windward rooms, then failure would occur for all interior partitions oriented normal to the direction of wave propagation.

Building Load. Although data are lacking for the nuclear blast load–time history on large multistory buildings with various percentage of window openings, procedures adequate for design have been established from data obtained in shock tube experiments and field tests with structures of relatively small size (i.e., small compared to large multistory buildings typical of American cities). To determine the design load it is generally assumed that reflection occurs in the normal manner from the net area of the front face (Ref. 22). However, calculation of a clearing time for the reflected pulse is exceedingly difficult, since it would be associated both with the overall size and percentage of open wall area. It is obvious that structures exist whose percentages of open wall area vary over a wide spectrum. To account for this range, only two cases are considered for design calculations; i.e., either less or greater than 30 percent window opening.*

Although this arbitrary division is considered conservative for design purposes, it is obviously unrealistic for damage prediction. For the purpose of estimating damage to the type of NFSS structures considered in this study, the loading was calculated by one method for building damage determination and by another for exterior wall damage determination (see following subsection). The rationale for adopting this procedure was based on consideration of the relationship between the diffraction phase, the drag phase, and the response time for large multistory buildings.

---

* There are several methods available to determine an average or weighted distance for clearing time calculations, e.g., Refs. 22 and 25.

For the building considered as a unit, the impinging shock front reflects from the building and expands as a weakened front into the room, exerting a pressure on the back face of the exterior wall panel. Because of the failing interior panels, the interior pressure buildup cannot be calculated by the method outlined previously for the nonfailing interior partition case. In any event, the diffraction of the wave around the front wall and subsequent relatively rapid failure of the interior partitions normal to the direction of wave propagation would transfer impulsive loads into the structural framing at various times during engulfment. These loads can be considered as impulsive, since the duration of each, as well as the time interval over which they occur, is small when compared to the period of the structure. This is so,even if the pressure level is sufficient to fail the exterior walls. Subsequent to engulfment time, the building would be subjected primarily to the drag loading indicated in Fig. 8. Since the determination of the magnitude of the impulsive loadings is primarily speculative and since, intuitively, it would appear unlikely that they could be of sufficient magnitude to cause major damage to the structural framing, it was assumed for this study that the drag phase loading is more critical.

Front Exterior Wall Load. After initial reflection on the front exterior wall, both the unloading waves on the front surface and the diffraction of the blast wave around the rear surface of the wall tend to reduce the pressure differential. However, for this case the interior walls would fail, and pressure buildup within the room would not occur. (Of course, there would be a pressure buildup prior to partition failure.) To determine the net exterior wall pressure – time history, it is necessary to know the decay time of the reflected wave on the exterior surface and the pressure exerted on the rear surface by the wave front entering the windows. The degradation of the reflected pressure reservoir is a function of the building size and the percent window opening. Although experimental information for full-size structures is insufficient to obtain quantitative values for the clearing time, the data presented in Ref. 28 for shock waves entering tunnels and chambers indicate that the time is considerably longer than that calculated by the design procedures using window spacing (for the case of less than 30 percent openings). That is, for buildings with window areas less than about

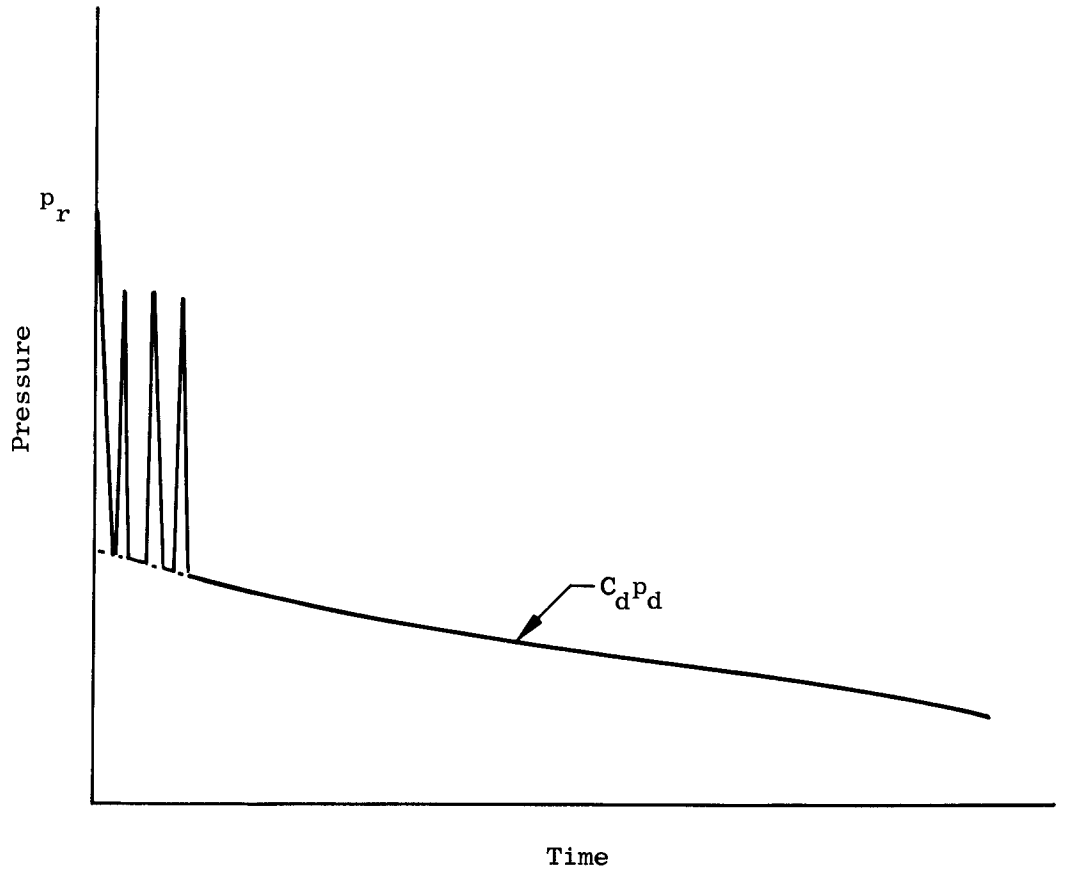

Fig. 8. Average Loading for a Multistory Panel Wall Structure — Interior Walls Failed, Exterior Walls Failed or Unfailed

50 percent, the clearing time for full-size buildings would probably be on the order of tens of milliseconds. For damage prediction for the front wall, it is only necessary to describe the load history until the time to failure. For the structures selected for this study, it is estimated that exterior wall failure will require approximately 50 to 100 msec (Ref. 29).

Based on the above discussion, the calculated failure loading for an exterior wall with windows is shown in Fig. 9. To calculate the net loading, it was assumed that the front wall loading was equal to the loading on the front face of a windowless building minus the overpressure exerted on the rear face of the front wall plus the drag component on the rear face. The initial impulse due to the time required for the rear face pressure to reach the incident overpressure level was neglected when estimating the failure load.

Case No. 3

For the final case, the exterior walls of the building fail at a lower incident overpressure level than the interior partitions. The types of exterior walls that fit this category are constructed of light-gauge metals or frangible material. Even though the time of diffraction of the blast wave around the back face of the front wall occurs rapidly, failure time for the walls in this category are very short. Therefore, the walls are peak-pressure-sensitive, and the failure pressure is calculated in the usual manner for reflected shock waves.

At incident overpressure levels greater than front-wall failure pressure, it was assumed for this study that a pressure wave equivalent to the free-field pressure prior to initial interaction enters the room and strikes the interior partition. Therefore, by consideration of the building geometry, the blast forces are calculated by the generalized loading schemes.

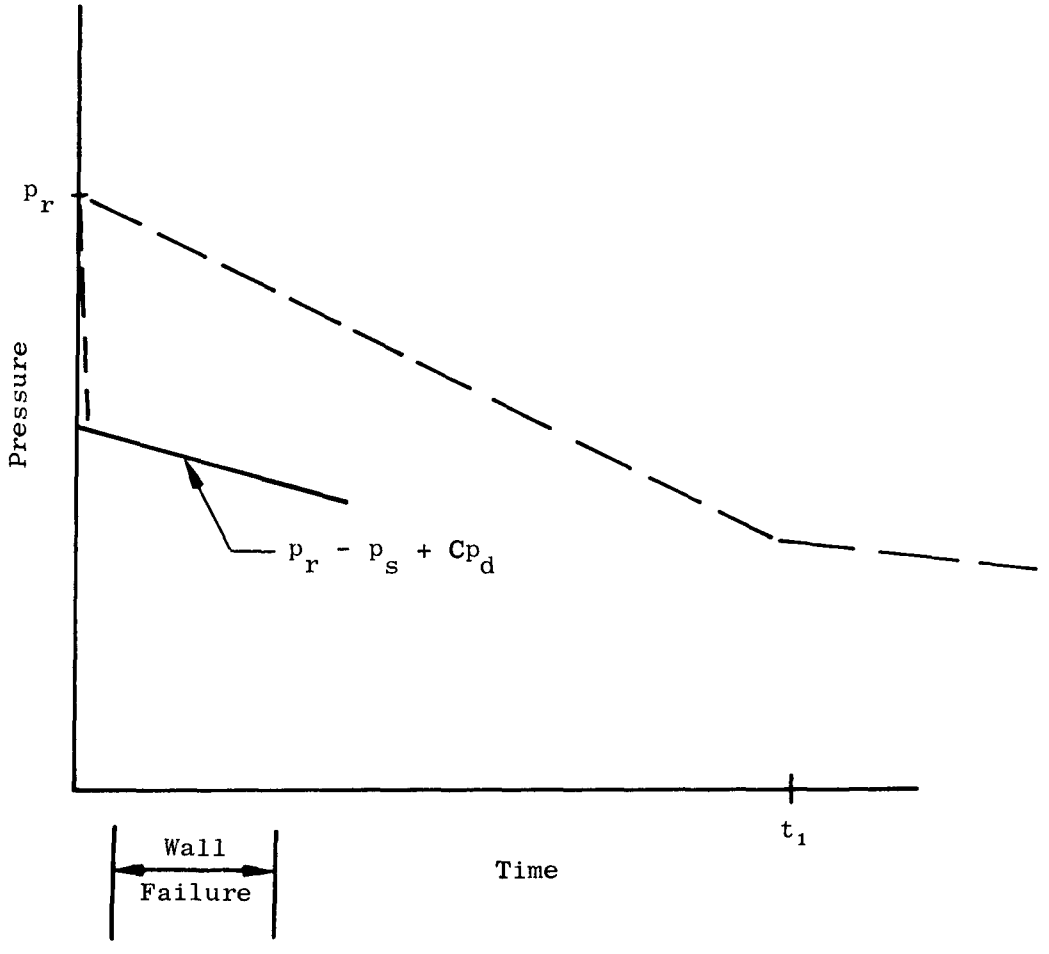

Fig. 9. Net Loading on Exterior Panel Wall — Interior Wall Failed

Section 3
APPLICATIONS OF PREDICTION METHODS

INTRODUCTION

As discussed in Section 1, the selection of the buildings for detailed damage analysis was based on the types of NFSS shelter construction described in the available information. Because of the limitations of the present program, it was only possible to perform damage predictions on three structures in the two major categories of multistory frame and load-bearing wall structures. No distinction was made between a reinforced concrete and steel frame structure for damage assessment purposes. That is, if a structure of either type was designed for the same load conditions and in accordance with the same fire code, then it was assumed that the behavior was the same. It is obvious that differences in damage would exist if such factors as the stability of various structural members, the continuity of joints, and the ultimate strength under blast loads were considered. However, such distinctions were beyond the scope of this effort.

The buildings selected for detailed investigation were two typical 12-story, steel-frame office buildings (one with brick and one with light-weight-metal exterior walls) and a 4-story, brick-load-bearing-wall building. In the following subsections, the protection level sensitivity of the three idealized structures is presented. The procedure was to first estimate the damage which occurs to each structure as a result of increasing levels of overpressure; second, to estimate the fire damage; and finally, to evaluate the change in PF of each building as a result of the estimated blast and fire damage.

It should be noted that to calculate the incident overpressure corresponding to the failure load for each structural element, it was assumed in this study that the structure was in an undamaged condition. This is essentially a process of examining the structure as though it were placed simultaneously at various ranges from a single detonation. Also, it was assumed for the air blast damage predictions that the structures were

located in the Mach region and subjected to a clean, sharp-fronted, classical wave from a 20-kt and 20-Mt weapon.* For clarity, the air blast damage predictions for each structure examined in this report are ordered in accordance with increasing incident overpressure levels up to 15 psi, the upper limit of interest for this study.

As mentioned in Section 2, the most practical way to handle fire damage in this study appeared to be on a go/no-go basis. In the examples below, the net results of a fire in each structure are presented for the following two conditions:

(1) without consideration for blast

(2) in combination with blast effects

The principal criterion for determining the significance of fire damage was the effect that damage had on the PF. That is to say, no consideration was given to the habitability of the structure.

Although the PF was supposed to be the parameter of primary concern, it became apparent in the course of the study that significant levels of damage could not always be related directly to a change in PF. For instance, it will be shown that the removal of the suspended ceiling has a negligible effect on the PF per se, but it can produce a marked reduction in the fire resistance.

The damage predictions are summarized in tables following the discussion of each structure.

DAMAGE PREDICTIONS

Structure No. 1a

Description

Structure No. 1a is a 12-story, steel frame building with full basement, measuring 300 by 55 ft in plan and 144 ft high, as shown in Figs. 10 and 11.

---

* In an actual application of the prediction methods presented herein, many of the assumptions that were made for illustrative purposes would in fact be known quantities.

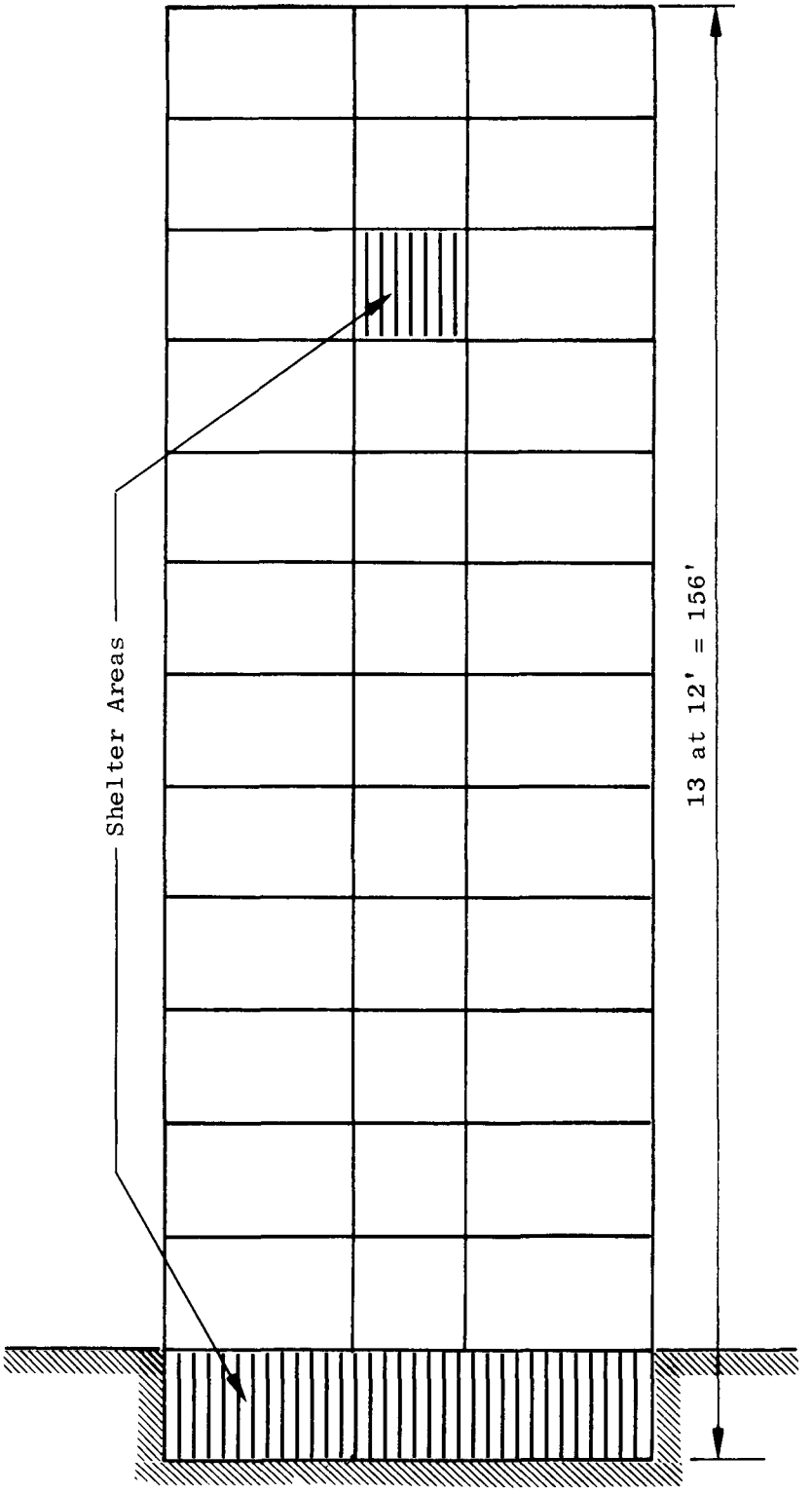

Fig. 10. Section View of Structure No. 1a

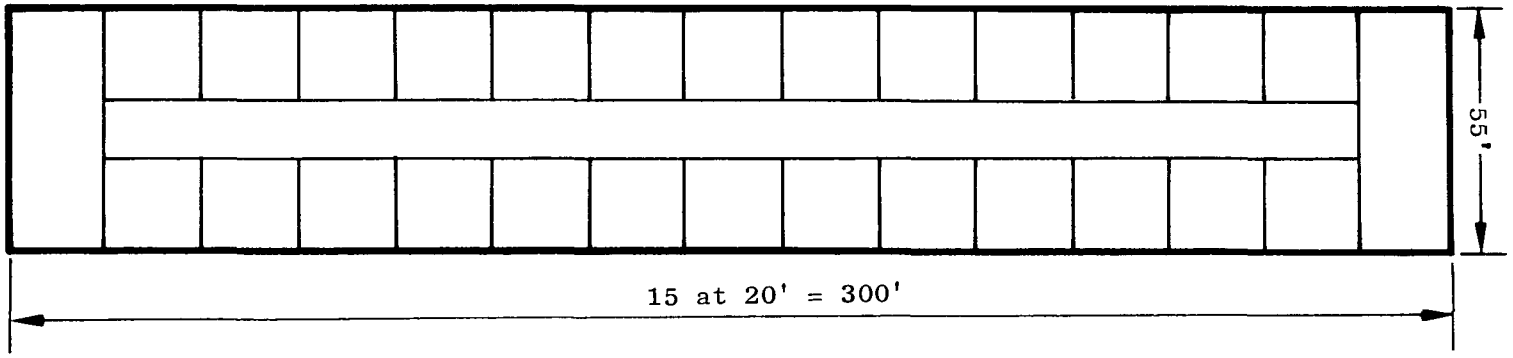

Fig. 11. Plan of Structure No. 1a

The floor is of reinforced concrete pan construction as shown on Fig. 12, and the roof is a 4-in.-thick reinforced concrete flat slab. The exterior walls are constructed of 12-in.-thick unreinforced brick, and the interior walls are 4-in.-thick masonry with 3/4-in.-thick plaster on both sides as shown on the figure. Each 20- by 20-ft room contains two 6- by 6-ft windows, which yields a window area equal to approximately 33 percent of the exterior building area. The building was assumed to be classified as fire resistive with a 3-hr classification. The fire-resistance ratings for the components were as follows:

(a) Columns - 4 hr (Design A, p. 8-120, Ref. 15)
(b) Beams & Girders - 4 hr (Design B-4, p. 8-117, Ref. 15)
(c) Interior Partitions - 4 hr
(d) Exterior walls - > 4 hr
(e) Floors - 3 hr (including suspended ceiling)

The fallout shelters were located in the basement and the central corridor on the 10th floor.

Air Blast Damage

Window. The first incident overpressure level of interest for damage prediction purposes is that which causes window failure. Assuming a thickness of 1/4 in. (requirement for a design load of 30 psf), it was determined that window failure would occur at a peak incident overpressure of less than 1/4 psi.

Suspended Ceiling. The second incident overpressure level of interest is that required to fail the suspended ceiling. The pressure for this case is determined by the method outlined for case No. 1 in Section 2 for calculating the average interior room pressure. It should be mentioned at this point that to calculate this pressure, it was assumed that the doors and interior walls would sustain the same load to failure and that the doors were closed. Since failure information was unavailable for suspended ceilings, it was necessary to estimate the failure loading from field tests on interior partitions constructed of 2-in. thick plaster on metal lath, which failed at an incident overpressure level of 4.2 psi (Ref. 30). Since the interior pressure for the test conditions was unknown, a calculation by the chamber-filling method outlined in Section 2, using predicted exterior wall pressures,

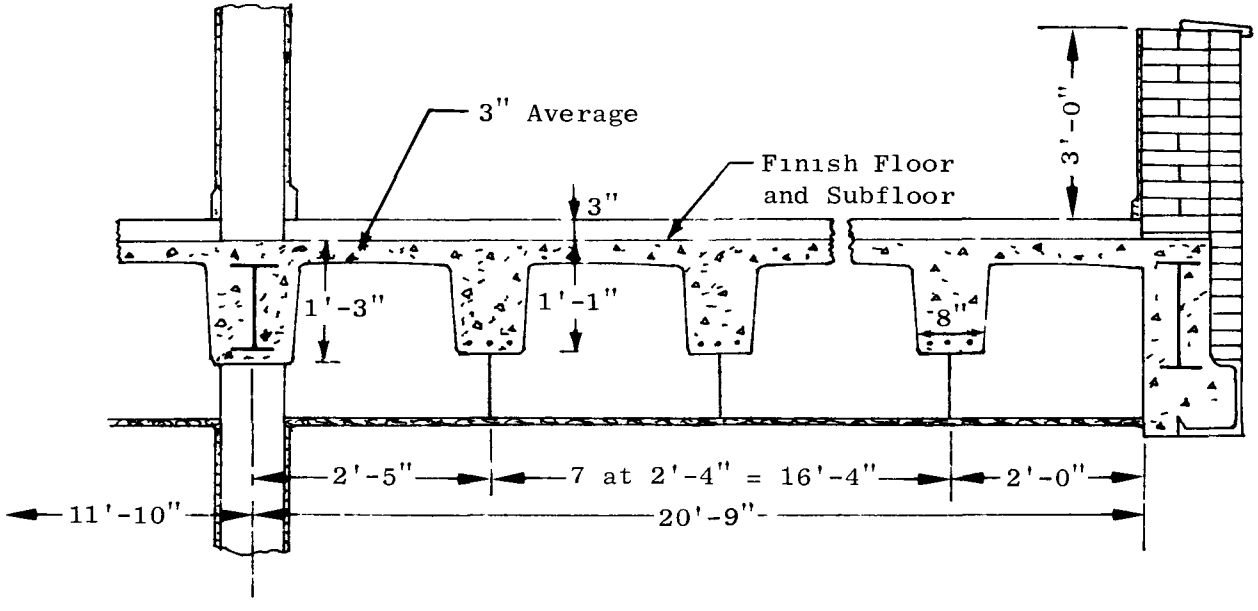

Fig. 12. Typical Floor Section of Structure No. 1a

indicated a peak average pressure of approximately 6 psi. Because of the lack of better information for ceilings, it was assumed that the 1-in.-thick metal-lath suspended ceiling for Structure No. 1a would fail at approximately 3 psi peak interior pressure. The general method of calculation for the average interior room pressure is shown in Appendix B. From similar calculations, it was determined that a peak incident overpressure of 1-1/2 to 2 psi would result in failure of the suspended ceiling in the rooms facing ground zero, for both the 20-kt and 20-Mt weapon yields. Although it is obvious that the ceilings in the downstream-facing rooms would require a higher incident overpressure to cause failure, that case is not considered because of the interior partition failure, as noted in the next section.

Interior Partition. The third incident overpressure level of interest is that which results in failure of the interior 4-in.-thick masonry walls oriented normal to the direction of wave propagation, i.e., the walls at the back of the room, which separate the room from the hall shelter space. The method outlined for Case No. 1 in Section 2 was used for determining the average interior pressure resulting from the large reflected pressure reservoir on the exterior of the front wall. The failure pressure for the 4-in.-thick masonry wall units was obtained from the nuclear test results (Ref. 29), and was estimated as 4 psi for Structure No. 1a. Therefore, from the sample calculations shown in Appendix B, it can be estimated that the peak incident overpressure which would fail the interior walls in the back of the rooms was between 2 and 2-1/2 psi from either the 20-kt or 20-Mt yield. Although there are no methods available to estimate the failure of interior walls located downstream from the first wall, it is obvious that failure of all walls, at normal incidence, would occur over a range of overpressure rather than a single pressure level. It was estimated, however, for Structure No. 1a that the failure-pressure range would be small. First, increasing the room volume by adding the hall volume would not appreciably change the average interior room pressure. Second, because of the relatively long diffraction time on the front face of a large structure, the reflected pressure would decay only a small amount during the time required for failure of the first interior partition. For this case, the reflected pressure reservoir would maintain sufficient differential pressure during filling of the

additional volume of the hall to fail the next partition with, at most, only a modest increase of side-on overpressure. Therefore, it seems reasonable to estimate that all interior partitions, oriented at normal incidence, would fail at a peak incident overpressure level between 2 and 2-1/2 psi for both weapon yields.

Building (First Critical Load). Since it is possible that the building could be subjected to a more severe loading prior to the failure of some component than after failure of the component, it is necessary to investigate the loading for critical conditions. As noted for Case No. 1 in Section 2, the net building loading can be calculated by the conventional techniques for overpressure levels below those resulting in failure of the interior or exterior walls. Such loading was calculated for Structure No. 1a for a peak incident overpressure of 2 psi, which is less than the estimated incident overpressure corresponding to failure of the interior partitions. The results are shown in Fig. 13.

It is obvious that the drag loading subsequent to diffraction would be insufficient to cause structural distress, since it is of the same order of magnitude as a 30-psf design wind loading. The structure would, however, respond to the impulse delivered during engulfment. Although a detailed calculation for the dynamic response of a multistory building was beyond the scope of this program, a first approximation was obtained by using the method outlined in Ref. 31. Based on assumed values for the building's natural period, ductility factor, and load duration, the ratio of the allowable dynamic load to the static yield resistance was greater than two. Although the static resistance of the structure was not known, it was estimated from the design wind load stresses and other related evidence (Refs. 7, 23, 24, 32), that the 2-psi peak incident overpressure level would not produce a critical loading on Structure No. 1a.

Roof and Floor Slab. As incident overpressure levels in excess of the interior partition failure pressure are considered, it is not obvious which structural component will be the next to fail. The primary difficulty in determining the next critical overpressure level is due to the paucity of experimental

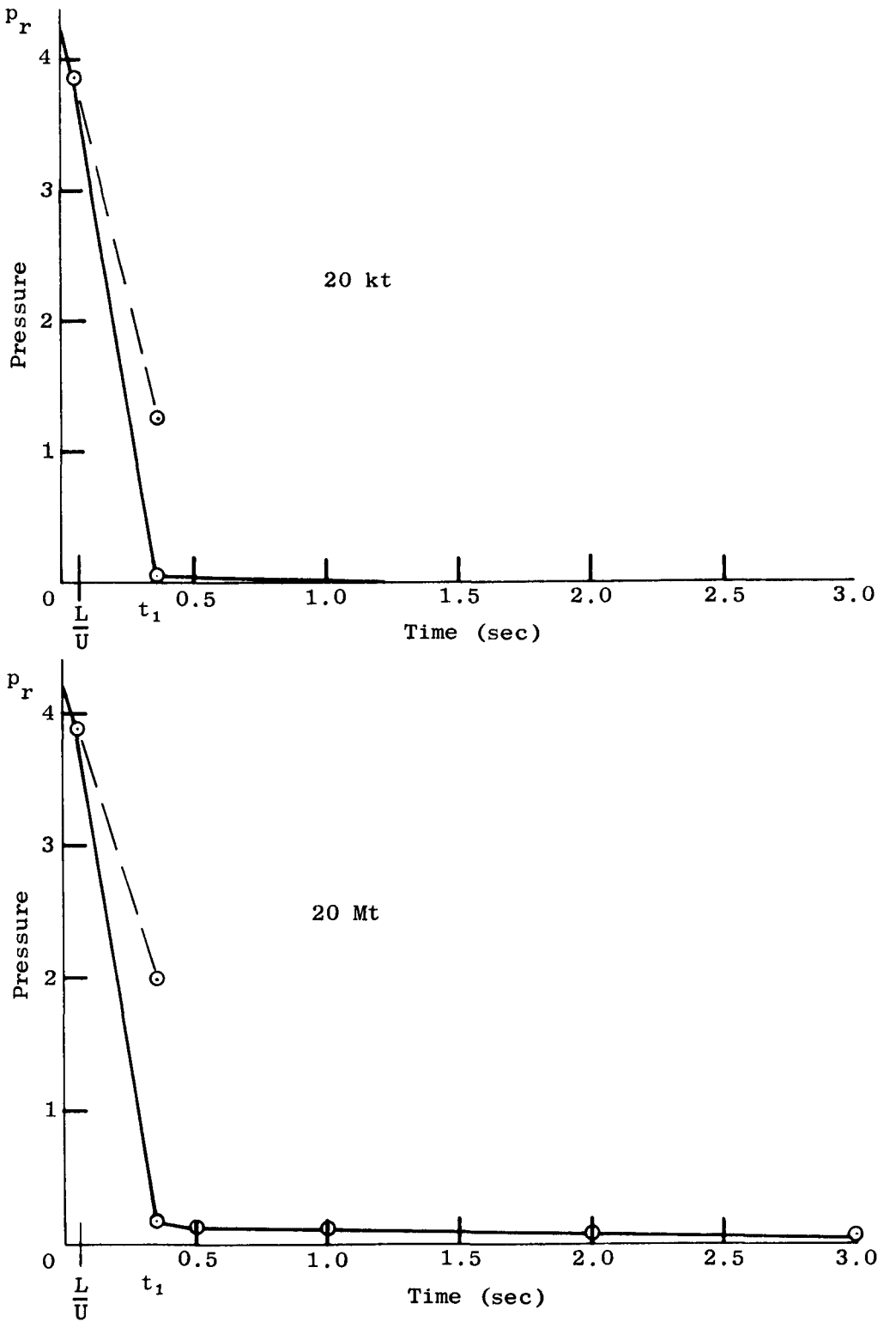

Fig. 13. Net Building Load Prior to Failure of Interior Partitions or Exterior Walls, Structure No. 1a

information for the behavior of roof and floor slabs typical of multistory buildings located in the Mach region. Except for the basement ceiling slab, the floor slabs throughout the idealized structure would be loaded approximately simultaneously on the top and bottom surface. Therefore, it can be concluded that, for the blast environments considered in this study, the floor slabs will not receive a critical failure load. The roof slab and the ground-floor slab (basement roof) should be considered separately.

For the 4-in.-thick reinforced concrete roof of Structure No. 1a, a differential pressure is exerted on the slab for a short period during the diffraction phase. This differential pressure is a function of the overpressure on the roof and the average room pressure. It is probable that during the load cycle, the interior pressure would increase from zero, at $t = 0$, to a value, at some later time, which is in excess of the exterior pressure on the roof (as calculated by conventional techniques). In any event, since the differential pressure would not be large relative to the strength of the slab, such calculations were not warranted for this structure.* It can be concluded, for the maximum free-field overpressure level of 15 psi in the Mach region, that failure of the roof slab would probably not occur. This conclusion is supported by the test results from a similar roof slab subjected to a peak incident overpressure of 12 psi in the regular reflection region (Ref. 29).

The ground-floor slab for Structure No. 1a was identical to the floor slab shown in Fig. 12. Because of insufficient information concerning the loading and response of slabs in the configuration for the selected building, it was necessary to utilize the loading methods previously discussed, together with conventional ultimate-strength concepts for reinforced concrete, to estimate a failure loading.

For this building, the ground-floor slab was found to fail at an overpressure level greater than the interior partition failure pressure but less than exterior wall failure pressure. The net loading on the slab is a function

* Both the uncertainty and the legitimacy of predicting roof failure is discussed in Ref. 29. Even when extrapolating test results for similar roof construction, such factors as different building geometry, as well as unknowns for both the detailed load–time history and the roof response, preclude accurate damage predictions. However, for the type of NFSS structures of primary interest, the ability to accurately predict roof failure would not generally be crucial for shelter evaluations.

of the differential pressure on the top and bottom surfaces. The pressure on the top of the slab is a function of the exterior reflected pressure, the percentage of window opening, and the volume of the interior of the first floor; this is analogous to the chamber-filling problem. The pressure on the botton of the slab is a function of the pressure within the first-floor volume, the area of the openings into basement, and the basement volume; this is also a chamber-filling problem. Because of the unknowns involved in determining the actual differential pressure—time on the slab for such a complex system, a simplification of the calculation was warranted. Therefore, for this study, it was assumed that the loading applied to the top slab surface was equal to the free-field overpressure and that the average basement pressure could be determined by the chamber-filling method discussed for Case No. 1 in Section 2.

To determine the failure load for the floor slab, conventional techniques for calculating the ultimate strength of reinforced concrete members (Ref. 33) were utilized together with the simplified dynamic analysis presented in Refs. 7 and 31. Although both techniques are well established in structural engineering, their applicability as used herein could not be verified for predicting damage for the wide variety of loadings and structural configurations of interest. However, it was possible to compare the method with the test results presented in Ref. 34 for dynamically loaded 15-ft-long reinforced concrete beams. For this case, the calculated failure loading was found to be within 15 percent of the experimental values.

From these calculations it was determined that the ground-floor slab for Structure No. 1a would fail at a peak incident overpressure level of about 5 psi for a weapon yield of 20 kt and 4 psi for 20 Mt.*

Exterior Wall. As discussed for Case No. 2 in Section 2, the loading on the building is significantly affected by the condition of the exterior walls (i.e., failed or unfailed). For a given peak side-on overpressure, above the interior-partition failure pressure, both the diffraction and drag

* It should be noted that floor slab failure at these relatively low overpressures is due to the lack of reserve strength for this type of construction. Field tests indicate that for other types of construction, the failure load could be much greater (Ref. 29).

phase loadings on the structure are a maximum for an unfailed-exterior-wall condition.* However, since it is not obvious whether the structure or the walls fail at the lower incident overpressure, the approach used in this study was to first determine the incident overpressure at which failure of the exterior wall would be expected and then to examine the structure's behavior at some lesser overpressure level, at which the walls would be intact. As noted in the subsequent subsection, it may also be necessary to examine the structure's behavior at overpressure levels in excess of wall failure pressure.

The incident overpressure level at which exterior-wall failure occurs for Structure No. 1a was calculated by the method outlined for Case No. 2 in Section 2. The failure criterion for the 12-in.-thick unreinforced brick curtain walls was obtained from the data presented in Refs. 6, 24, 29, and 30. From this information it was estimated that the wall for the assumed building would fail at a net loading of 17 to 20 psi.** It was determined that a pressure of this magnitude would be imposed on the exterior wall of Structure No. 1a by a peak incident overpressure level of approximately 11 psi. As indicated by the heavy dashed line in Fig. 14, the diffraction of the wave front around the rear of the front wall reduces the net pressure on the wall. Since the impulse associated with this diffraction was small, it was neglected for failure determination. Consequently, it was found that a wall failure pressure of 19 psi would result from a peak incident overpressure of 11 psi. Since the wall failure would probably occur within approximately 50 to 100 msec, it can be seen from the figure that the incident overpressure corresponding to exterior-wall failure would be the same for both 20-kt and 20-Mt weapon yields, since the net wall loading is essentially identical for both yields during the clearing time.

Building (Second Critical Load). In the previous subsection the behavior of the building was examined for a possible critical load condition at pressure

---

* Of course, this is not to imply that there is no critical building loading condition at incident overpressure levels in excess of the exterior-wall failure loading.

** For the windowless test structure reported in Ref. 30, this loading was imposed by a peak incident overpressure of 7 to 8 psi.

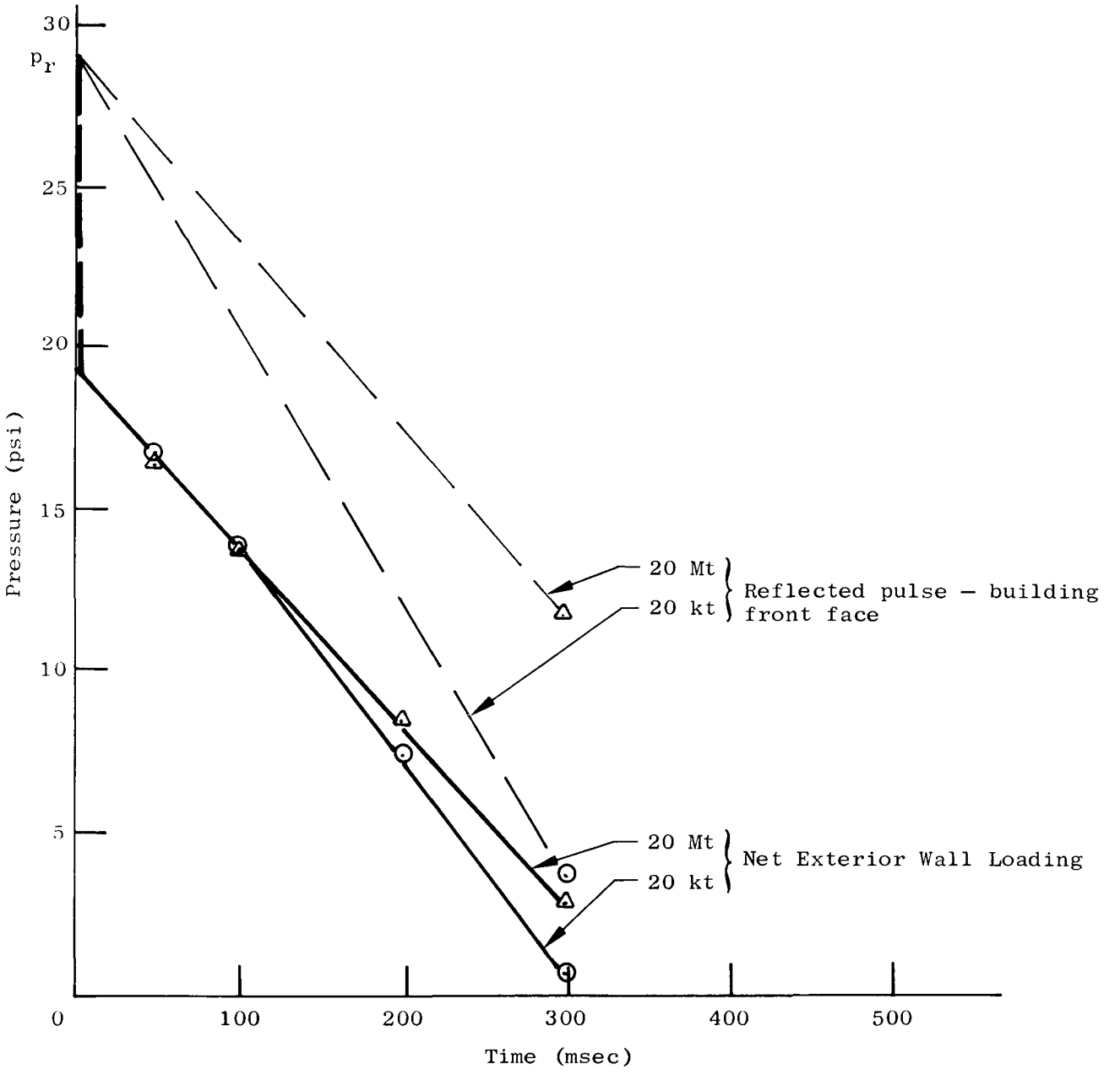

Fig. 14. Net Front Exterior Wall Load for p_{so} = 11 psi, With Interior Partitions Failed, Structure No. 1a

levels less than the failure pressure for the interior partition. For such pressure levels, it was concluded that a critical loading would not be imposed on Structure No. 1a prior to interior partition failure. It is also possible that the structure could be subjected to a critical loading at some pressure level between the interior- and exterior-wall failure pressures. Since it was determined that the exterior brick walls failed at a peak incident overpressure of about 11 psi for either a 20-kt or a 20-Mt yield, the structure behavior should be examined for a lower pressure level, e.g., 10 psi.

As noted in Section 2, during the diffraction phase impulsive loads would be transmitted to the structural framing by the differential pressure on the exterior walls and the interior partitions during failure. Because of the unknowns involved in predicting damage to typical American multistory buildings subjected to nuclear blast, the effect of the impulsive loads were neglected in this initial study. Although the impulses could contribute to the damage, it was felt that the drag phase loadings would be a more important factor for the gross building response* at the overpressure levels of interest.

Subsequent to diffraction, the loading on the building is a function of the wall area projected on a vertical plane (including all remaining members) times the dynamic pressure, times some average drag coefficient. For a peak side-on overpressure of 10 psi, the peak dynamic pressure is equal to 2.0 psi. The dynamic pressure at various times was calculated by standard techniques (Ref. 6) for both 20-kt and 20-Mt yields. It should be noted that for the 20-kt weapon, the dynamic pressure has decreased to 0.4 psi at a time of 0.25 sec and is insignificant at 0.5 sec; however, for the 20-Mt yield, the pressure is 1 psi at 1 sec and 0.5 psi at 2 sec. Since the natural period of multistory buildings is generally in the range of 0.5 to 1.5 sec (Ref. 35), it is probable that Structure No. 1a is capable of responding during the early period of high wind forces for the megaton case but not for the kiloton. To estimate whether the short-duration drag loading from the 20-kt yield is a

---

* That is, gross structure reponse such as overturning, foundation failure or motion, and general column failure.

critical building load would require a more sophisticated analysis than was possible under the current effort (see Refs. 36 and 37).* However, based on limited field test data (Ref. 38) and on the data from the nuclear attacks on Japanese cities (Refs. 23 and 24), it is most probable that a gross failure of the structure would not occur for the 20-kt weapon.

Although a dynamic analysis of the structure would be required to better predict gross building damage for any weapon yield, it is possible to make a more meaningful estimate (when supporting analyses are unavailable) for a blast wave whose duration is long relative to the natural period of the building. For this case, it was felt sufficient to compare the design wind loading with the blast-induced drag loading. In this manner, the basis for an estimate of building overturning, foundation distress, or column failure under dynamic conditions could be related to conventional static analysis.

If the design wind load for Structure No. 1a is assumed to be 20 psf,** then it can be shown that an average equivalent lateral unit load for the transient drag phase (for a 20-Mt weapon) varies from an initial value of 30 times the design wind load to a value 8 times as large at 2 sec. That is, considering only the drag forces, the building is subjected to a wind loading (due to the blast wave) which averages greater than 15 times the design wind loading for a period of time exceeding several natural periods of the structure. This indicates that the lateral shear at the basement level and the overturning moment for the structure could be more than 15 times the static design conditions. For the assumed structure, it is estimated that this overturning moment is approximately 1-1/2 times the resisting moment calculated using the building dead plus live load. Although such a load would be catastrophic if applied statically, it is not known

---

* It should be noted, however, that any dynamic analysis based on elasto-plastic response and developed for the design of multistory buildings may not necessarily be adequate for predicting the failure mode for large multistory buildings.

** The design and analysis for a similar structure are presented in Ref. 39.

whether a duration of a few seconds is sufficient to cause similar damage. However, it is entirely possible that a massive column failure or foundation displacement could occur along the downstream column line.

If it is assumed that the structure survives an incident overpressure level which results in exterior wall failure, it is interesting to calculate a drag loading on the remaining structural components (e.g., floor slabs and columns) that is equivalent to the 10-psi loading discussed previously. That is, what overpressure level, above exterior-wall failure pressure, would be required to produce a loading equivalent to the second critical loading? Calculations indicate that such a loading would be imposed on the structural framing by a 22-psi peak incident overpressure level from a 20-Mt weapon yield.

Fire Damage

In order to apply the fire damage prediction model to the selected structures, certain characteristics had to be assumed with regard to the contents of the buildings. It was assumed that the occupancy of Structure No. 1a was general office use, the unit fire load was equal to 15 psf,* and the surface area of combustibles per 20-by 20-ft office was equal to 300 sq ft.

Based on these assumptions, the burning rate for a fuel-surface-controlled fire, R_s, was calculated to be 27 lb/min. On the other hand, the burning rate for a ventilation-controlled fire, R_v, was calculated to be 266 lb/min. Consequently, the burning rate is surface-controlled since the lesser of the two values controls.**

Based on a burning rate of 27 lb/min, the duration of the peak fire was found to equal 110 min. As a result, due to the high fire resistance (a minimum of 3 hr), the only anticipated fire damage was window breakage and penetration of the doors. Penetration of the doors would not lead to further

---

* Although this fire load is higher than it probably would be for office occupancy, it was chosen to illustrate a subsequent point.

** It was anticipated that most all of the fires in blast-damaged buildings will be surface-controlled; however, this is not necessarily so for the structures located beyond the area of blast damage.

fire spread since there is nothing combustible in the corridors.

Fire and Blast Damage Combined

There are three ways in which the blast could affect the fire damage predictions:

(1) changing the burning rate

(2) changing the fire load

(3) reducing the fire resistance

The first one can be eliminated for this structure, since the only possible change would be due to increasing R_v, and it was already determined that R_s controls. Since the structure is constructed of noncombustible materials, the only way the fire load can be altered would be by removal of the contents by the air blast.

There are a number of ways in which the fire resistance of the components could be changed. The first significant level of blast damage affecting the fire resistance is destruction of the ceilings, i.e., at 1-1/2 to 2 psi incident overpressure. It was difficult to ascertain exactly what this effect would be; however, Ref. 15 attributes a rating of 1 hr and 45 min to a ceiling protecting a similar floor slab. In addition, Ref. 40 states: "...typically the presence or absence of the drop ceiling could make a difference of 1-1/2 to 2-1/2 hr in the fire resistance." Consequently, it was assumed that the suspended ceiling accounted for half of the 3-hr rated resistance for the floors. Comparing the resulting fire resistance of 1-1/2 hr with the anticipated duration of peak fire of 110 min, it is apparent that the floors could be damaged by the fire. This case illustrates a condition wherein although the fire alone would not induce failure and the blast damage itself would not be critical, the combination of the two might be.

The next significant blast damage to the fire resistance of Structure No. 1a occurs at a pressure level sufficient to damage the fire protection to columns. With plaster on metal lath fire protection for the columns, it appeared as though gross deformations of the columns would be required before

the fire protection would be damaged significantly. If the structure could sustain gross deflections of this magnitude without collapsing, then consideration would have to be given to the reduced fire protection for the columns.

Post-Damage Protection Factors

In the previous sections, the damage to Structure No. 1a was examined through a range of overpressure up to 15 psi, the critical failure pressure for each element was calculated, and the fire damage was estimated. In this subsection, the change in PF for the damaged structure is presented. As mentioned in Section 1, the change in PF was the criterion adopted in this study to demonstrate the sensitivity of the structures to the effects of nuclear weapons. However, it is well to keep in mind that the use of the PF as a basis for comparison has certain shortcomings. For instance, as the overpressure level is increased, the resulting change in PF does not necessarily indicate the extent of the damage to the structure or the shelterees. In fact for certain situations, severe damage to the structural elements can occur without appreciably affecting the PF.

In calculating the PF, it was assumed that the building was isolated and exposed to an infinite field of view, and the contribution from entranceways or stair wells was neglected. In addition, when the windows were the only damaged component, the ingress was distributed uniformly in the areas surrounding the interior corridor and was equal to 10 percent of the exterior mass loading. When the core partitions were destroyed, the ingress was spread uniformly over the entire floor. Again, the assumed interior density was 10 percent of the exterior (naturally this would amount to a greater quantity of ingress than in the previous case). When the PF dropped below 20, the shelter was considered to be inadequate.

As mentioned, there were two shelter locations in Structure No. 1a, the entire basement and the interior corridor on the 10th floor. The latter was selected as the optimum aboveground shelter area by maximizing the height above the contaminated plane while keeping the overhead mass thickness sufficient to reduce the roof contribution to a negligible amount.

For the undamaged structure, the initial PF was calculated to be 350 for the 10th-floor shelter and greater than 3000 for the basement shelter. As noted from the summary in Table 3, the initial air blast damage that causes a degradation of the protection afforded by the shelter is approximately 1/4 psi, i.e., when the windows are shattered. The primary effect on the shelter area is the subsequent ingress of fallout radiation, which decreases the PF to 85 and 1500, for the 10th-floor and basement shelters, respectively. At a peak incident overpressure of 1-1/2 to 2 psi, the suspended ceilings were destroyed; and although there was no significant direct effect on the PF, it has been shown in the previous subsection that this can have a serious effect on the fire resistance. The next blast level of interest is 2 to 2-1/2 psi, at which failure of the interior partitions occurs. Although ingress would degrade the PF for this condition, both shelters would provide adequate fallout protection for the postattack environment. At an incident overpressure level of 4 psi for the 20-Mt yield and 5 psi for the 20-kt, the ground-floor slab fails and the basement area ceases to function as an adequate shelter area. The aboveground shelter area provides a PF of 30 until an incident overpressure of about 11 psi is reached and failure of the exterior walls occurs.

In addition to the affect of blast damage on the protection factor, there can also be an interaction between fire and PF. For many realistic structures, fire could consume combustible barriers* intended for attenuating the nuclear radiation; however, in this example, the structure was almost totally noncombustible. Nonetheless, for ranges beyond the initial blast damage, fire did cause a reduction in the PF for Structure No. 1a by shattering the windows and permitting fallout to enter the outer offices. More important, though, is the affect that fire can have on the stability of a structure.

---

* In addition, consumption of combustible contents as a result of fire could reduce the PF significantly. However, in making PF calculations, the contents of the building are usually neglected.

Table 3

BLAST DAMAGE VERSUS PF
STRUCTURE NO. 1a

Incident Overpressure (psi)			Resulting PF	
20 kt	20 Mt	Failed Element	Basement Shelter	10th-Floor Shelter
<1/4	<1/4	None	>3,000	350
~1/4	~1/4	Window	1,500	85
1-1/2 to 2	1-1/2 to 2	Suspended ceiling	1,500	85
2 to 2-1/2	2 to 2-1/2	Interior partition	550	30
5	4	Ground-floor slab	< 20	<30
	10	Possible building collapse	–	–
11	11	Exterior wall	<20	<20
>15		Building collapse	–	–

Structure No. 1b

Description

Structure No. 1b is similar to Structure No. 1a except that the exterior walls were assumed to be constructed of lightweight panels instead of brick panels. The detail for a typical lightweight metal panel is shown in Appendix A, Fig. A-5.

Air Blast Damage

Window. The discussion of window damage presented for Structure No. 1a also applies to this structure.

Exterior Wall. The substitution of a lightweight metal exterior wall for the 12-in.-thick brick wall has a profound effect on both the loading and response of the structure. Although definitive damage information is lacking for the specific wall panel selected, experimental data for similar walls indicate that the failure pressure would be approximately 3 to 4 psi. Since tests also show that the time to failure for such lightweight panels is less than 20 msec, (e.g., Ref. 29), the exterior walls for Structure No. 1b would be primarily peak-pressure-sensitive. This means that when the failure pressure is reached, failure will be very rapid and the net loading on the wall will, therefore, not be appreciably affected by the wave front entering the window and diffracting around the back face. The failure pressure can be calculated in the usual manner for a normal reflecting wave; and for the selected panel, failure could be expected to occur at a peak side-on overpressure of about 1-1/2 to 2 psi.

Suspended Ceiling and Interior Partition. As noted for Structure No. 1a, it was estimated that the suspended ceiling would fail at an incident overpressure of 1-1/2 to 2 psi and the interior partitions at approximately 2 to 2-1/2 psi. Obviously, this is in the same pressure range as that determined for the failure of the lightweight exterior panel walls for Structure No. 1b. This complicates the problem of establishing a rational basis for estimating the sequence of failure for the various components, since the small difference in the calculated failure loading is probably less than the error inherent in the prediction techniques.

It is probable, however, that the suspended ceiling would fail at a slightly lower overpressure level than the exterior panel walls. To estimate whether the interior or exterior walls would fail at the lower incident overpressure, it is convenient to consider in more detail the chamber-filling method for determining the average interior room pressure described in Section 2. In that method, an experimental relationship was established between the exterior pressure reservoir and the time required (fill-time) for the average pressure in the chamber to build up to the exterior pressure value. An important factor in the relationship is the ratio of the window opening and the chamber volume. It is apparent that a rapidly failing* exterior wall panel would drastically decrease the fill-time. Therefore, the interior pressure would approximate the peak exterior reflected pressure. Since the failure pressure is approximately the same for both the lightweight exterior walls and the interior masonry partition of Structure No. 1a, it is estimated that failure of both walls would occur at an incident overpressure of about 2 psi.

Roof and Floor Slabs. The discussion of the roof and floor slabs presented for Structure No. 1a also is applicable for Structure No. 1b. The behavior of roof and floor slabs would not be appreciably affected by the lightweight exterior-wall panel construction; and for the overpressure levels of interest in this study, failure of the slabs (excluding the ground-floor slab) would not be anticipated. Although failure of the exterior wall panels would affect the rise-time and the magnitude of the loading on the ground-floor slab, it would not significantly affect the overpressure level at which failure occurs. Therefor, for Structure No. 1b, the slab failure would be predicted at an incident overpressure of about 4 psi for a yield of 20 Mt and 5 psi for 20 kt.

Building. As discussed previously, failure of both the exterior walls and interior partitions for Structure No. 1b is expected to occur at an incident overpressure around 2 psi. Based on the information presented for Structure No. 1a, a critical failure load for the structure would not be anticipated at this pressure level for either the kiloton or megaton weapon yields. Since the next critical loading was determined to be above the 15-psi overpressure

---

* That is, the panel failure time is much less than the chamber fill-time calculated for a similar situation but with nonfailing walls.

level (i.e., ~ 22 psi), it is concluded that a gross failure of Structure No. 1b would not occur for the pressure levels of interest.

Fire Damage

For Structure No. 1b the exterior walls were lightweight prefabricated glass-and-aluminum curtain walls, instead of 12-in. brick panels. This difference results in a significant decrease in the fire rating for the exterior walls compared to Structure No. 1a. Because of the low melting point for aluminum, these walls would have, essentially, a zero fire rating. Consequently, if ignitions are assumed for this structure, the exterior walls would have to be eliminated from consideration. However, the remainder of the structure, i.e., frame, floors, and interior partitions, would remain in place, since the fire ratings of these components were greater than the duration of peak fire as calculated for Structure No. 1a.

Fire and Blast Damage Combined

The combination of fire and blast effects on Structure No. 1b would be virtually the same as it was for Structure No. 1a. The first important effect was again found to be a reduction of the fire rating for the floors when the incident overpressure was sufficient to destroy the suspended ceilings at 1-1/2 to 2 psi. The other blast damage that could conceivably alter the fire rating was the exposure of the steel frame by removal of the fireproofing materials as a result of excessive deflections of the frame. Since damage sufficient to produce such large deflections was not predicted for Structure No. 1b at overpressures less than 15 psi, it was estimated that gross damage to the plaster-on-lath fire protection for the columns would not occur. As a result, it was concluded that the only combined effect of fire and blast was the destruction of the suspended ceiling.

Post-Damage Protection Factors

As in the previous example, there were two shelter locations to consider in Structure No. 1b, i.e., the basement and the 10th-floor corridor. Because of the lightweight exterior walls, the initial PF for each of the two shelters was less than it was for Structure No. 1a. For Structure No. 1b, the initial PF was 130 for the 10th-floor shelter and 1600 for the basement shelter.

As can be seen from Tables 3 and 4, the results of the combined effects on Structure No. 1b are qualitatively similar to those for Structure No. 1a, except for a few differences that warrant discussion. First, the initial PF is markedly less for the building with low-mass curtain walls, especially for the 10th-floor shelter, where the initial PF is approximately one-third that for Structure No. 1a. This difference is most pronounced initially and less so when fallout ingress occurs as a result of window breakage, at about 1/4 psi. Second, even though the exterior walls for Structure No. 1b were destroyed at less than 2 psi, there was no significant reduction in PF, since this type of curtain wall has a low mass thickness (~10 psf). Nonetheless, there would probably be a greater amount of ingress for Structure No. 1b at an overpressure just sufficient to fail the lightweight curtain walls. Finally, it can be seen by referring to Tables 3 and 4 that the interior partitions fail at a slightly lower overpressure, and the resulting PF was slightly less for both shelters in Structure No. 1b than it was for Structure No. 1a. In both cases, the most devastating effect on the basement shelter occurred when the ground-floor slab was destroyed at a peak incident overpressure of 4 psi for the 20-Mt yield and 5 psi for the 20-kt yield; this pressure was essentially unaltered by changing the exterior-wall construction.

Structure No. 2

Description

Structure No. 2 is a 4-story, typical, masonry-load-bearing-wall apartment building. The plan dimensions are 40 ft wide by 70 ft long, as shown in Fig. 15. The 12-in.-thick exterior brick walls have 20 percent window area and are supported on reinforced concrete basement walls. The floors and roof are of wood joist construction similar to that shown in Appendix A, Fig. A-14. The interior partitions are typical lath and plaster supported on wood studs.

For the purpose of this study, it was assumed that the structure is bounded on both sides by adjacent structures of comparable height. For Structure No. 2 the fallout shelter occupied the entire basement.

Table 4

BLAST DAMAGE VERSUS PF
STRUCTURE NO. 1b

Incident Overpressure (psi)			Resulting PF	
20 kt	20 Mt	Failed Element	Basement Shelter	10th-Floor Shelter
< 1/4	< 1/4	None	1,600	130
~1/4	~1/4	Window	1,000	60
1-1/2 to 2	1-1/2 to 2	Suspended ceiling	~1,000	~60
< 2	< 2	Exterior wall	~1,000	54
2	2	Interior partition	480	< 20
5	4	Ground-floor slab	< 20	< 20
>15	>15	Building collapse	–	–

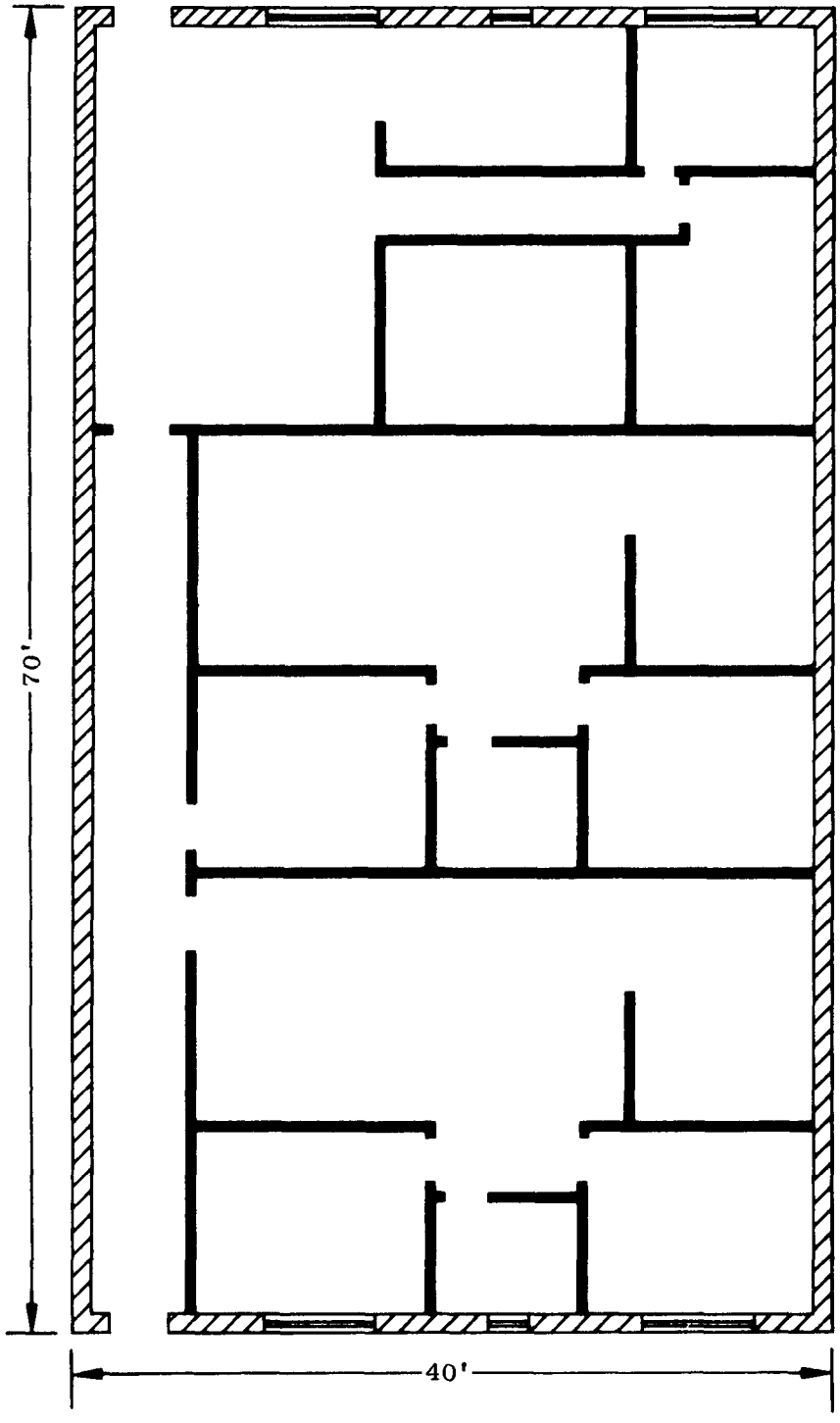

Fig. 15. Floor Plan of Structure No. 2

Window. The discussion of window damage presented for Structure No. 1a, also applies to Structure No. 2, except that the windows are of smaller size and thickness. It was estimated that window failure would occur at a peak incident overpressure of approximately 1/4 to 1/2 psi.

Interior Partition, Floors, and Roof. The methods outlined in Section 2 together with the appropriate established generalized loading schemes were used to calculate the load-time history on the various building components, such as roof, interior partitions, and floor. As discussed previously, to predict structural damage for various overpressure levels, it is also necessary to determine a failure pressure for the building and its component parts. Unfortunately, because definitive information concerning the behavior of multistory load-bearing wall structures subjected to blast forces is unavailable, the prediction of detailed damage for this type of structure is less certain than for the framed structure previously considered. Even so, it was felt important to examine a typical load-bearing-wall structure during this study, since the type comprises a significant portion of NFSS structures.

Although load-bearing-wall structures of current interest were investigated during the early nuclear tests (e.g., Ref. 38), the primary emphasis was on the loading and response of various structural components. Therefore, to estimate the failure pressure for Structure No. 2, it was necessary to use experimental field test results on components, together with the information from Hiroshima and Nagasaki.

Since the composite action of load-bearing structures is difficult to predict for small changes in overpressure level, the estimate of the failure of interior partition, roof, and floor will be included in one subsection, rather than treated separately. For Structure No. 2 it was estimated that the lath and plaster interior partitions would fail at an applied pressure of approximately 5 psi. Although no experimental data were found during this study for the specific partition, the failure pressure estimate was based on field test results for similar panels (Refs. 29 and 30).

The failure pressure calculated by the chamber-filling method was reached in the front rooms of the building at an incident overpressure level of approximately 3 psi. Although the prediction of failure for the interior partitions of the outer room is straightforward, the prediction of failure for subsequent partitions is very difficult.

For Structure No. 1a, the clearing time of the reflected pulse on the front face of the structure was approximately 350 msec. Since the time required for the pressure to build up to the failure pressure in the outer rooms plus the time of partition failure was much less than the clearing time for the reflected pulse, it was reasonable to assume that all interior partitions would fail at about the same incident overpressure level. However, for Structure No. 2, the clearing time is less than 100 msec, and the room fill-time and the partition failure-time would be a significant portion of the clearing-time. Therefore, by the time of failure of the first partition, the reflected pressure reservoir on the front face of the building would be significantly degraded so that failure of subsequent partitions would probably not occur at the initial failure pressure. Because of the unknowns involved in both load prediction and structural response, the calculations required to estimate subsequent partition failure are unwarranted for this study. The 3-psi incident overpressure level can be considered as a lower bound for interior partition damage for Structure No. 2, and failure of all partitions within the building would not occur unless the overpressure level was increased.

An examination of the ground-floor (basement ceiling) and the roof behavior indicates that considerable damage to these elements can be expected at a pressure level sufficient to fail the interior partitions. For conventional floor construction similar to that in Structure No. 2, field tests* indicate that minor damage can be expected at less than 2 psi incident

---

* There are, however, major differences between the test structures and the idealized structure used in this study. These include the size and geometry, floor span, surrounding structures, and the duration of the reflected pulse.

overpressure and considerable damage at 5 psi (Refs. 41 and 42). Because of the geometry of the test structures, the clearing-time of the reflected pulse was very short and the interior pressure was probably not significantly greater than the incident overpressure. Therefore, extensive damage to the floor system for Structure No. 2 could be expected at the 3-psi incident overpressure level, which corresponds to an estimated room pressure of about 5 psi for both the 20-kt and 20-Mt weapon yields.

In an attempt to predict the overpressure level at which roof failure would occur, it is necessary to determine the differential time-varying load on the roof. The generalized load prediction method (e.g., Ref. 6) was used to calculate the average exterior roof pressure for comparison with the previously determined average interior room pressure at 3 psi incident overpressure. The results of these calculations are presented on Fig. 16 for the 20-kt weapon yield. From the figure it can be seen that during the first 100 msec, the average net pressure on the roof varies initially from about 1-1/2 psi, downward, to about 2 psi, upward, at 40 msec. Although the failure pressure of roofs for the predicted loading could not be established within the time and effort available, it was estimated that the roof above the front outer room would fail upward. The prediction of the failure of the roof over the remainder of the building involves the same degree of uncertainty as predicting the interior partition failure pressure throughout the building.

Building. In order to assist in establishing a failure pressure for Structure No. 2, the data in Refs. 3, 23, 24, 29, 30, and 38 were examined. Although the evidence was conflicting, it was felt to be sufficient to permit assuming that the method used for predicting the loading and failure of 12-in.-thick brick panel walls for Structure No. 1a would be applicable to load-bearing-wall structures.

For these conditions, the incident overpressure at which failure of Structure No. 2 could occur was approximately 11 psi for either the kiloton or megaton weapon yields. As noted for Structure No. 1a, the calculated failure overpressure for the exterior brick walls was also 11 psi.

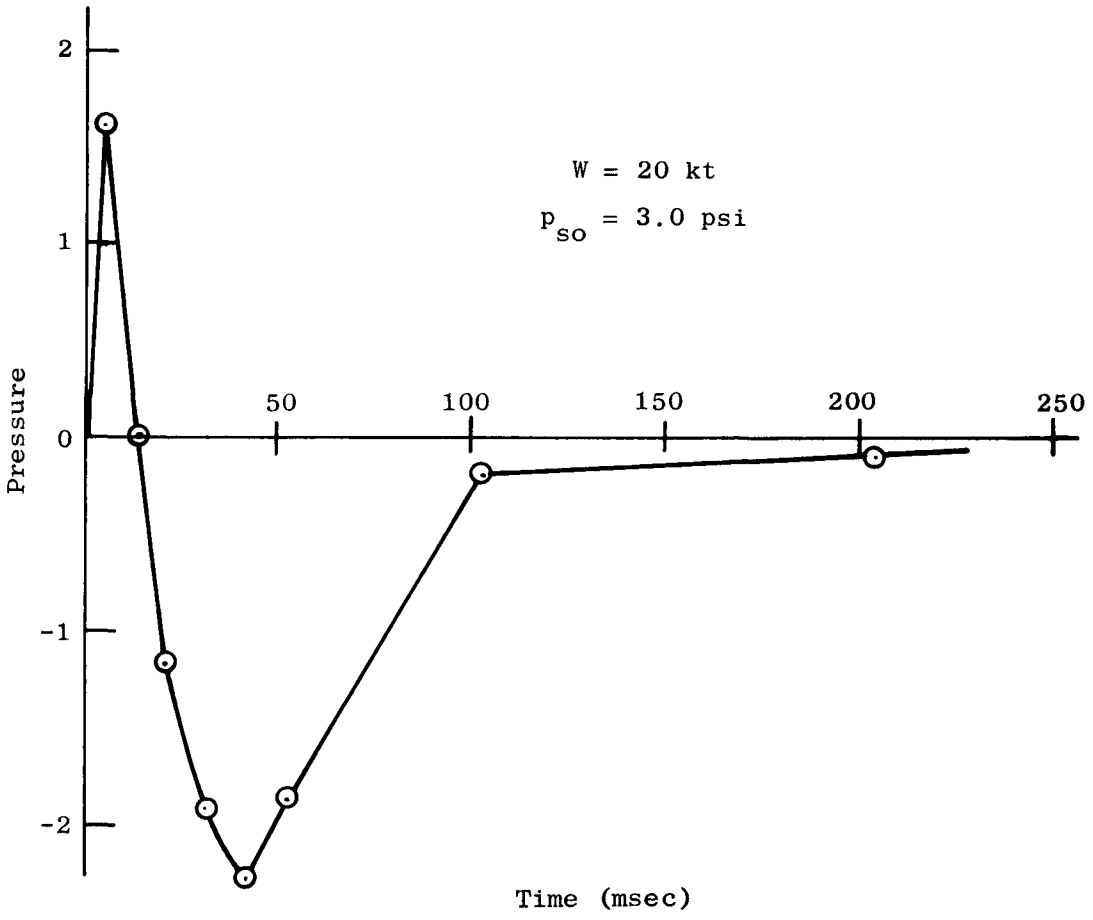

Fig. 16. Differential Roof Loading, Structure No. 2

The pressures are the same for two reasons; first, the failure criterion selected was the same for both walls; and second, it is implicit in the methods used in this study that the load–time histories for elements subjected to blast loads are similar, at least up to failure. However, for the two structures under discussion, an examination of the load for the initial 50 to 100 msec shows considerably more decay for the smaller structure. In an attempt to estimate the effect of this difference in decay, the impulse to failure for the 12-in.-thick brick test panels (Ref. 30) was compared with the idealized structure. It was found that the walls for Structure No. 1a received approximately the same impulse at failure as the test panel, whereas for the walls of Structure No. 2, the impulse was only about two-thirds as great. It would appear reasonable, therefore, to expect that the incident overpressure level required to cause gross failure of the exterior walls for Structure No. 2 would be somewhat greater than the 11 psi calculated.

Fire Damage

Because of the combustible nature of the materials used in the construction of Structure No.2, it is anticipated that any structure of this type will sustain a complete burnout if subjected to any ignition, regardless of the source.

Fire and Blast Damage Combined

In view of the above discussion, there is little need for considering the combined effects of fire and blast for this structure. That is, regardless of the blast damage (if less than the building failure overpressure), an ignition of Structure No. 2 results in burnout of the shelter area.

Post-Damage Prediction Factors

The initial PF of 50 for the basement shelter in Structure No. 2 represents the lower level of protection factor of interest. Window breakage would occur between 1/4 and 1/2 psi. However, even though the initial PF of the shelter is marginal, the resulting ingress would not be serious, because of the small window area and the relatively low initial PF.*

---

* Studies have shown that the reduction in PF for similar conditions was on the order of 10 to 20 percent for 2 percent ingress (Refs. 9 and 12).

The next building damage resulting from blast was the removal of the roof due to uplift at less than 3 psi incident overpressure. This produced some reduction in mass thickness and decrease in PF; however, the resulting change in PF was small (see Table 5). At an overpressure of 3 psi the interior partitions and the ground floor were destroyed, in which case the building was considered to be inadequate as a shelter.

Table 5

BLAST DAMAGE VERSUS PF
STRUCTURE NO. 2

Incident Overpressure (psi)			Resulting PF Basement Shelter
20 kt	20 Mt	Failed Element	
< 1/4	< 1/4	None	50
1/4 – 1/2	1/4 – 1/2	Window	50
< 3	< 3	Roof	~50
3	3	Interior partitions and ground floor	< 20
> 11	> 11	Building collapse	–

Section 4
CONCLUSIONS AND RECOMMENDATIONS

From the foregoing, it is apparent that the prediction of the combined effects of nuclear weapons on the various types of NFSS shelter structures is a difficult task, requiring individual attention to each structure. Essentially, this is a result of the lack of definitive information for the blast loading and response and the effect of thermal radiation on typical multistory buildings located in city complexes. Although the applicability of the procedures outlined in this report is limited by the available information, this investigation has emphasized a number of factors from which general conclusions can be drawn and recommendations for further research made.

CONCLUSIONS

Due to the nature of this investigation and the limits of current knowledge, the following conclusions must be considered as tentative. However, they are important for estimating the relative usefulness of typical NFSS shelter structures for resisting the combined effects of nuclear weapons. It can be concluded that:

- From a consideration of the combined effects of nuclear weapons on the three idealized building situations examined in this investigation, it is apparent that degradation of the protection afforded by typical NFSS shelter areas can occur at very low overpressures. For instance, as noted in the previous section and summarized in Tables 3, 4, and 5, (pp. 56, 61, and 68, respectively), degradation of the PF of typical aboveground and basement shelter areas occurred at overpressures as low as 1/4 psi due to the ingress of fallout radiation through broken windows.

- It was also found that failure of conventional non-load-bearing interior partitions in large multistory structures with usual window openings can be expected at incident overpressure levels of only a few psi. Although not examined specifically in this study, this suggests that in addition to the hazard of a degradation of the shelter radiation protection and fire resistance by removal of an important barrier for the fallout shelter area,

considerable direct blast and missile damage to shelterees can occur at lower overpressure levels than is generally assumed for typical NFSS shelters. Therefore, from the damage analysis for the building situations considered in this report, it is axiomatic that to increase the protection level of many existing shelter areas against fire and blast would usually require extensive modification or replacement of building components such as walls, partitions, floors, or frames.

- For large multistory buildings with lightweight metal panels and conventional interior partitions, a blast wave of modest overpressure level could result in the destruction of the aboveground shelter area. For the building of this type examined in this study, failure of the exterior wall panels, interior partitions, and suspended ceiling occurred at a peak incident overpressure of 1-1/2 to 2 psi. Not only was the PF of the 10th-floor shelter area found to be unacceptable (< 20) for this level of damage, but the existence of the area as a "designated shelter area" to house people in the postattack environment is primarily academic.

- Due to their greater blast and fire resistance and high radiation protection, basement areas of modern multistory buildings are inherently superior to aboveground areas as shelters. For the two large multistory buildings considered, failure of the interior partitions at 2 to 2-1/2 psi incident overpressure resulted in an unacceptable or marginal radiation protection (PF 20 to 30) for the aboveground shelter areas. However, the basement shelters provided more than adequate radiation protection ($PF \sim 500$) until failure of the ground floor slab at a peak incident overpressure of 4 to 5 psi. In addition, the basement area would be shielded from the direct thermal radiation.

- Long-duration, drag-phase loadings of intermediate magnitude from megaton-yield weapons can be a major damage parameter (e.g., by producing gross structure response, such as overturning) for typical multistory buildings with brick masonry curtain walls and conventional interior partitions. This factor was emphasized in this study by a consideration of the detailed blast wave interactions with brick non-load-bearing exterior walls of the large multistory building having typical window openings. Because of the relationship between the relatively long failure time and the short blast wave diffraction process around the back face of the wall, the incident overpressure required to cause failure in conventional brick walls with windows was found to be considerably higher (about 50 percent) than for the field test data for windowless panel walls.

Since the failure of the exterior walls drastically modifies the building loading, this indicates that a distinct possibility exists for a gross building failure of many typical NFSS shelter structures due to the drag forces at overpressure levels insufficient to cause a failure of the exterior brick wall panels.

- For purposes of analysis of the response of multistory buildings to blast load, the usual assumption that the exterior walls fail at modest overpressure levels can be misleading for many typical multistory buildings of interest. In the dynamic analysis of multistory structures, it is generally assumed that the relationship between the rapidly failing exterior wall panels and the response of the structure is such that is is permissible to assume that the actual time-dependent reaction of the wall can be replaced by an impulse (e.g., see Ref. 6). However, because the unreinforced brick curtain walls examined in this study failed at a higher peak incident overpressure (11 psi) than usually assumed for this type of construction, the arbitrary substitution of an impulse for a more realistic wall reaction—time history could result in large errors in the building analysis.

- Shelters located in load-bearing-wall structures (non-monumental type) with conventional roofs, floors, and interior partitions are highly vulnerable to the individual and combined effects of fire and air blast. This applies to all regions subjected to direct ignitions or fire spread and to overpressure regions greater than a few psi. For instance, the examination of the blast loading of a 4-story, load-bearing-wall apartment building showed that failure of the interior partitions and basement ceiling at about 3 psi resulted in degradation of the PF for the basement shelter area to less than 20. In addition, the inherent susceptibility of this class of structure to complete burnout if subjected to ignitions, regardless of source, is apparent.

- Buildings dependent upon suspended ceilings or other frangible fire-protective coverings for a major part of their total fire protection could be seriously damaged by the combined effects of fire and blast at low overpressures. In this study, it was estimated that the suspended ceilings for typical multistory buildings failed at a peak incident overpressure of only 1-1/2 to 2 psi. It was estimated that the removal of the suspended ceiling reduced the fire resistance of the floor slab from a 3-hr rating to a 1-1/2-hr rating. Even though it was not necessarily a critical factor for the particular fire-resistant structure examined, for many structures the suspended ceiling provides a more significant portion of the fire resistance of the floor (Ref. 15), and its removal would considerably alter the fire resistance of the building.

RECOMMENDATIONS

Although reasonably detailed damage predictions can be made on an individual basis for certain structures at the present time, a significant improvement in prediction ability must be based on the development of additional fundamental information. Such information is needed especially for the development of rational methods adequate for general application to a wide variety of structures. The approach should be to examine the available experimental and analytical information for the purpose of both upgrading the interim damage prediction methods and providing guidance for the most meaningful research program to pursue.

There are two principal problems inherent in establishing rational methods for the prediction of air blast damage to large structures in American cities. These are the determination of the time-dependent load function at any point on or within the building and the establishment of adequate failure criteria for the buildings and members of interest. The investigation conducted under the current URS contract has emphasized the inadequacy of generalized air blast loading schemes for use in attempting to determine the failure loading on a particular structural member. Although it was necessary for the purposes of this study to utilize these load prediction methods, certain limited modifications were employed. This was essentially a process of applying engineering judgment to modify, or tailor, the generalized scheme for the investigation of a specific situation. This procedure is only a first step toward the development of more rational damage prediction methods, but the limited results do demonstrate a few of the difficulties and possible errors in damage prediction that can occur by the application — without modification — of current generalized loading methods, which were developed for design purposes.

Basically, the development of satisfactory air blast loading schemes for the analysis of existing structures involves a solution to, or at least sufficient understanding of, a number of specific problem areas, including the following:

- Blast shielding in city complexes
- Point-by-point load distribution for large multistory buildings

- The effect of openings on the load distribution on multistory buildings
- The effect of building and member orientation on the load functions
- Load–time function on all interior building surfaces, including the effect of failing walls
- Importance of nonideal waveforms, including the effect of airborne debris on blast wave parameters

This study has also indicated the need for failure criteria that are more reliable than those currently available for multistory structures and structural elements. For purposes of this study, it was possible to apply the limited data from specific nuclear field tests to obtain solutions to idealized building situations. Although this type of extension and extrapolation of limited information yields reasonable damage predictions, the reliability, or even the limits, of the predictions are unknown. Furthermore, the ability to predict detailed damage for the wide variety of structural systems found in NFSS buildings requires the establishment of more reliable failure criteria for the following:

- Structural elements, including exterior walls, interior partitions, floors, and roof slabs
- Multistory frames
- Load-bearing masonry structures
- Gross structure behavior, i.e., overturning, massive column buckling, foundation failure, and settlement which may create subsequent instability

The fire prediction model presented in this study was based on experimental evidence obtained from fires in combustible buildings. Since it is expected that many of the NFSS spaces are in fire-resistive construction, the experimental studies of fires in structures need to be expanded to include this latter type of construction.

Realistic determination of the protection factor associated with a shelter building, as well as formulation of adequate countermeasures, requires consideration of ingress of radioactive fallout. Since the information determined to date (both with regard to total quantity and distribution of particles) was preliminary in nature, it is recommended that further studies in this area be considered.

Section 5
REFERENCES

1. White, Clayton S., Tentative Biological Criteria for Assessing Potential Hazards From Nuclear Explosions, Lovelace Foundation, Albuquerque, New Mexico, Dec 1963 (AD 437 253)

2. Kaplan, Kenneth and Carl Wiehle, Air Blast Loading in the High Shock Strength Region (U), Part I — Analysis and Correlation (SFRD), Part II — Prediction Methods and Examples (U), Final Report URS 633-3, DASA 1460, Contract No. DA-49-146-XZ-209, URS Corporation for the Defense Atomic Support Agency, Washington, D. C., Feb 1965 (Part II - AD 464 651)

3. Rotz, J., J. E. Edmunds, and K. Kaplan, Effects of Fire on Structural Debris Produced by Nuclear Blast, Research Report URS 639-9, Contract No. OCD-PS-64-19, URS Corporation for the Office of Civil Defense, Washington, D. C., Jan 1965 (AD 615 156)

4. Hill, E. L., et al., Determination of Shelter Configuration for Ventilation, R-OU-177, Contract No. OCD-PS-64-56, Research Triangle Institute for Office of Civil Defense, Washington, D. C., April 1965

5. Davis, L. W., et al., Prediction of Urban Casualties From the Immediate Effects of a Nuclear Attack, The Dikewood Corporation, Albuquerque, New Mexico, April 1963

6. Glasstone, S., The Effects of Nuclear Weapons, Department of Defense and the Atomic Energy Commission, Feb 1964

7. Edmunds, J. E., C. K. Wiehle, and K. Kaplan, Structural Debris Caused by Nuclear Blast, Research Report URS 639-4, Contract No. OCD-PS-64-19, URS Corporation for the Office of Civil Defense, Washington, D. C., Oct 1964 (AD 450 115)

8. "Instructions for Filling out DD Form 1356 (1 Nov 61) National Fallout Shelter Survey - Phase I," Office of Civil Defense, Washington, D. C., Dec 1961

9. Kawahara, F. K., and R. J. Crew, Distribution of Volcanic Fallout In and About a One-Story Residence, USNRDL-TR-953, OCD Work Unit No. 3118A, U.S. Naval Radiological Defense Laboratory, San Francisco, Calif., 11 Aug 1965

10. Crew, R. J., and F. K. Kawahara, Studies of Volcanic Fallout Related to OCD Problems, Phase II, U.S. Naval Radiological Defense Laboratory, San Francisco, Calif.

11. Brusse, Joseph C., A Study of the Infiltration of Radioactive Fallout Particles Into Shelter Spaces Through Large Openings, Contract No. OCD-OS-63-197, Texas Engineering Experiment Station for Office of Civil Defense, Washington, D. C., June 1964

12. Howard, Burl W., The Investigation of the Effect of Building Protection Factors of Ingress of Fallout Through Apertures, NRDL Contract N 288 (62479)-66109, Research Triangle Institute for U.S. Naval Radiological Defense Laboratory, San Francisco, Calif., Dec 1964 (RM 196-1)

13. Office of Civil Defense, Shelter Design and Analysis, Vol. 1, TR-20, Fallout Protection, Washington, D. C., May 1964

14. Renner, R. H., S. B. Martin and R. E. Jones, Parameters Governing Urban Vulnerability to Fire From Nuclear Bursts (Phase I), USNRDL-TR 1040 U.S. Naval Radiological Defense Laboratory, San Francisco, Calif., June 1966

15. Fire Protection Handbook, Tryon, George H., ed., National Fire Protection Association, Boston, Mass., 1962

16. Troxell, G. E., J. G. Degenkolb, K. L. Benuska, and B. R. Loya, Reusability of Buildings After a Warfire, Contract No. OCD-OS-63-172, T. Y. Lin and Associates for Office of Civil Defense, Washington, D. C., Jan 1964

17. Salzberg, F., W. G. Labes, H. Nielsen and T. E. Waterman, Prediction of Fire Damage to Installations and Built-up Areas From Nuclear Weapons, Final Report - Phase II, Study of Initiation and Spread of Fires in Typical Structures, Contract No. DA-49-146-XZ-021, Armour Research Foundation for Defense Atomic Support Agency, Washington, D. C., Dec 1960

18. Waterman, T. E., W. G. Labes, F. Salzberg, J. E. Tamney, F. J. Vodvarka, Prediction of Fire Damage to Installations and Built-up Areas From Nuclear Weapons, Final Report - Phase III, Experimental Studies - Appendices A - G, Contract No. DCA-8, Illinois Institute of Technology Research Institute for National Military Command System Support Center, Washington, D. C., Nov 1964

19. Salzberg, F., M. M. Gutterman, and A. J. Pintar, Prediction of Fire Damage to Installations and Built-up Areas From Nuclear Weapons, Phase III, Theoretical Studies, Contract No. DA-49-146-XZ-021, Illinois Institute of Technology Research Institute for National Military Command Support Center, Washington, D.C., July 1965

20. Rotz, J. V., J. E. Edmunds and K. Kaplan, Formation of Debris From Buildings and Their Contents by Blast and Fire Effects of Nuclear Weapons, URS 651-4, Contract No. B-70924(4949A-20)-US, URS Corporation for Stanford Research Institute, Menlo Park, California, Jan 1966

21. Vortman. L. J., and W. J. Francy, Effects of a Nonideal Shock Wave On Blast Loading of a Structure, WT-1162, Sandia Corporation, Albuquerque, New Mexico, May 1956

22. Newmark, N. M., and J. D. Haltiwanger, Air Force Design Manual, AFSWC-TDR-62-138, prepared by the University of Illinois for Air Force Special Weapons Center, Kirtland Air Force Base, N. M., 1962

23. U.S. Strategic Bombing Survey, The Effects of the Atomic Bomb on Hiroshima, Japan, Vols. I – III, May 1947

24. U.S. Strategic Bombing Survey, The Effects of the Atomic Bomb on Nagasaki, Japan, Vols. I – III, June 1949

25. The Design of Structures to Resist the Effects of Atomic Weapons, EM 1110-345-414 to 421, Massachusetts Institute of Technology for the Office of Chief of Engineers, U.S. Army, Washington, D. C., 1957

26. Smith, B., Design Manual — AEC Test Structure, TID-16347, Vols. I, II, and III, Holmes and Narver for the Atomic Energy Commission, Los Angeles, Calif., 1961

27. Bultmann, E. H., Jr., Eugene Sevin, and T. H. Schiffman, Blast Effects On Existing Upshot-Knothole and Teapot Structures, WT-1423, Armour Research Foundation and Air Force Special Weapons Center, Kirtland Air Force Base, N. M., May 1960

28. Ballistic Research Laboratories, Information Summary of Blast Patterns In Tunnels and Chambers, BRL 1390, DASA 1273, Aberdeen Proving Ground, Maryland, Mar 1962

29. Sevin, Eugene, Tests on the Response of Wall and Roof Panels and the Transmission of Load to Supporting Structures, WT-724, Armed Forces Special Weapons Project, Sandia Base, Albuquerque, N. M., for Air Material Command, Wright-Patterson Air Force Base, Dayton, Ohio, May 1955

30. Taylor, Benjamin C., Blast Effects of Atomic Weapons Upon Curtain Walls and Partitions of Masonry and Other Materials, WT-741, Armed Forces Special Weapons Project, Sandia Base, Albuquerque, N. M., for Federal Civil Defense Administration, Battle Creek, Michigan, Aug 1956

31. Newmark, N. M., "An Engineering Approach to Blast Resistant Design," Trans. ASCE, Vol. 121, paper No. 2788, 1956, pp. 45 – 64

32. Massachusetts Institute of Technology, Army Structures Test, Appendix 12, Results of Second Engebi Shot, WT-95, Contract No. DA-49-129-eng-47, MIT for Office of Chief of Engineers, Washington, D. C., Aug 1951

33. Large, George Elwyn, Basic Reinforced Concrete Design: Elastic and Creep, The Ronald Press Company, New York, 1957

34. Allgood, J. R., S. K. Takahashi, W. A. Shaw, Blast Loading of 15 ft R/C Beams, Technical Report TR-086, U.S. Naval Civil Engineering Laboratory, Port Hueneme, California, Jan 1961

35. Zeitlin, E. A., The Blast Environment: Methodology and Instrumentation Techniques with Applications to New Facilities, Navweps Report 8782, U.S. Naval Ordnance Test Station, China Lake, California, Aug 1965

36. Berg, G. V., and D. A. DaDeppo, The Response of Tier Buildings to Blast Loads, AFSWC-TR-57-45, University of Michigan Engineering Research Institute for Air Force Special Weapons Center, Kirtland Air Force Base, N. M., May 1958

37. Office of Civil Defense, A Computer Program to Analyze the Dynamic Response of High Rise Building to Nuclear Blast Loading, Vols. I and II, PG 80-18-1 & 2, Review Draft for Department of Defense, Office of Civil Defense, Washington, D.C., Feb 1964

38. Pettitt, B. E., Scientific Director's Report Annex 3.3, U.S. Air Force Structures, WT-29, Operation Greenhouse, Aug 1951

39. Grinter, Linton E., Design of Modern Steel Structures, The Macmillan Company, New York, 1941

40. Personal communication with Fire Protection Engineer, Donald Wallace, Consultant to URS Corporation.

41. Byrnes, Joseph B., Effects of an Atomic Explosion on Two Typical Two-Story-and-Basement Wood-Frame Houses, WT-792, Federal Civil Defense Administration, Washington, D. C., Sept 1953

42. Randall, P. A., Damage to Commercial and Special Types of Residence Exposed to Nuclear Effects, Operation Teapot, WT-1194, Office of Civil Defense Mobilization, Washington, D.C., Mar 1961

43. Office of Civil Defense, Estimating Shelter Cost and Usable Space, PG 80-12, Washington, D. C., Sept 1962

44. Cannon, Ernest W., Building Materials as Commonly Used in Existing Urban Buildings in the United States, CD-GA-56-57, Institute of Engineering Research, University of California, Richmond, California, Jan 1958

45. Concrete Reinforcing Steel Institute, Reinforced Concrete, A Manual of Standard Practice, AIA File No. 4-E-2, Chicago, Illinois, 1961

Appendix A
TYPICAL BUILDING COMPONENTS

The following material was compiled from Refs. 43, 44, and 45. The mass thicknesses were either obtained from Ref. 44 or calculated from information presented in Ref. 45. These quantities were rounded off according to the following rule: 0 – 20 psf round to the nearest psf, 20 – 100 psf round to 5 psf, over 100 psf round to 10 psf.

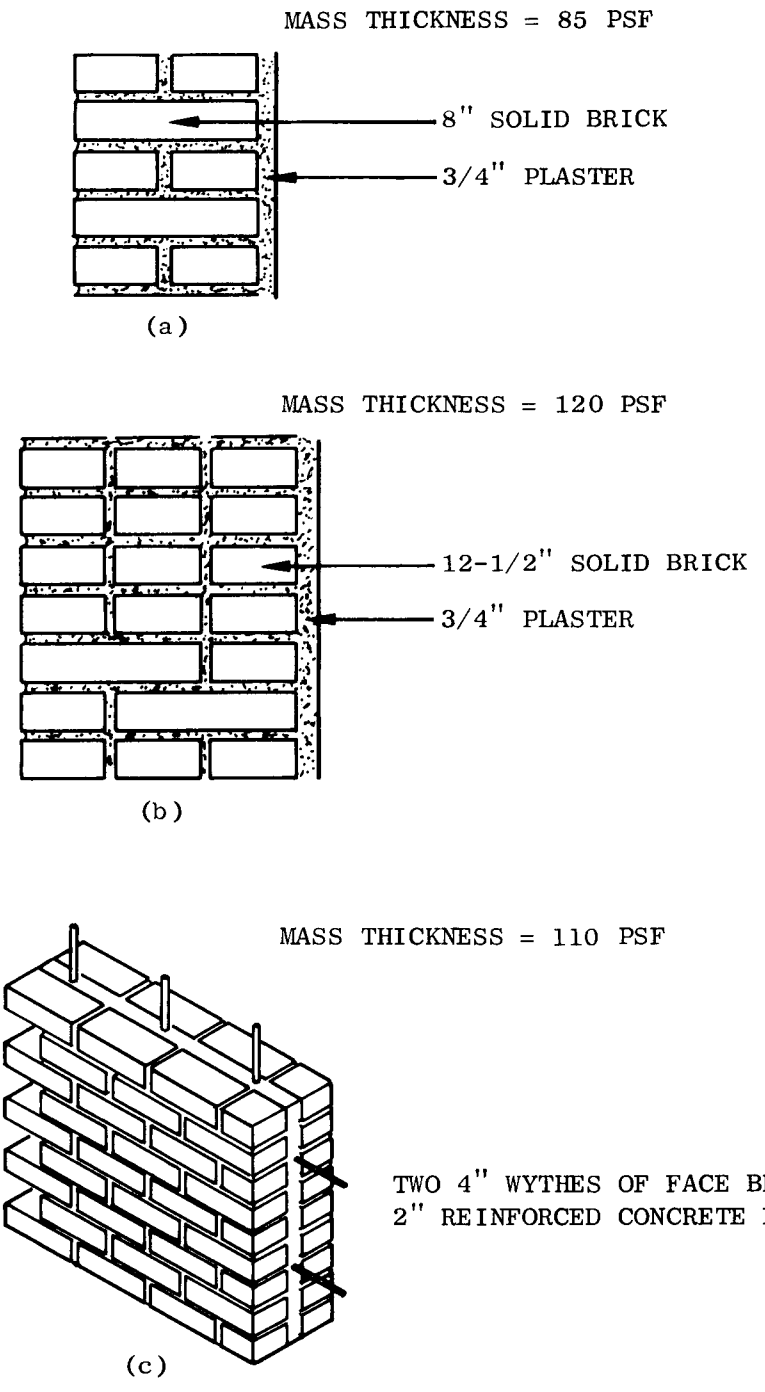

Fig. A-1. Exterior Wall Sections

MASS THICKNESS = 100 PSF

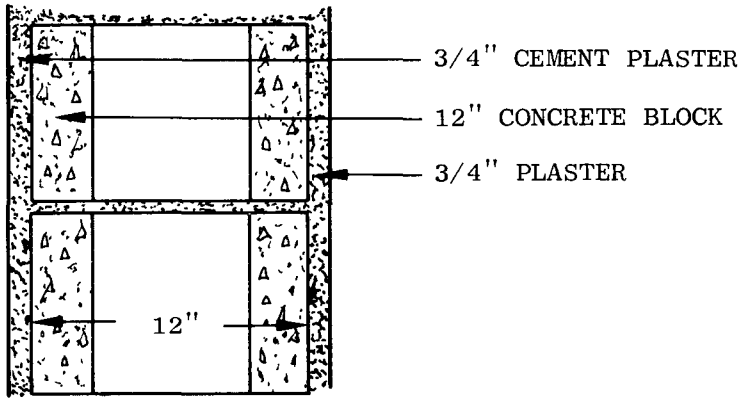

(a)

MASS THICKNESS = 55 PSF

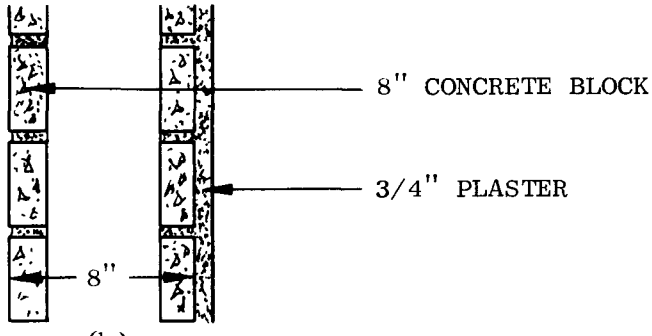

(b)

MASS THICKNESS = 30 PSF

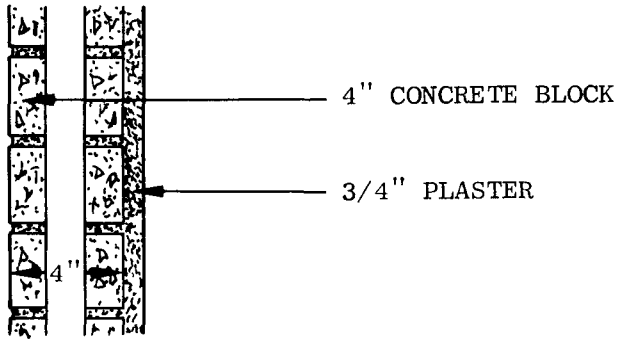

(c)

Fig. A-2. Exterior Wall Sections

MASS THICKNESS = 70 PSF

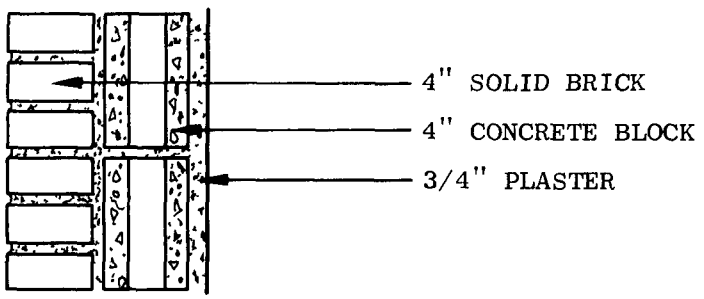

(a)

MASS THICKNESS = 95 PSF

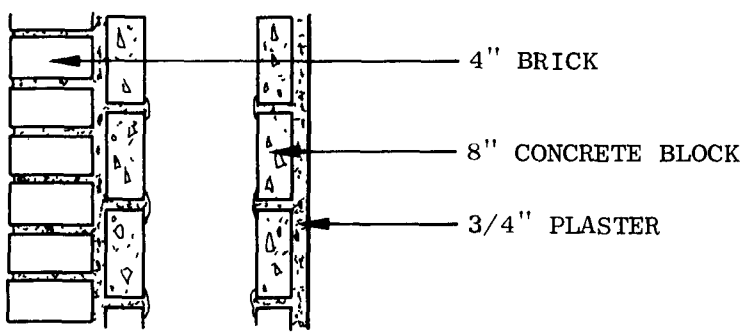

(b)

MASS THICKNESS = 65 PSF

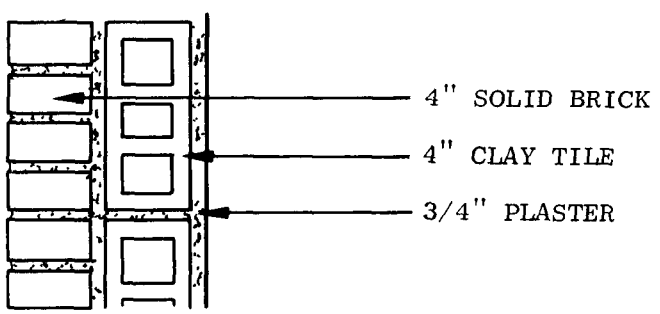

(c)

Fig. A-3. Exterior Wall Sections

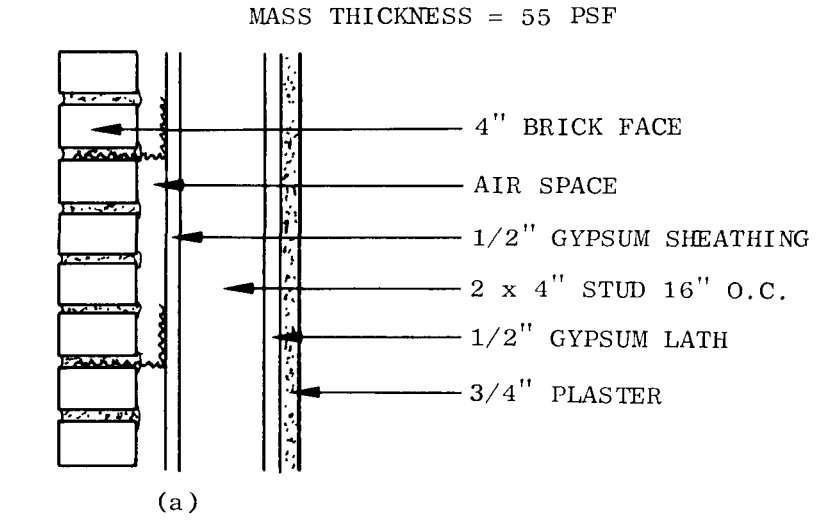

Fig. A-4. Exterior Wall Sections

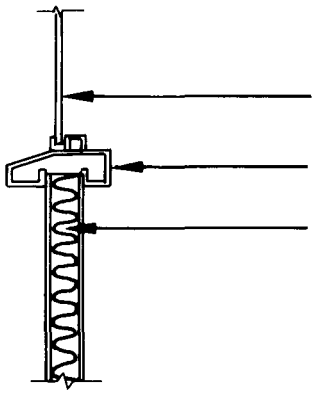

(MASS THICKNESS WAS ASSUMED EQUAL TO ZERO FOR PF CALCULATIONS)

PLATE GLASS

ALUMINUM MULLION

PORCELAINIZED STEEL PANEL WITH RIGID INSULATION

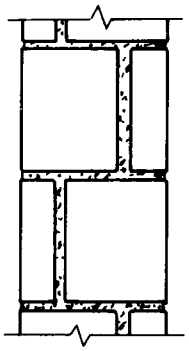

MASS THICKNESS = 25 PSF

6" GLAZED STRUCTURAL FACING TILE

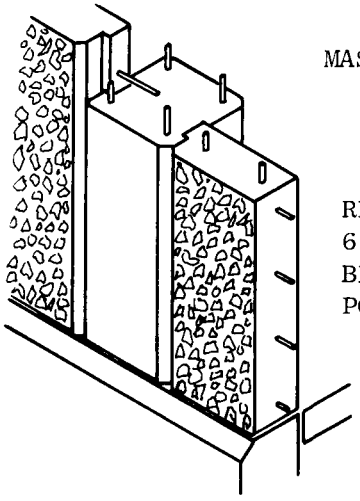

MASS THICKNESS = 75 PSF

REINFORCED CONCRETE TILT-UP PANELS
6" THICK
BROKEN STONE FACE
POURED IN PLACE REINFORCED CONCRETE COLUMNS

Fig. A-5. Exterior Wall Sections

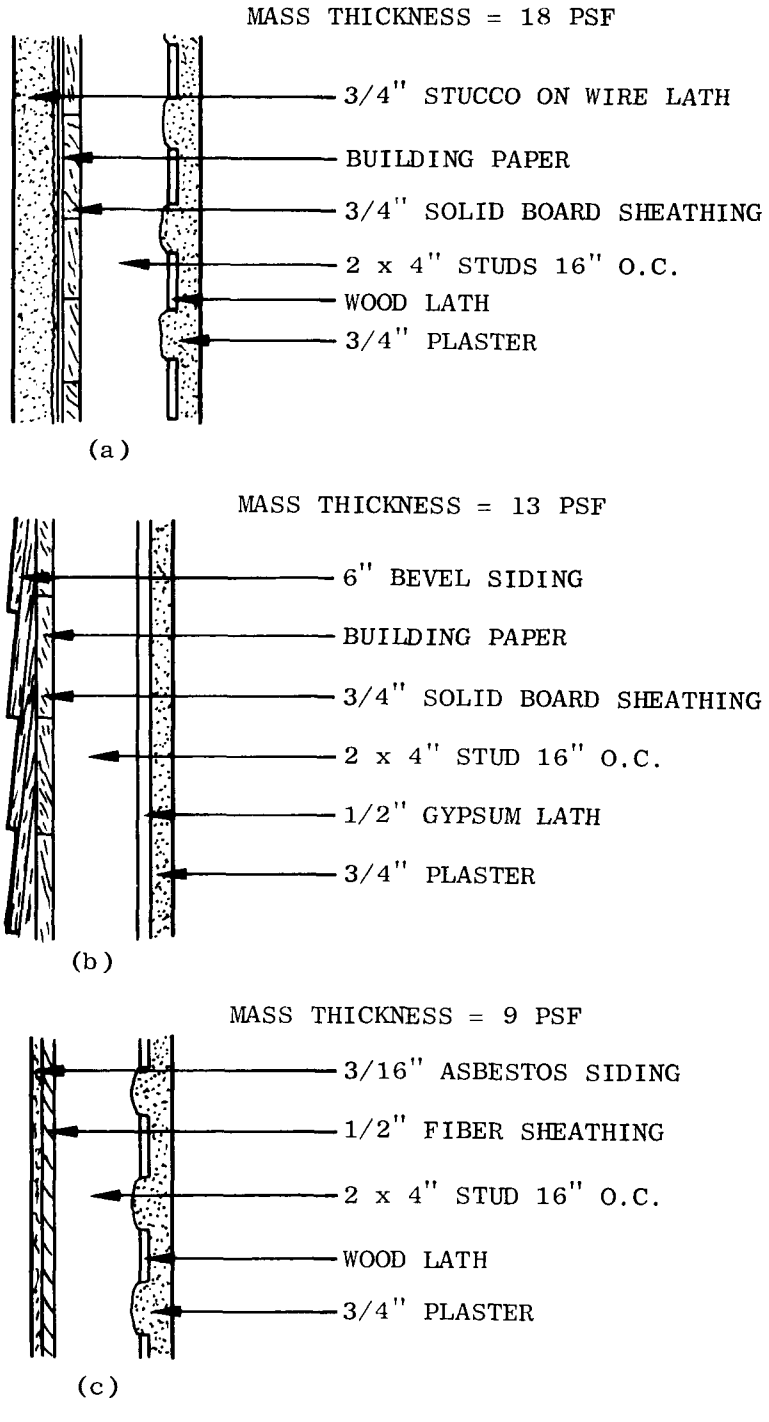

Fig. A-6. Interior Wall Sections

MASS THICKNESS = 45 PSF

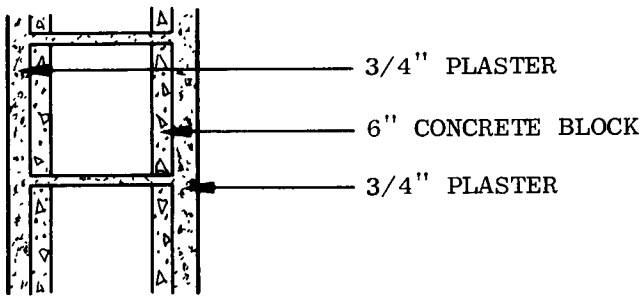

(a)

MASS THICKNESS = 40 PSF

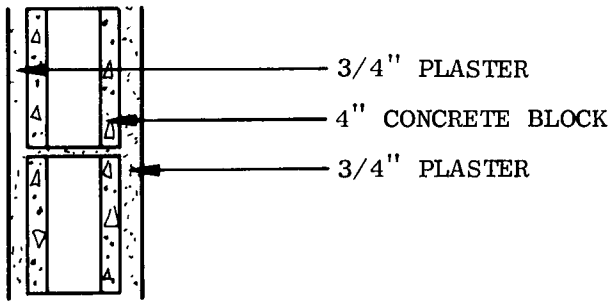

(b)

MASS THICKNESS = 30 PSF

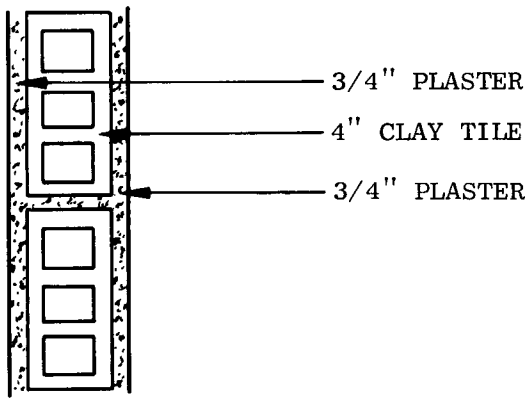

(c)

Fig. A-7. Interior Wall Sections

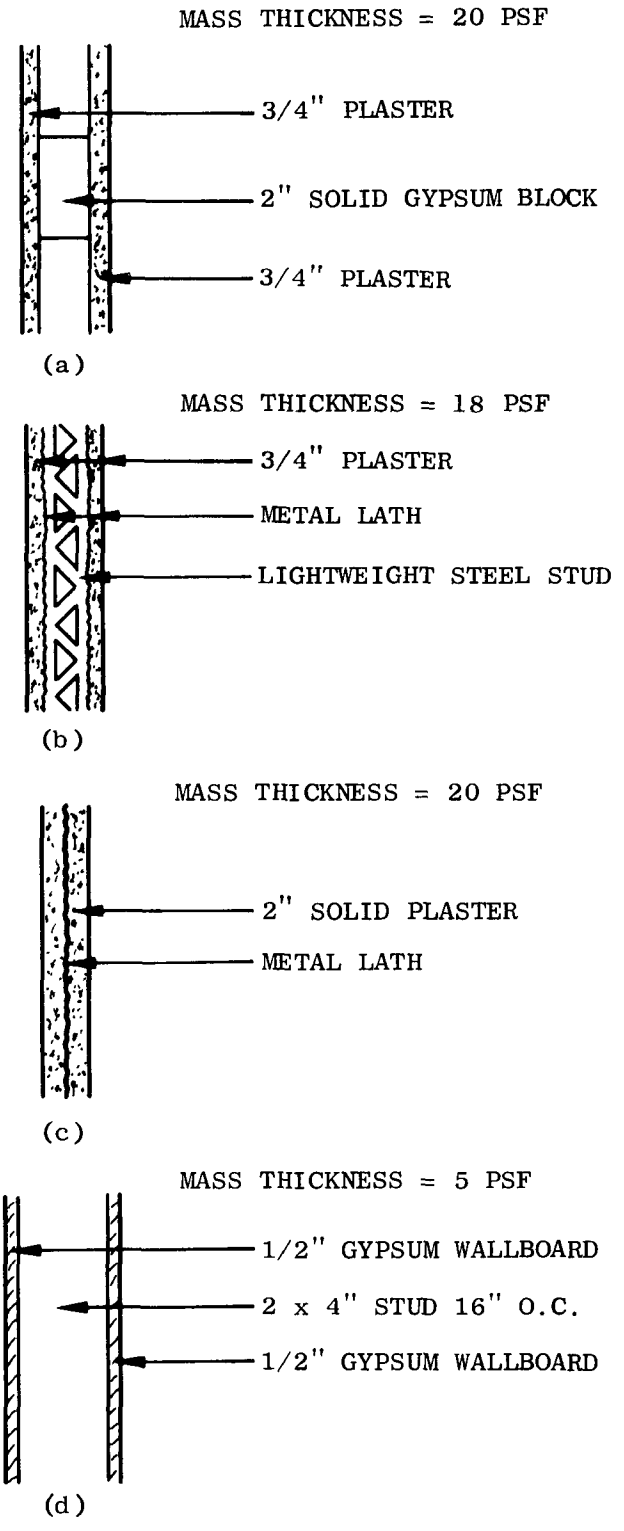

Fig. A-8. Interior Wall Sections

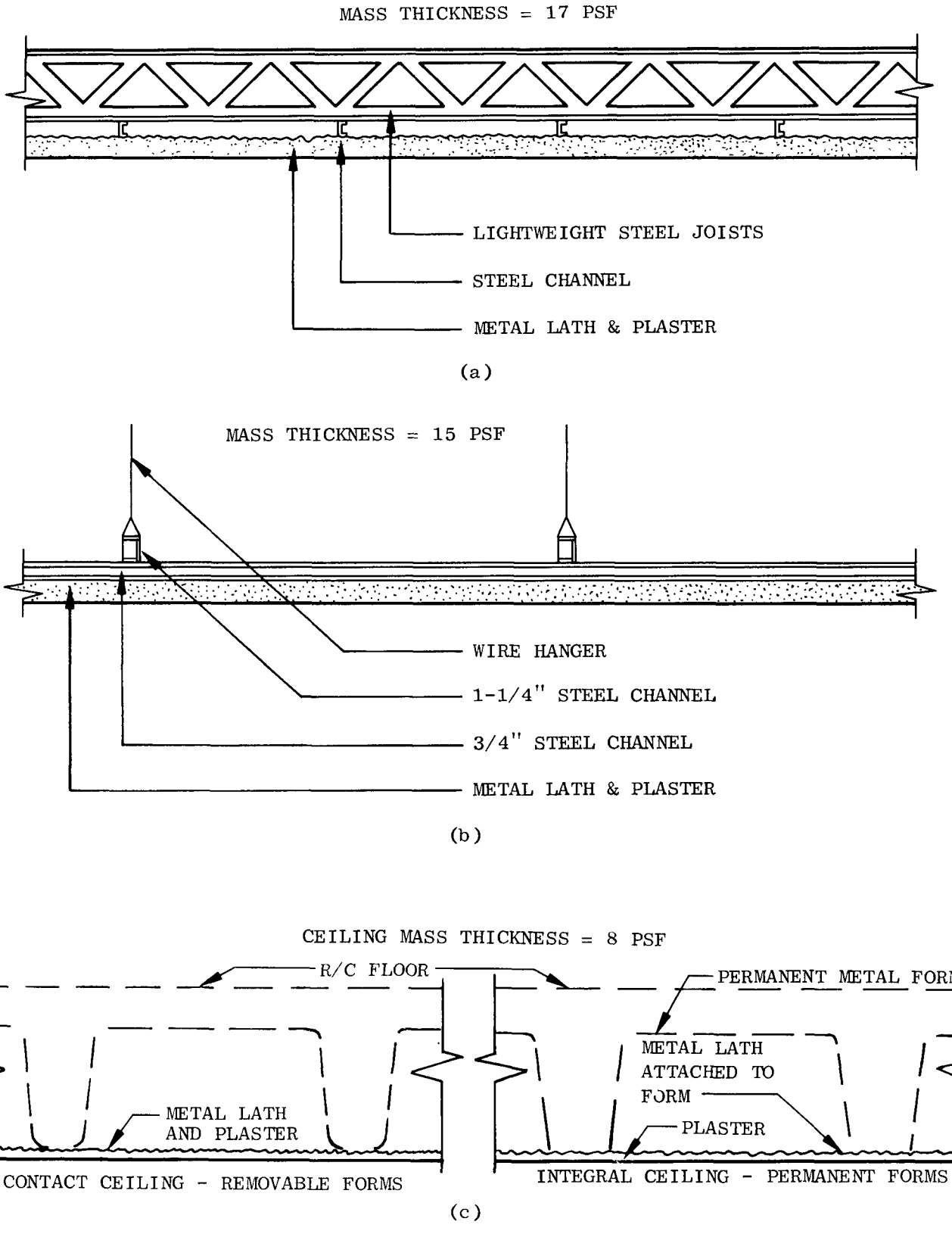

Fig. A-9. Sections of Typical Ceilings

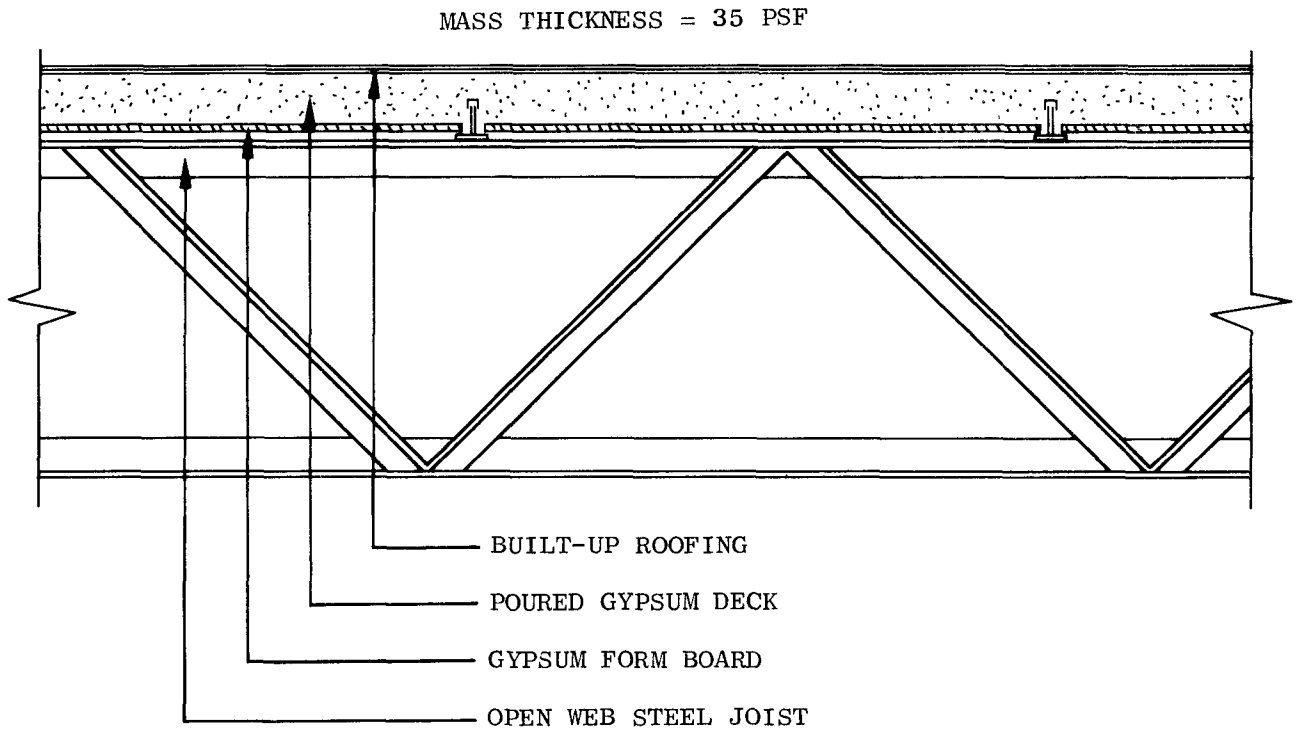

(a)

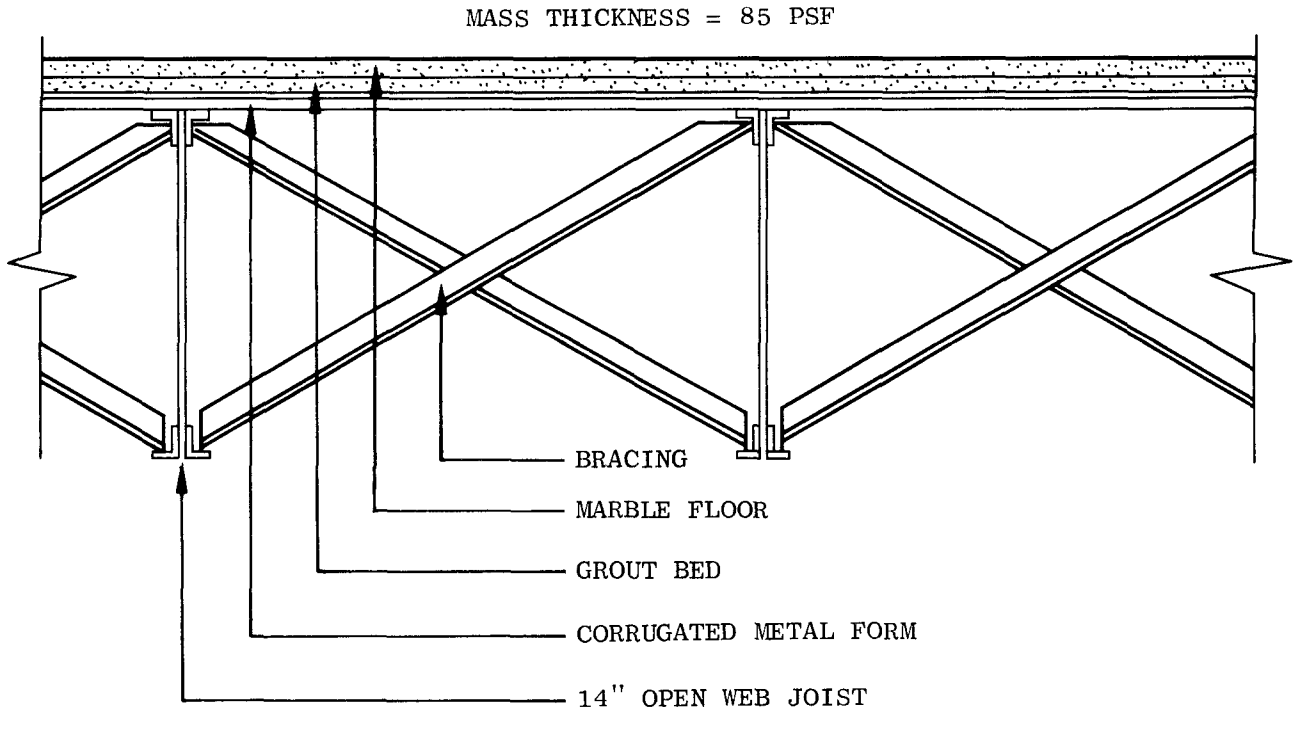

(b)

Fig. A-10. Roof or Floor Sections

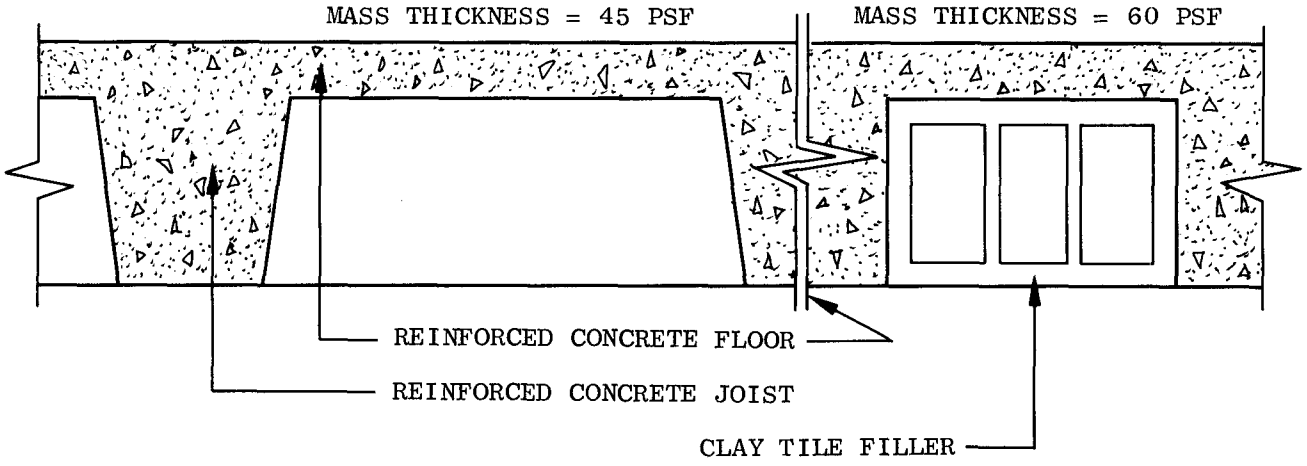

(a)

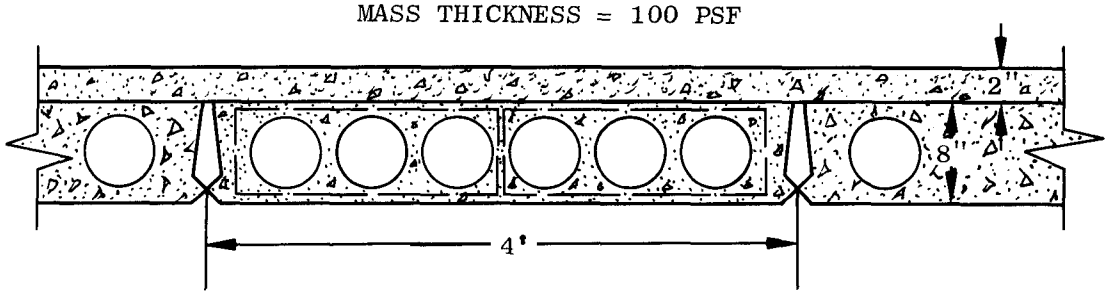

PRESTRESSED CONCRETE HOLLOW CORE SLAB WITH COMPOSITE CONCRETE FILL, SPAN 28', 100 PSF LIVE LOAD

(b)

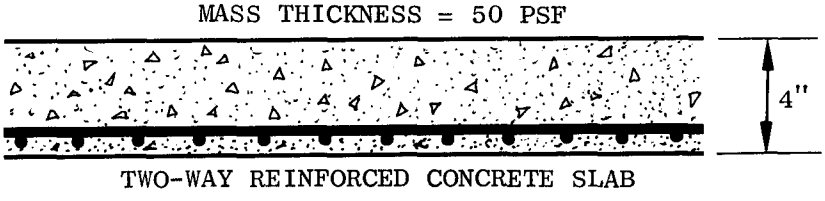

TWO-WAY REINFORCED CONCRETE SLAB

(c)

Fig. A-11. Roof or Floor Sections

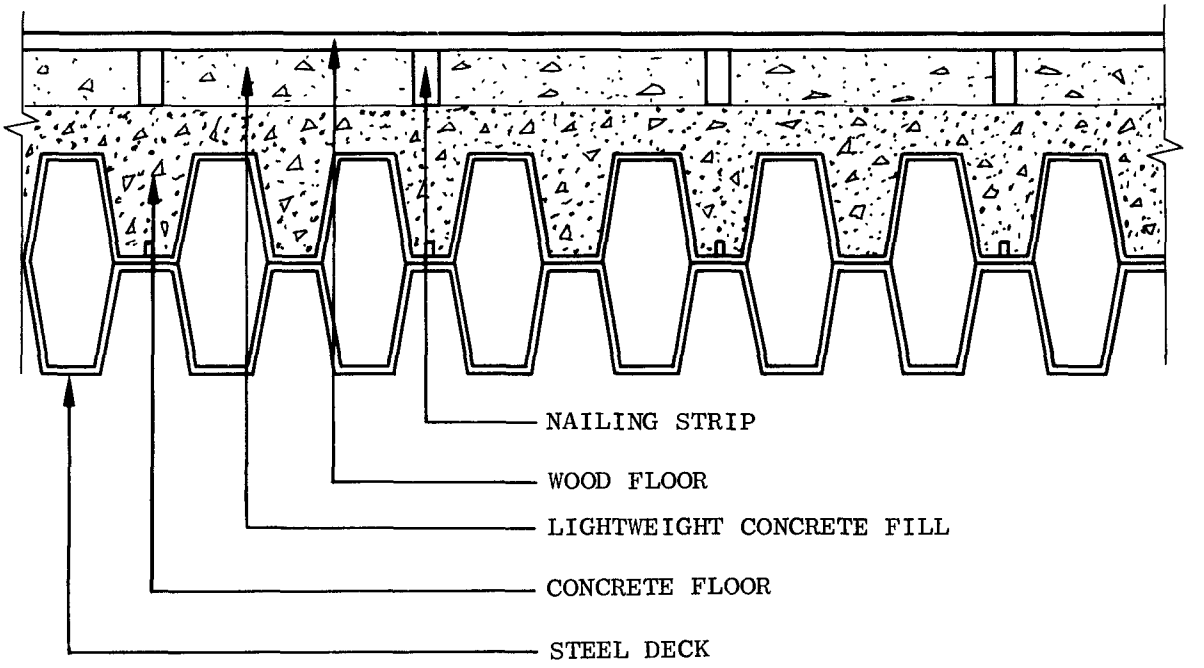

MASS THICKNESS = 25 PSF

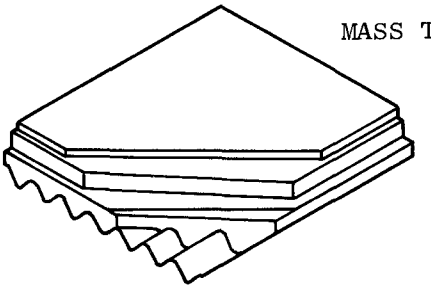

5 PLY BUILT-UP ROOFING
2" RIGID INSULATION, WITH VAPOR BARRIER
LIGHTWEIGHT REINFORCED CONCRETE ON
CORRUGATED STEEL DECK
SPAN 6'

MASS THICKNESS = 30 PSF

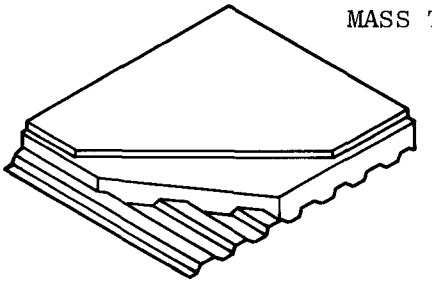

5 PLY BUILT-UP ROOFING
3" INSULATING CONCRETE
STANDARD CORRUFORM

Fig. A-12. Roof or Floor Sections

MASS THICKNESS = 30 PSF (EST.)

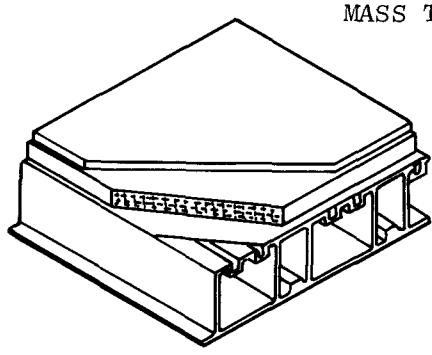

5 PLY BUILT-UP ROOFING
2" RIGID INSULATION, WITH VAPOR BARRIER
7-1/2" STEEL DECKING, SPAN 28'

MASS THICKNESS = 25 PSF (EST.)

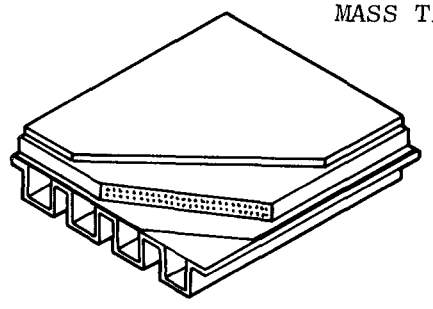

5 PLY BUILT-UP ROOFING
2" RIGID INSULATION, WITH VAPOR BARRIER
4-1/2" STEEL DECKING, SPAN 16'

MASS THICKNESS = 20 PSF (EST.)

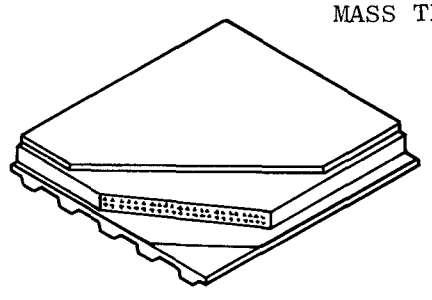

5 PLY BUILT-UP ROOFING
2" RIGID INSULATION, WITH VAPOR BARRIER
1-1/2" RIBBED STEEL DECKING, SPAN 8'

Fig. A-13. Roof Sections

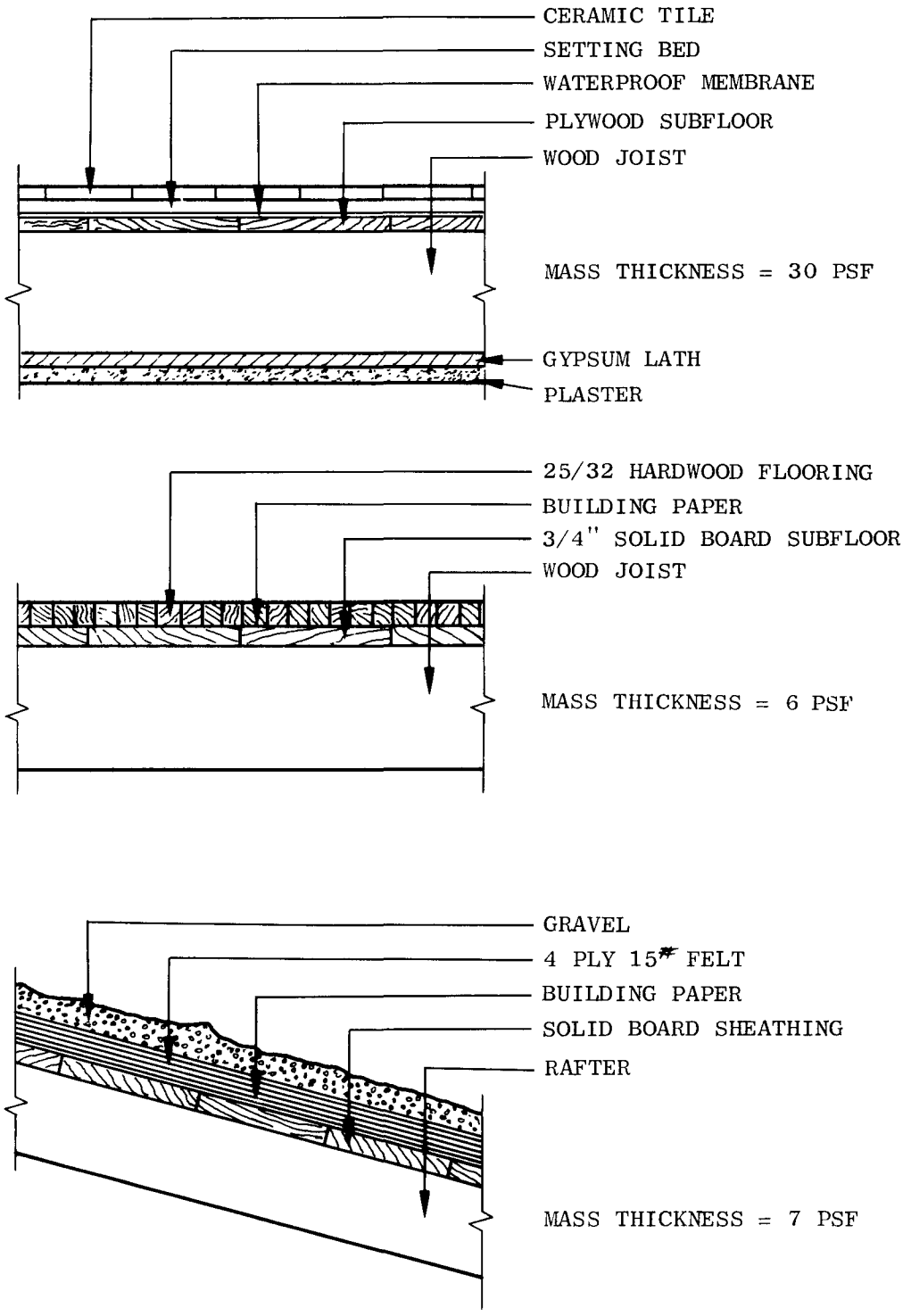

Fig. A-14. Roof or Floor Sections

Appendix B

SAMPLE CALCULATION — ROOM PRESSURE BUILDUP

NOTATION

p_{so}	Peak side-on overpressure
p_s	Side-on overpressure varying with time
p_{do}	Peak dynamic pressure
p_d	Dynamic pressure varying with time
p_r	Reflected pressure
U	Shock front velocity
t_+	Duration of positive overpressure phase
t	Time measured from instant of initial contact of blast wave with front face
t_1	Clearing time, front face
C_d	Drag coefficient
p_4	Overpressure in chamber
C	Experimental function
H	Building height
B	Building width
L	Building length
ℓ	Room length
A_w	Window area
A_B	Building area
V	Room volume
S	H or B/2, whichever is less

PROBLEM

To determine the overpressure causing failure of the 4-in. masonry interior partitions for Structure No. 1a (see Figs. 10–12, Section 3).

BLAST PARAMETERS

p_{so} = 2.0 psi

p_{do} = 0.1 psi

p_r = 4.2 psi

t_+ = 1.2 sec, 20 kt; 11.5 sec, 20 Mt

t_1 = 350 msec

U = 1,180 fps

BUILDING PARAMETERS

H = 144 ft

W = 300 ft

L = 56 ft

ℓ = 20 ft

$A_w = 0.30\ A_B$

S = H = 144 ft

FAILURE PRESSURE

$p \simeq 4$ psi, for 4-in.-thick masonry interior partition with 3/4-in. plaster.

ROOM PRESSURE*

$$C = \frac{V}{A}\frac{\Delta p_4}{\Delta t}$$

for

$A = 72\ ft^2$

$V = 4{,}400\ ft^3$

---

* Average chamber pressure as determined by the method presented in Ref. 28.

$\Delta t = 0.010$ sec

$\Delta p_4 = 0.164 \times 10^{-3} C$

20 kt

t	p	p_4	$p - p_4$	C (Fig. B-1)	Δp_4
0	4.2	0	4.2	9,500	1.6
0.010	4.1	1.6	2.5	6,000	1.0
0.020	4.0	2.6	1.4	3,500	0.6
0.030	3.9	3.2	0.7	1,500	0.2
0.040	3.8	3.4	0.4	1,100	0.2
0.050	3.8	3.6	0.2	500	0.1
0.060	3.7	3.7			

20 Mt

0	4.2	0	4.2	9,500	1.6
0.010	4.1	1.6	2.5	6,000	1.0
0.020	4.1	2.6	1.5	3,700	0.6
0.030	4.0	3.2	0.8	2,100	0.3
0.040	4.0	3.5	0.5	1,200	0.2
0.050	3.9	3.7	0.2	500	0.1
0.060	3.8	3.8			

From the above calculations and Fig. B-2, it can be seen that the interior room pressure would equal the 4-psi failure pressure at slightly greater than 2 psi incident overpressure level. Therefore, it can be concluded that the partitions for Structure No. 1a would fail at a peak incident overpressure between 2 and 2.5 psi.

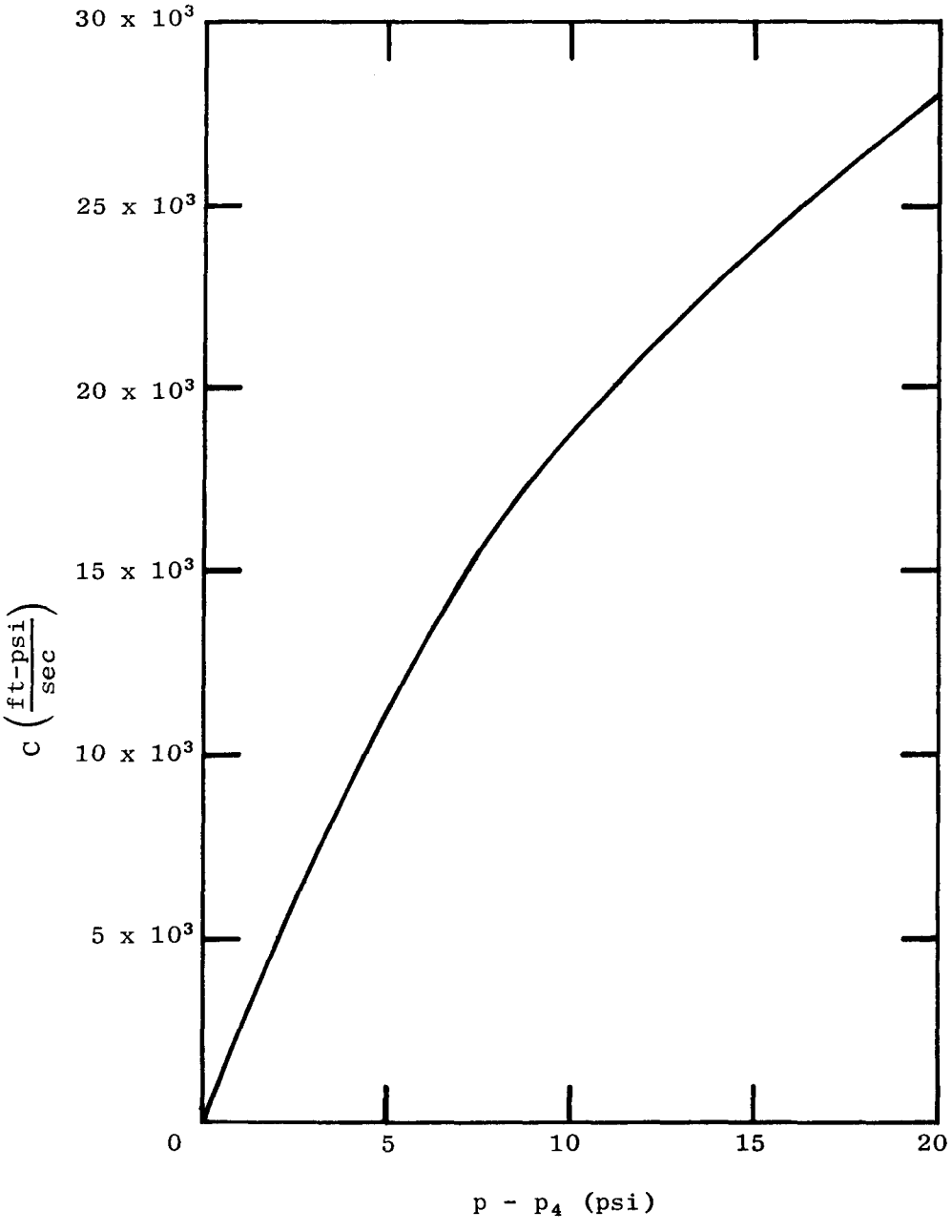

Fig. B-1. C Versus Pressure Differential Between Applied Wave and Chamber (From Ref. 28)

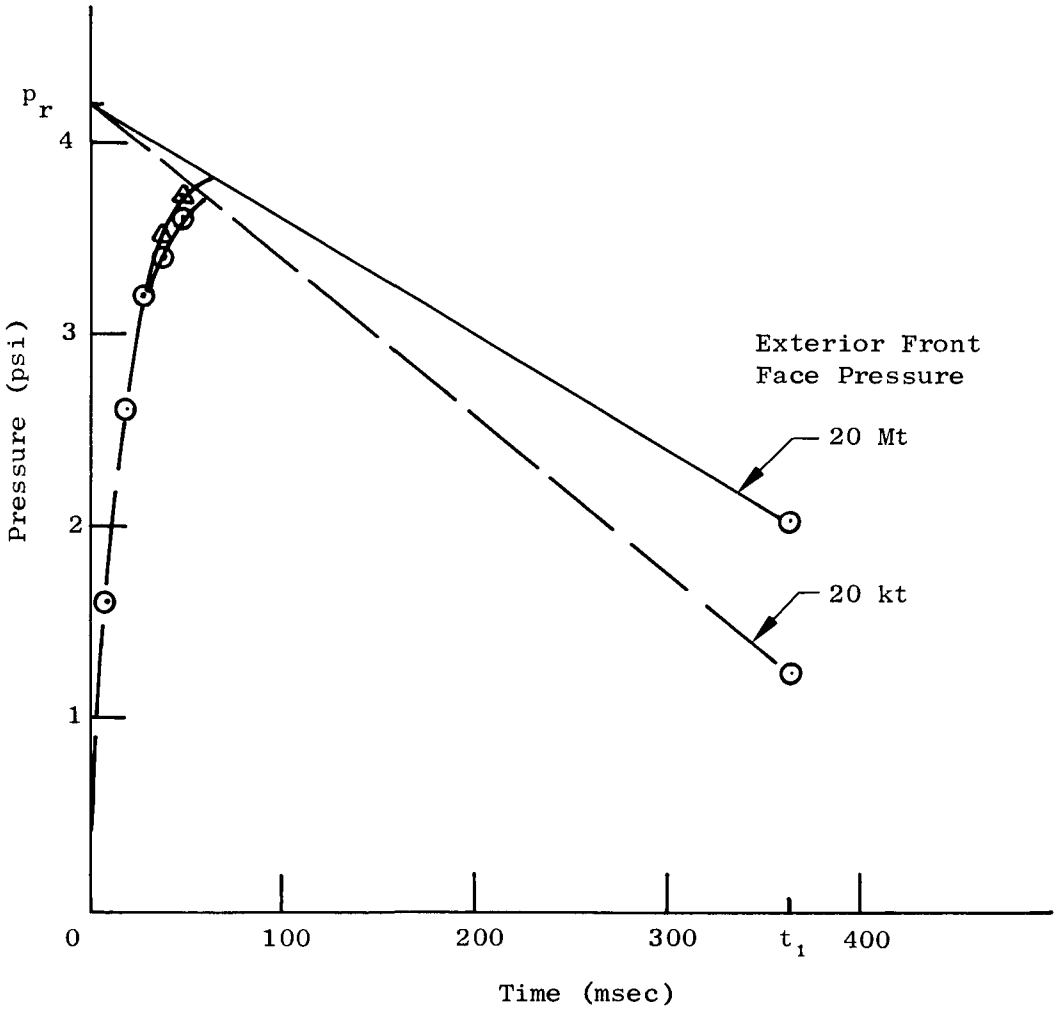

Fig. B-2. Room Pressure Buildup, Structure No. 1a

Appendix C

DISTRIBUTION LIST

Addressee	No. of Copies
Assistant Director of Civil Defense (Research) Office of Civil Defense Department of the Army - OSA Washington, D. C. 20310	47
Defense Documentation Center Cameron Station Alexandria, Virginia 22314	20
Dr. James O. Buchanan Director, Shelter Research Division Office of Civil Defense Department of the Army - OSA Washington, D. C. 20310	1
Mr. Norbert E. Landdeck Shelter Research Division Office of Civil Defense Department of the Army - OSA Washington, D. C. 20310	1
Assistant Secretary of the Army (R&D) Attn: Assistant for Research Washington, D. C. 20310	1
Commanding Officer U. S. Army Nuclear Defense Lab Attn: Civil Defense Coordinator SMUEA-CM-M-4A Edgewood, Maryland 21010	1
Army Library, TAGO Civil Defense Unit The Pentagon Washington, D. C. 20310	3
Director, U. S. Army Matls. Res. Agency Watertown Arsenal Attn: Dr. Dorothy Weeks Watertown, Massachusetts	1
Director, U. S. Army Ballistic Res. Lab Attn: Document Library Aberdeen Proving Ground, Maryland 21005	1

Addressee	No. of Copies
Commanding Officer Nuclear Group U. S. Army Combat Development Command Fort Bliss, Texas 79906	1
Director, U. S. Army Engineer Waterways Experiment Station Post Office Box 631 Attn: Nuclear Weapons Effects Branch Vicksburg, Mississippi	1
Director, U. S. Army Engineer Waterways Experiment Station Post Office Box 631 Attn: Document Library Vicksburg, Mississippi	1
Chief, Joint Civil Defense Support Group Office, Chief of Engineers Gravelly Point Washington, D. C.	3
Chief of Engineers Department of the Army Attn: ENGTE-E Washington, D. C. 20310	1
Mr. Strode L. Ely Office of the Secretary of Defense Installations and Logistics Room 3C771, The Pentagon Washington, D. C. 20301	1
Mr. Edward R. Saunders Office of Emergency Planning Executive Office of the President Washington, D. C. 20504	1
Mr. Charles F. Coffin Planning Officer Technical Analysis Division Office of Emergency Planning Executive Office of the President Washington, D. C. 20504	1
Director of Research and Development Office of Emergency Planning Washington, D. C. 20504	1

Addressee	No. of Copies
Director, Defense Atomic Support Agency Attn: Technical Library Washington, D. C. 20301	1
Director, Defense Atomic Support Agency Attn: Mr. John G. Lewis Washington, D. C. 20301	1
Director, Defense Atomic Support Agency Attn: Jack R. Kelso Washington, D. C. 20301	1
Commander, Field Command Defense Atomic Support Agency Sandia Base Albuquerque, New Mexico	1
Chief of Naval Research (Code 104) Department of the Navy Washington, D. C. 20310	1
Chief of Naval Operations (OP-07T10) Department of the Navy Washington, D. C. 20360	1
Chief, Bureau of Naval Weapons (Code RRRE-4) Department of the Navy Washington, D. C. 20360	1
Chief, Bureau of Medicine and Surgery Department of the Navy Washington, D. C. 20390	1
Chief, Bureau of Supplies and Accounts (Code L12) Department of the Navy Washington, D. C. 20360	1
Chief of Naval Personnel Code PERS M12 Department of the Navy Washington, D. C.	1
Chief, Bureau of Yards and Docks Research and Development (Code 74) Department of the Navy Washington, D. C. 20390	1
Commanding Officer and Director Attn: Document Library U. S. Naval Civil Engineering Laboratory Port Hueneme, California	1

Addressee	No. of Copies
Chief, Bureau of Ships (Code 203) Department of the Navy Washington, D. C. 20360	1
Coordinator, Marine Corps Landing Force Development Activities Quantico, Virginia	1
U. S. Naval Radiological Defense Laboratory Attn: Technical Library (Code 222A) San Francisco, California 94135	1
U. S. Naval Radiological Defense Laboratory Civil Defense Technical Group Attn: Mr. Paul E. Zigman San Francisco, California 94135	1
Air Force Special Weapons Laboratory Attn: Technical Library Kirtland Air Force Base New Mexico, 87117	2
Director, A. F. Nuclear Engineering Facility Air Force Institute of Technology Wright-Patterson AFB Dayton, Ohio 45433	1
Colonel Francis A. Sanders Department of the Air Force DCS Programs and Resources Engineering Division Building 626, Bolling Air Force Base Washington, D. C.	1
Civil Defense Technical Office Attn: Mr. William L. White Stanford Research Institute Menlo Park, California 94025	5
Civil Defense Technical Office Attn: Mr. James Halsey Stanford Research Institute Menlo Park, California 94025	1
Director, Civil Effects Branch Division of Biology and Medicine Atomic Energy Commission Attn: Mr. L. J. Deal Washington, D. C. 20545	1

Addressee	No. of Copies
U. S. Atomic Energy Commission Technical Information Service P. O. Box 62 Oak Ridge, Tennessee 37831	1
Radiation Shielding Information Center Oak Ridge National Laboratory P. O. Box X Oak Ridge, Tennessee 37831	1
Director, Oak Ridge National Laboratory P. O. Box X Attn: Dr. C. E. Clifford Oak Ridge, Tennessee 37831	1
Los Alamos Scientific Laboratory Attn: Document Library Los Alamos, New Mexico 87544	1
Hudson Institute Quaker Ridge Road Harmon-on-Hudson, New York	
Advisory Committee on Civil Defense National Academy of Sciences Attn: Mr. Richard Park 2101 Constitution Avenue, N. W. Washington, D. C. 20418	1
Mr. Arthur D. Gaster Chairman, Coordinating Committee on Civil Defense American Society of Civil Engineers 2864 McFarlan Park Drive Cincinnati 11, Ohio	1
The RAND Corporation 1700 Main Street Santa Monica, California Attn: Dr. Harold Brode	1
Dr. A. Sachs Institute of Defense Analysis 400 Army-Navy Drive Arlington, Virginia 22202	1

Addressee	No. of Copies
Mr. Luke J. Vortman Division 5412 Sandia Corporation Box 5800 Sandia Base Albuquerque, New Mexico 87115	1
Dr. Nathan M. Newmark 111 Talbot Laboratory University of Illinois Urbana, Illinois	1
Dr. William Hall 111 Talbot Laboratory University of Illinois Urbana, Illinois	1
Dr. Merit P. White Head, Civil Engineering Department School of Engineering University of Massachusetts Amherst, Massachusetts	
Dr. Robert J. Hansen Department of Civil and Sanitary Engineering Massachusetts Institute of Technology Cambridge, Massachusetts	1
Mr. Bill Miller Department of Civil Engineering 307 More Hall University of Washington Seattle, Washington	1
Mr. Carl Koontz Department of Civil Engineering Worcester Polytechnic Institute Worcester, Massachusetts	1
Franklin J. Agardy Department of Civil Engineering San Jose State College San Jose, California	1
Mr. M. B. Scott School of Civil Engineering Civil Engineering Building Purdue University Lafayette, Indiana	1

Addressee	No. of Copies
Mr. John A. Samuel Department of Mechanical Engineering University of Florida Gainesville, Florida	1
Mr. C. K. Vetter School of Architecture University of Colorado Boulder, Colorado	1
Mr. Charles H. Samson, Jr. Head, Civil Engineering Department Texas A&M University College Station, Texas	1
ITT Research Institute 10 West 35th Street Attn: Dr. Eugene Sevin Chicago, Illinois 60616	1
The Dikewood Corporation 1009 Bradbury Drive, S. E. University Research Park Albuquerque, New Mexico 87106	1
Research Triangle Institute Post Office Box 12194 Durham, North Carolina 27709	1
United Research Services 1811 Trousdale Drive Burlingame, California	1
General American Transportation Corporation MRD Division 7449 North Natchez Avenue Niles, Illinois 60648	1
T. Y. Lin and Associates 14656 Oxnard Street Van Nuys, California	1
Amman & Whitney 111 Eight Avenue New York, New York 10011	1
Bechtel Corporation Attn: Mr. L. Pinzow 190 Shady Grove Road Gaithersburg, Maryland	1

COMBINED EFFECTS OF NUCLEAR WEAPONS ON NFSS TYPE STRUCTURES, URS 658-3
URS Corporation, Burlingame, California
September 1966 100 pp. Contract OCD-PS-64-201 Work Unit 1126B

Unclassified

The primary objective of this program was to examine and evaluate the protection afforded by the types of structures found in the National Fallout Shelter Survey (NFSS) against the combined effects of nuclear weapons. Since a major criterion for the designation of the NFSS structures was the radiation protection factor (PF) of the structure, the approach adopted in this investigation was to examine the sensitivity of the PF for idealized building situations to alteration by air blast and fire damage. To accomplish this, interim techniques were developed for estimation of the air blast loading and damage to selected types of structures. These techniques were developed by utilizing available experimental data together with engineering judgment to modify current generalized blast loading schemes. The procedure adopted to predict damage was to determine the blast loading on each building component and then to compare this loading with the failure loading for the component.

Similarly, by utilizing fire prediction information, a method was developed for determining the fire damage within the building. To predict damage to the various building elements by this procedure, the duration of the peak fire was calculated and then compared with the rated resistance of the components.

COMBINED EFFECTS OF NUCLEAR WEAPONS ON NFSS TYPE STRUCTURES, URS 658-3
URS Corporation, Burlingame, California
September 1966 100 pp. Contract OCD-PS-64-201 Work Unit 1126B

UNCLASSIFIED

The primary objective of this program was to examine and evaluate the protection afforded by the types of structures found in the National Fallout Shelter Survey (NFSS) against the combined effects of nuclear weapons. Since a major criterion for the designation of the NFSS structures was the radiation protection factor (PF) of the structure, the approach adopted in this investigation was to examine the sensitivity of the PF for idealized building situations to alteration by air blast and fire damage. To accomplish this, interim techniques were developed for estimation of the air blast loading and damage to selected types of structures. These techniques were developed by utilizing available experimental data together with engineering judgment to modify current generalized blast loading schemes. The procedure adopted to predict damage was to determine the blast loading on each building component and then to compare this loading with the failure loading for the component.

Similarly, by utilizing fire prediction information, a method was developed for determining the fire damage within the building. To predict damage to the various building elements by this procedure, the duration of the peak fire was calculated and then compared with the rated resistance of the components.

COMBINED EFFECTS OF NUCLEAR WEAPONS ON NFSS TYPE STRUCTURES, URS 658-3
URS Corporation, Burlingame, California
September 1966 100 pp. Contract OCD-PS-64-201 Work Unit 1126B

UNCLASSIFIED

The primary objective of this program was to examine and evaluate the protection afforded by the types of structures found in the National Fallout Shelter Survey (NFSS) against the combined effects of nuclear weapons. Since a major criterion for the designation of the NFSS structures was the radiation protection factor (PF) of the structure, the approach adopted in this investigation was to examine the sensitivity of the PF for idealized building situations to alteration by air blast and fire damage. To accomplish this, interim techniques were developed for estimation of the air blast loading and damage to selected types of structures. These techniques were developed by utilizing available experimental data together with engineering judgment to modify current generalized blast loading schemes. The procedure adopted to predict damage was to determine the blast loading on each building component and then to compare this loading with the failure loading for the component.

Similarly, by utilizing fire prediction information, a method was developed for determining the fire damage within the building. To predict damage to the various building elements by this procedure, the duration of the peak fire was calculated and then compared with the rated resistance of the components.

COMBINED EFFECTS OF NUCLEAR WEAPONS ON NFSS TYPE STRUCTURES, URS 658-3
URS Corporation, Burlingame, California
September 1966 100 pp. Contract OCD-PS-64-201 Work Unit 1126B

UNCLASSIFIED

The primary objective of this program was to examine and evaluate the protection afforded by the types of structures found in the National Fallout Shelter Survey (NFSS) against the combined effects of nuclear weapons. Since a major criterion for the designation of the NFSS structures was the radiation protection factor (PF) of the structure, the approach adopted in this investigation was to examine the sensitivity of the PF for idealized building situations to alteration by air blast and fire damage. To accomplish this, interim techniques were developed for estimation of the air blast loading and damage to selected types of structures. These techniques were developed by utilizing available experimental data together with engineering judgment to modify current generalized blast loading schemes. The procedure adopted to predict damage was to determine the blast loading on each building component and then to compare this loading with the failure loading for the component.

Similarly, by utilizing fire prediction information, a method was developed for determining the fire damage within the building. To predict damage to the various building elements by this procedure, the duration of the peak fire was calculated and then compared with the rated resistance of the components.

UNCLASSIFIED

Security Classification

DOCUMENT CONTROL DATA - R&D

(Security classification of title, body of abstract and indexing annotation must be entered when the overall report is classified)

1 ORIGINATING ACTIVITY *(Corporate author)*
URS Corporation
1811 Trousdale Drive
Burlingame, California

2a REPORT SECURITY CLASSIFICATION
UNCLASSIFIED

2b GROUP

3 REPORT TITLE
Combined Effects of Nuclear Weapons on NFSS Type Structures

4 DESCRIPTIVE NOTES *(Type of report and inclusive dates)*
Final Report

5 AUTHOR(S) *(Last name, first name, initial)*
Wiehle, Carl K.; Durbin, William L.

6 REPORT DATE	7a TOTAL NO OF PAGES	7b NO OF REFS
September 1966	103	45

8a CONTRACT OR GRANT NO.
OCD-PS-64-201

b. PROJECT NO
Work Unit No. 1126B

c

d

9a ORIGINATOR'S REPORT NUMBER(S)
URS 658-3

9b OTHER REPORT NO(S) *(Any other numbers that may be assigned this report)*

10. AVAILABILITY/LIMITATION NOTICES
Distribution of this document is unlimited.

11. SUPPLEMENTARY NOTES

12. SPONSORING MILITARY ACTIVITY
Office of Civil Defense
Office of the Secretary of the Army
Washington, D.C. 20310

13 ABSTRACT

The primary objective of this program was to examine and evaluate the protection afforded by the types of structures found in the National Fallout Shelter Survey (NFSS) against the combined effects of nuclear weapons. Since a major criterion for the designation of the NFSS structures was the radiation protection factor (PF) of the structure, the approach adopted in this investigation was to examine the sensitivity of the PF for idealized building situations to alteration by air blast and fire damage. To accomplish this, interim techniques were developed for estimation of the air blast loading and damage to selected types of structures. These techniques were developed by utilizing available experimental data together with engineering judgment to modify current generalized blast loading schemes. The procedure adopted to predict damage was to determine the blast loading on each building component and then to compare this loading with the failure loading for the component.

Similarly, by utilizing fire prediction information, a method was developed for determining the fire damage within the building. To predict damage to the various building elements by this procedure, the duration of the peak fire was calculated and then compared with the rated resistance of the components.

DD FORM 1 JAN 64 1473

UNCLASSIFIED

Security Classification

14 KEY WORDS	LINK A		LINK B		LINK C	
	ROLE	WT	ROLE	WT	ROLE	WT
Building damage Protection factor NFSS shelters Nuclear weapon Air blast Fire damage Structural response Structural dynamics Dynamic loading						

INSTRUCTIONS

1. ORIGINATING ACTIVITY: Enter the name and address of the contractor, subcontractor, grantee, Department of Defense activity or other organization *(corporate author)* issuing the report.

2a. REPORT SECURITY CLASSIFICATION: Enter the overall security classification of the report. Indicate whether "Restricted Data" is included. Marking is to be in accordance with appropriate security regulations.

2b GROUP. Automatic downgrading is specified in DoD Directive 5200.10 and Armed Forces Industrial Manual. Enter the group number Also, when applicable, show that optional markings have been used for Group 3 and Group 4 as authorized

3. REPORT TITLE. Enter the complete report title in all capital letters. Titles in all cases should be unclassified. If a meaningful title cannot be selected without classification, show title classification in all capitals in parenthesis immediately following the title.

4. DESCRIPTIVE NOTES. If appropriate, enter the type of report, e.g., interim, progress, summary, annual, or final. Give the inclusive dates when a specific reporting period is covered.

5. AUTHOR(S): Enter the name(s) of author(s) as shown on or in the report. Enter last name, first name, middle initial. If military, show rank and branch of service. The name of the principal author is an absolute minimum requirement.

6. REPORT DATE. Enter the date of the report as day, month, year, or month, year. If more than one date appears on the report, use date of publication.

7a TOTAL NUMBER OF PAGES: The total page count should follow normal pagination procedures, i.e., enter the number of pages containing information.

7b NUMBER OF REFERENCES. Enter the total number of references cited in the report.

8a CONTRACT OR GRANT NUMBER. If appropriate, enter the applicable number of the contract or grant under which the report was written.

8b, 8c, & 8d. PROJECT NUMBER: Enter the appropriate military department identification, such as project number, subproject number, system numbers, task number, etc.

9a ORIGINATOR'S REPORT NUMBER(S): Enter the official report number by which the document will be identified and controlled by the originating activity. This number must be unique to this report.

9b OTHER REPORT NUMBER(S): If the report has been assigned any other report numbers *(either by the originator or by the sponsor)*, also enter this number(s).

10. AVAILABILITY/LIMITATION NOTICES: Enter any limitations on further dissemination of the report, other than those imposed by security classification, using standard statements such as:

(1) "Qualified requesters may obtain copies of this report from DDC."

(2) "Foreign announcement and dissemination of this report by DDC is not authorized."

(3) "U. S. Government agencies may obtain copies of this report directly from DDC. Other qualified DDC users shall request through _____."

(4) "U. S. military agencies may obtain copies of this report directly from DDC. Other qualified users shall request through _____."

(5) "All distribution of this report is controlled. Qualified DDC users shall request through _____."

If the report has been furnished to the Office of Technical Services, Department of Commerce, for sale to the public, indicate this fact and enter the price, if known.

11. SUPPLEMENTARY NOTES. Use for *additional* explanatory notes.

12. SPONSORING MILITARY ACTIVITY: Enter the name of the departmental project office or laboratory sponsoring *(paying for)* the research and development. Include address.

13 ABSTRACT: *Enter an abstract giving a brief and factual* summary of the document indicative of the report, even though it may also appear elsewhere in the body of the technical report *If additional space is required, a continuation sheet shall* be attached

It is highly desirable that the abstract of classified reports be unclassified Each paragraph of the abstract shall end with an indication of the military security classification of the information in the paragraph, represented as *(TS) (S) (C) or (U)*

There is no limitation on the length of the abstract However, the suggested length is from 150 to 225 words

14 KEY WORDS: Key words are technically meaningful terms or short phrases that characterize a report and may be used as index entries for cataloging the report Key words must be selected so that no security classification is required Identifiers, such as equipment model designation, trade name, military project code name, geographic location, may be used as key words but will be followed by an indication of technical context. The assignment of links, rules, and weights is optional